

BAK activation: a multiple step mechanism

Thesis submitted for the degree of
Doctor of Philosophy
at the University of Leicester

by

Kathrin Weber
MRC Toxicology Unit
University of Leicester

November 2010

BAK activation: a multiple step mechanism

Kathrin Weber

Medical Research Council Toxicology Unit,
Hodgkin Building, Lancaster Road, Leicester LE1 9HN, U.K.

Abstract

Although the pro-apoptotic BCL-2 family proteins BAK and BAX play a key role in mitochondrial perturbation their transition from an inactive closed conformation to a membrane permeabilising pore remains unclear. I found that BAK in viable cells existed in a primed state which was characterized by an occluded N-terminus and an exposed BH3 domain. This conformation facilitated binding to the hydrophobic groove of BCL-X_L and served as a checkpoint maintaining cell survival by preventing its further activation. Isolation of BAK by immunoprecipitation suggests that only a discrete portion is present in this primed conformation. Reconstitution of the BCL-X_L BAK complex into a BAK/BAX null background rendered cells more sensitive to the BAD BH3 mimetic ABT-737 indicating that primed BAK is primarily involved in ABT-737 induced apoptosis.

Primed BAK was displaced from BCL-X_L by ABT-737 followed by an N-terminal conformational change and subsequent formation of dimers and higher molecular weight complexes. These sequential BAK activation steps occurred independently of cell fate and did not represent the rate limiting steps in BAK activation as a BAK BH3 mutant L78A lost proapoptotic function but still oligomerised as efficiently as wt BAK.

Thus the transition from inactive BAK to a membrane permeabilising pore requires an additional activation step. I demonstrate that after 30 min of ABT-737 exposure primed BAK, after its displacement from BCL-X_L, interacts with BIM_{EL} reflecting the transient nature of this interaction. This interaction represented an additional step in BAK activation as BAK pro-apoptotic function was enhanced when BIM_{EL} and BAK were co-expressed. However BIM_{EL} did not induce the N-terminal conformational change nor oligomerisation of BAK and its interaction occurred downstream of both these events. In addition the pool of BIM_{EL} involved in the further activation of BAK did not represent that sequestered by the antiapoptotic proteins BCL-2 and BCL-X_L.

These data suggest that BAK activation occurs in multiple steps in which a further activation event is required after the exposure of the BH3 domain, the N-terminal conformational change and the formation of high molecular weight complexes but prior to cytochrome *c* release. I propose that this event may be represented by interaction of N-terminal conformational changed/oligomerised BAK with BIM_{EL}.

Acknowledgments

I thank my supervisor Prof. Gerry Cohen.

I am grateful to all members of the lab both past and present and especially to Dr. Nicholas Harper for his helpful discussions and experimental support. I also thank Prof. John Schwab for support in designing the mutants and discussions.

Ausserdem möchte ich ganz lieb meiner Familie danken. Ganz besonders meiner kleinen Hanni ohne deine ansteckende Lebensfreude hätte ich es nie geschafft. Ausserdem Nick vielen Dank, dass du immer für mich da warst und bist und alle Höhen und Tiefen mit mir meisterlich durchgestanden hast. Zudem ein riesengrosses Dankeschön an meine Eltern für eure kontinuierliche Unterstützung, ohne Euch wäre es nie möglich gewesen. Danke, dass ihr immer für uns da wart.

Contents

1	CHAPTER: INTRODUCTION.....	1
1.1	Apoptosis.....	2
1.2	Apoptosis in <i>Caenorhabditis elegans</i>.....	2
1.3	Apoptosis in the mammalian system.....	3
1.3.1	Caspases.....	5
1.3.2	Mitochondria: central to the intrinsic apoptotic pathway.....	5
1.4	The BCL-2 family.....	6
1.4.1	Anti-apoptotic, multidomain BCL-2 proteins: mitochondrial protectors.....	6
1.4.2	Pro-apoptotic, multidomain BCL-2 proteins: triggers for death.....	9
1.4.3	The BH3-only proteins: the cellular damage sensors.....	12
1.5	Activation of BAX and BAK: direct vs indirect.....	13
1.5.1	Direct activation.....	13
1.5.2	Indirect activation displacement model.....	14
1.5.3	BAK and BAX: different mechanisms of activation.....	15
1.6	Conformational changes leading to active BAK and BAX.....	17
1.6.1	Reorganisation of the N-terminal region.....	17
1.6.2	Exposure of the BH3 domain.....	18
1.7	BH3 mimetics in cancer therapy.....	21
1.8	Aims and objectives:.....	25

2	CHAPTER 2: MATERIALS AND METHODS	26
2.1	Materials	27
2.2	Cell Biology Techniques	27
2.2.1	Cell Culture.....	27
2.2.2	Annexin V and Propidium Iodide Staining.....	28
2.2.3	Measurement of the Ψ_m	28
2.2.4	Subcellular fractionation.....	29
2.3	Biochemical Techniques	30
2.3.1	Preparation of Samples for SDS-PAGE	30
2.3.2	Immunostaining of proteins on Nitrocellulose Membranes (Western blotting).....	31
2.4	Molecular Biology Protocols	34
2.4.1	Plasmids	34
2.4.2	Bacterial Strains and Culture Conditions.....	34
2.4.3	Transformation of <i>E. Coli</i>	34
2.4.4	Preparation of Plasmid DNA	34
2.4.5	Quantification of DNA	35
2.4.6	DNA Electrophoresis on Agarose Gels	35
2.4.7	Mutagenesis	35
2.5	Reconstitution of BCL-X_L:BAK complexes.....	35
2.6	siRNA transfections.....	36
2.7	Analysis of BAK activation	36
2.7.1	Intracellular AB-1 staining	36
2.7.2	Immunohistochemistry	36
2.7.3	Limited Trypsin proteolysis.....	37
2.7.4	Copper(II)(1,10-phenanthroline) ₃ (CuPhe).....	37

2.7.5	Sucrose density centrifugation.....	38
2.7.6	Immunoprecipitation.....	38
3	CHAPTER 3: Specificity of BH3 mimetics: ABT-737 as a tool to analyse the activation of BAK.....	39
3.1	Introduction	40
3.2	Results	42
3.2.1	Involvement of BAK/BAX in cell death induced by a variety of BH3 mimetics.....	42
3.2.2	Involvement of caspase-9 in cell death induced by a variety of BH3 mimetics.....	44
3.2.3	ABT-737 induces the intrinsic apoptotic pathway in a BAX-deficient Jurkat cell line.....	46
3.2.4	ABT-737 induced apoptosis requires BAK in BAX-deficient Jurkat cell line.	52
3.3	Discussion.....	54
4	CHAPTER 4: A discrete pool of cellular BAK is sequestered by BCL-X_L and can be displaced by ABT-737	56
4.1	Introduction	57
4.2	Results	59
4.2.1	A distinct proportion of total cellular BAK is associated with BCL-X _L and displaced by ABT-737	59
4.2.2	Reconstitution of a BCL-X _L :BAK complex sensitises resistant cells to ABT-737.....	63
4.2.3	Role of MCL-1 and BCL-2 as inhibitors of BAK	67
4.2.4	The BAK BH3 domain mediates interaction with BCL-X _L	70
4.3	Discussion.....	73

5	CHAPTER 5: BAK undergoes an N-terminal conformational change and oligomerizes during apoptosis – both do not represent the point of no return	74
5.1	Introduction	75
5.2	Results	77
5.2.1	BAK unmaskes the N-terminal region during apoptosis.....	77
5.2.2	Primed BAK exposes the AB-1 epitope after displacement from BCL-X _L	81
5.2.3	Primed BAK is not N-terminally changed.....	84
5.2.4	The N-terminal conformational change: a reorganisation of the N-terminal region	87
5.2.5	BAK forms dimers and high molecular weight complexes during apoptosis ..	90
5.2.7	Auto-activation	92
5.2.8	N-terminal conformational change occurs before BAK oligomerisation	92
5.2.9	N-terminal conformational change as well as aggregation of BAK are not sufficient for the commitment to apoptotisis	95
5.3	Discussion.....	101
6	CHAPTER 6: BIM_{EL} interacts with “active” BAK after its displacement from BCL-X_L.....	104
6.1	Introduction	105
6.2	Results	107
6.2.1	BIM _{EL} resides in a complex with BAK	107
6.2.2	BIM _{EL} interacts with primed BAK after displacement from BCL-X _L	109
6.2.3	BIM _{EL} enhances the pro-apoptotic function of BAK	112
6.2.4	BIM _{EL} does not induce N-terminal conformational change or oligomerisation of BAK.....	114
6.2.5	ABT-737 displaces BIM _{EL} from BCL-X _L but not BCL-2.....	117

6.3	Discussion.....	121
7	CHAPTER 7: Discussion.....	123
7.1	Exposure of the BH3 domain	126
7.2	N-terminal conformational change and oligomerisation of primed BAK	127
7.3	Interaction with BIM _{EL}	129
7.4	Direct or indirect activation	131
8	CHAPTER 8: References	133
9	CHAPTER 9: APPENDIX.....	139

Table of Figures/Tables

Figure 1.1	The apoptotic pathway in <i>C. elegans</i>	3
Figure 1.2	Pathways to apoptosis in mammalian cells.....	4
Figure 1.3	Classes of BCL-2 Proteins and their selectivity for each other.....	8
Figure 1.4	BH3:groove interaction.....	11
Figure 1.5	Schematic representation of the indirect and direct activation model.....	16
Figure 1.6	Inactive BAK- occluded N-terminus and BH3 domain/groove.....	20
Figure 1.7	Structures of some BCL-2 inhibitors.....	23
Tabel 1.1	Binding affinities of different BH3 mimetics for specific antiapoptotic BCL-2 proteins.....	24
Table 2.1	Recipes for resolving and stacking polyacrylamide gels.....	31
Table 2.2	Sources of antibodies used in studies	33
Table 2.3	Sense strands of used BAK siRNAs	36
Figure 3.1	Only ABT-737 induces BAX/BAK dependent cell death.....	43
Figure 3.2	Only ABT-737 induces caspase-9 dependent cell death.....	45
Figure 3.3	ABT-737 induces PS externalisation and reduction in $\Delta\Psi_m$	47
Figure 3.4	ABT-737 induces cytochrome <i>c</i> release.....	49
Figure 3.5	ABT-737 initiates the caspase cascade.....	51
Figure 3.6	ABT-737 requires BAK to induce apoptosis in Jurkat cells.....	53
Figure 4.1	BAK is bound to BCL-X _L and can be displaced by ABT-737.....	61
Figure 4.2	A distinct proportion of total cellular BAK is associated with BCL-X _L	62
Figure 4.3	Discrete proportion of primed BAK is sufficient to launch apoptosis.....	65
Figure 4.4	Reconstituted BCL-X _L :BAK complex is disrupted by ABT-737.....	66
Figure 4.5	BAK is sequestered by MCL-1 but not by BCL-2.....	68
Figure 4.6	Failure to reconstitute a BCL-2:BAK complex, MCL-1 associates with BAK but is not targeted by ABT-737	69
Figure 4.7	The BAK BH3 domain mediates interaction with BCL-X _L	72

Figure 5.1	BAK undergoes an N-terminal conformational change during apoptosis.....	79
Figure 5.2	Exposure of the AB-1 epitope occurs after displacement of primed BAK from BCL-X _L	83
Figure 5.3	N-terminus is not exposed in primed BAK.....	86
Figure 5.4	The epitopes of the AB-1 antibody reside on helix α 1.....	89
Figure 5.5	Formation of BAK oligomers during apoptosis.....	91
Figure 5.6	N-terminal conformational change is required for BAK proapoptotic function.....	94
Figure 5.7	N-terminal conformational change is required for BAK proapoptotic function.....	96
Figure 5.8	N-terminal conformational change does not represent the point of no return in BAK activation.....	98
Figure 5.9	Formation of BAK oligomers does not represent the point of no return in BAK activation.....	100
Figure 6.1	BIM _{EL} interacts with BAK.....	107
Figure 6.2	BIM _{EL} interacts with primed BAK.....	111
Figure 6.3	BIM _{EL} enhances the proapoptotic function of BAK.....	113
Figure 6.4	BAK is N-terminal conformationally changed and oligomerised when reconstituted in HEK293T cells.....	116
Figure 6.5	BIM _{EL} is displaced from BCL-X _L by ABT-737.....	119
Figure 6.6	Reconstituted BCL-X _L :BIM _{EL} is disrupted by ABT-737.....	120
Figure 7.1	BAK activation- a multiple step mechanism.....	125

Abbreviations

APAF-1	apoptotic protease activating-factor 1
ATP	adenosine triphosphate
BAK	BCL-2 homoloug antagonist/killer
BAX	BCL-2 associated X protein
BIM _{EL}	BCL-2-interacting mediator of cell death (isoform extra long)
BCL-X _L	BCL-2 like protein 1 (isoform beta, long)
BCL-2	B cell lymphoma 2
CuPhe	Copper(II)(1,10-phenanthroline) ₃
DKO	double knock out
DMEM	Dulbecco's modified Eagle's medium
DMSO	di-methyl sulphoxide
FITC	fluorescein isothiocyanate
FSC	Forward scatter
MOMP	Mitochondrial outer membrane permeabilisation
MCL-1	Induced myeloid leukemia cell differentiation protein
ng	nano gramm
PBS	phosphate-buffered saline
PS	phosphatidylserine
PI	propidium iodid
RPMI	Roswell Park Memorial Institute
SDS	sodium dodecyl sulphate
TBS	TRIS-buffered saline
TBST	TBS containing 0.1% Tween-20
TBSMT	TBST containing 5% (w/v) Marvel TM
TEMED	N,N,N',N'-tetramethylethylenediamine
TMRE	Tetramethylrhodamine, ethyl ester
TOM	Mitochondrial import receptor subunit
Ψ _m	mitochondrial membrane potential

CHAPTER 1:
Introduction

1.1 Apoptosis

Programmed cell death (Lockshin and Williams 1965) and its morphologic manifestation of apoptosis (Kerr, Wyllie et al. 1972) is a conserved pathway that is vital for development and functioning of multicellular organisms. Apoptosis ensures the elimination of redundant, damaged or infected cells, shapes the embryo and maintains tissue homeostasis and defence against pathogens in adults.

The characteristic changes within the cell during programmed cell death include morphological changes such as cell shrinkage, nuclear condensation, plasma membrane blebbing, DNA fragmentation and translocation of phosphatidylserine to the outer leaflet of the plasma membrane (reviewed in (Green and Evan 2002)). Finally cells are packaged into “apoptotic bodies” which are rapidly phagocytosed by neighbouring cells. This highly controlled mechanism ensures that the cellular contents are not released into the extracellular milieu preventing a potentially damaging inflammatory response which is associated with other uncontrolled forms of cell death such as necrosis.

Tight control of this mechanism is essential as too much apoptosis contributes to pathological degenerative conditions such as Alzheimer’s and Huntington’s disease whereby too little apoptosis sets the stage for cancer and autoimmune disease.

1.2 Apoptosis in *Caenorhabditis elegans*

Important insights regarding the genetic basis of programmed cell death were obtained by studies using the nematode *C. elegans* (Horvitz 1999). During worm development out of 1090 somatic cells the same 131 cells die. Two genes, *CED-3* and *CED-4*, were observed to promote cell death whereas another *CED-9* prevented cell death (Ellis and Horvitz 1991; Hengartner, Ellis et al. 1992). *CED-3* was found to be related to mammalian cysteine protease that activates the cytokine interleukin-1 β (Yuan 1993) and activation of *CED-3* requires *CED-4* (human homologue APAF-1) in order to kill cells. *CED-9* prevents cell death and its functional and structural mammalian counterpart was identified to be *BCL-2* (Hengartner and Horvitz 1994). A fourth protein *EGL-1* (Conradt and Horvitz 1998) equivalent to the mammalian BH3-only proteins releases the *CED-9* block and induces cell death of somatic cells.

Mammalian orthologues of these cell death genes were subsequently identified (reviewed in (Meier, Finch et al. 2000)), whereby the complexity and importance of the apoptotic process increased with the complexity of the organism.

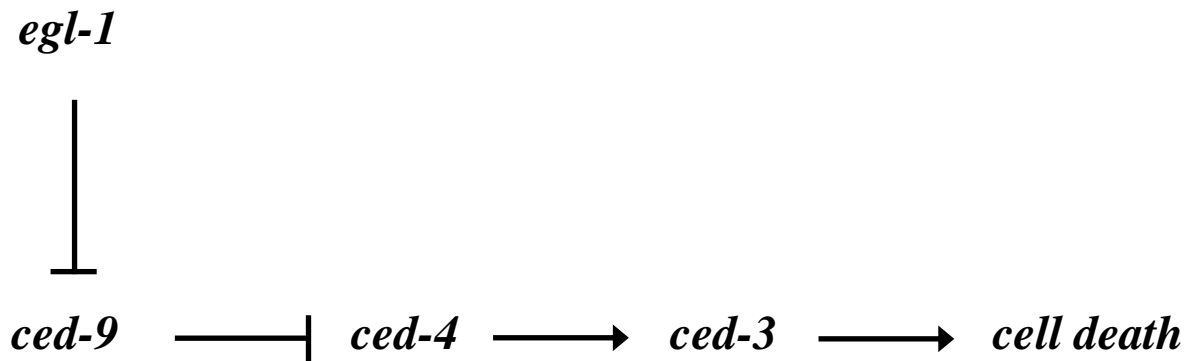


Figure 1.1 Apoptotic pathway in *C. elegans*.

1.3 Apoptosis in the mammalian system

In mammals two major apoptotic pathways exist: the extrinsic receptor mediated and intrinsic stress induced pathways. The extrinsic pathway is triggered when ligands of the tumor necrosis factor (TNF) family engage with their cognate receptors on the cell surface. This initiates formation of the death-inducing signaling complex (DISC), which results in activation of the initiator caspase-8 (reviewed (Danial and Korsmeyer 2004)). The intrinsic pathway involves the mitochondria, whereby diverse stress stimuli converge at the mitochondria provoking permeabilisation of the outer mitochondrial membrane (MOMP). This results in the release of apoptogenic proteins (e.g. cytochrome c) from the mitochondrial intermembrane space into the cytosol leading to the activation of the initiator caspase-9 (reviewed (Danial and Korsmeyer 2004)). Although both pathways are largely independent in certain cell types the two pathways can converge. Caspase-8 can process the pro-apoptotic BCL-2 protein BID into its active form (tBID) (Fig. 1.2), which then acts directly at the mitochondria to induce MOMP. However both pathways merge in the activation of caspases, which are responsible for all the stereotypical morphological changes during apoptosis and are the executioners of apoptosis

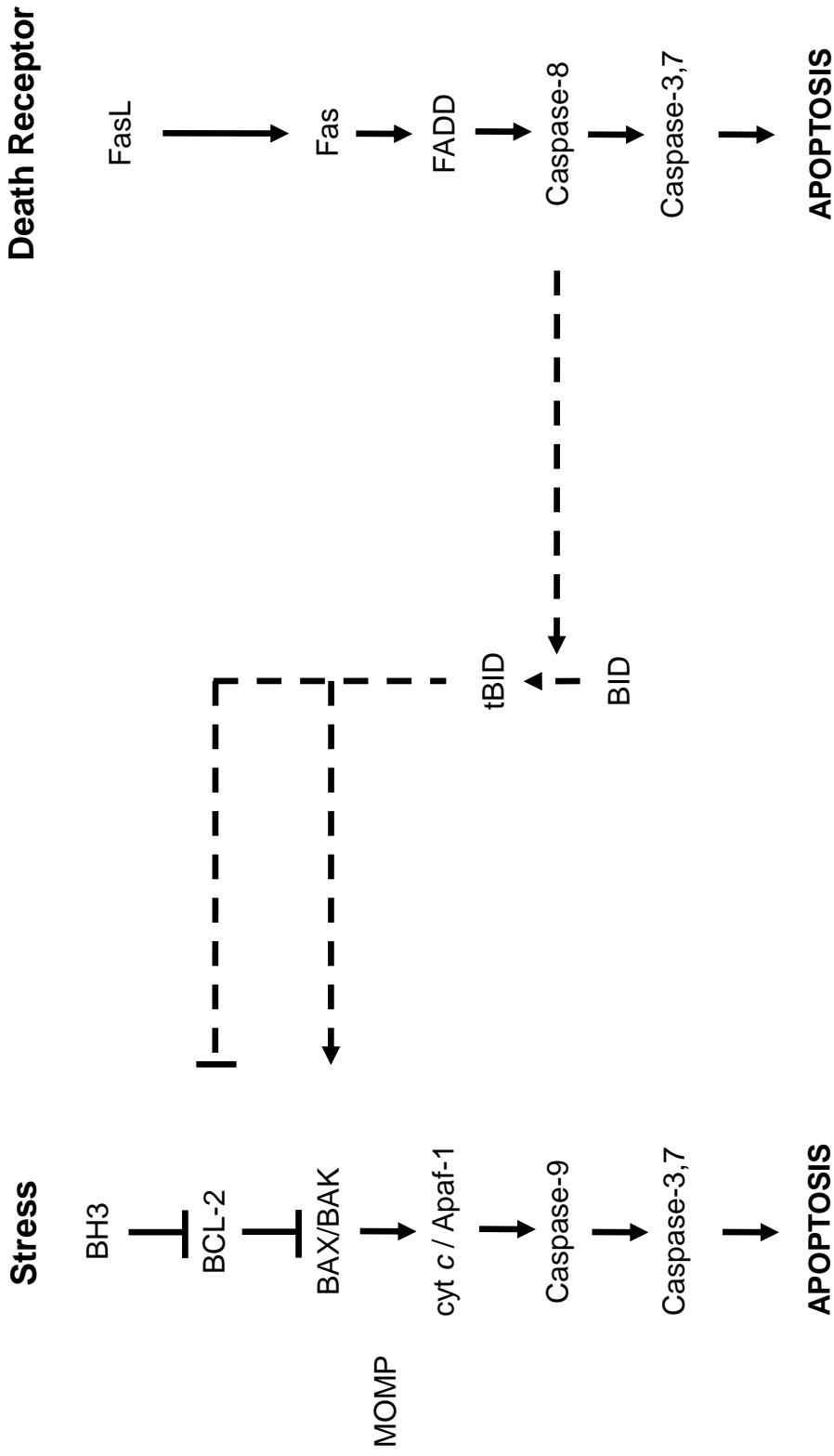


Figure 1.2 Pathways to apoptosis in mammalian cells

Stress pathway (right panel) triggered by several cytotoxic stimuli. Involves members of the BCL-2 protein family and leads to perturbation of the mitochondria and activation of initiator caspase-9. Receptor pathway (left panel) triggered by aggregation of death receptors of the TNF family (here typified by FAS) on the plasma membrane leading to activation of initiator caspase-8. Both pathways may be linked BID .

1.3.1 Caspases

Caspases are intracellular cysteine proteases so termed because of the cysteine residue in their active site and their specificity for cleavage after aspartate residues (Thronberry and Lazebnik 1998, Earnshaw 1999, Shi 2002 Yuan 2003). They are synthesized as inactive zymogens and become activated during apoptosis. Activation includes cleavage between their small subunit and the large subunit followed by a second cleavage to remove the prodomain. The structure of an active caspase is a heterotetramer, where the p20 and p10 dimers represents the smallest subunit (reviewed (Cohen 1997)).

Caspases involved in apoptosis can be subdivided into those involved in the initiation of apoptosis - the initiator caspases (caspase-8: extrinsic pathway, caspase-9: intrinsic pathway) and those involved in the execution phase - the effector caspases (caspase-3 and 7).

Caspase-9 is the initiator caspase of the intrinsic apoptotic pathway. Pro-caspase-9 shares the characteristic features found for other initiator caspases mainly a long prodomain facilitating binding to a scaffold protein (APAF-1) which acts as a platform for its activation. Once caspase-9 is activated it processes and activates downstream effector caspases (caspase-3, 6 and 7) which are responsible for cleavage of multiple cellular substrates. For example, caspase-3-mediated cleavage of ICAD (Inhibitor of Caspase-Activated DNase) releases CAD (Caspase-Activated DNase) a nuclease whose action leads to chromatin condensation. Cleavage of nuclear (lamins) and cytoskeletal (actin and fodrin) structural proteins contribute to nuclear/cellular shrinkage and the classical morphological changes that occur during apoptosis (Takahashi, Alnemri et al. 1996; Wolf and Green 1999).

1.3.2 Mitochondria: central to the intrinsic apoptotic pathway

The intrinsic apoptosis pathway is activated by a wide range of cytotoxic stimuli including cytokine deprivation, ionising radiation and chemotherapeutic drugs. These death signals converge at the mitochondria leading to the perturbation of the outer mitochondrial membrane and consequently release of apoptogenic factors from the mitochondrial intermembrane space into the cytoplasm (Fig. 1.2). Among these is cytochrome *c*, which facilitates together with dATP (or ATP) the assembly of APAF-1 into a large (~700 kD) caspase-activating complex - the 'apoptosome' (Cain, Brown et al. 1999; Zou, Li et al. 1999). The apoptosome provides a platform for the autocatalytic activation of the initiator caspase-9 and subsequent

activation of the caspase cascade. Formation of the apoptosome can also be initiated by cytochrome *c* released by an extrinsic death signal through tBid.

The point of no return in this pathway is the release of cytochrome *c* from the mitochondria and is controlled by members of the BCL2 protein family. BAK and/or BAX oligomerise and form pores in the outer mitochondrial membrane, which facilitates cytochrome *c* release from the mitochondrial intermembrane space (Martinou and Green 2001). However, the exact nature of this pore is not determined yet. In artificial membranes BAX can permeabilize liposomes without assistance of other proteins (Kuwana, Bouchier-Hayes et al. 2005). In a cellular context a variety of proteins are described to play a potential role in MOMP. For example BAX was described to interplay with components of the mitochondrial fission and fusion machinery that regulate the dynamics and plasticity of mitochondria. During apoptosis mitochondria are fragmented by increased fission and components of the mitochondrial fission and fusion machinery (DRP-1 and mitofusins) are recruited to mitochondrial scission sites colocalizing with BAX (Frank, Gaume et al. 2001; Karbowski, Lee et al. 2002).

1.4 The BCL-2 family

The intrinsic apoptotic pathway is regulated by the members of the BCL-2 protein family (Danial and Korsmeyer 2004) and the decision to survive or to commit apoptosis is mediated through interactions between anti- and pro-apoptotic subclasses of this family. Further subclassification includes their structural composition and presence of *BCL-2 homology* (BH) domains (Fig 1.3 A).

1.4.1 Anti-apoptotic, multidomain BCL-2 proteins: mitochondrial protectors

The first molecular regulator of the cell suicide programme identified was the oncogene BCL-2 which was linked in human follicular lymphoma by a chromosomal translocation to the heavy chain locus (Tsujimoto, Yunis et al. 1984). In contrast to all other identified oncogenes BCL-2 was shown to inhibit cellular proliferation instead of promoting it (Vaux, Cory et al. 1988), reinforcing the concept that impaired apoptosis is central in tumor development (Hanahan and Weinberg 2000; Green and Evan 2002).

BCL-2 as well as its closely related proteins BCL-X_L and BCL-w display homology within four α -helical BH domains BH1-4. The anti-apoptotic proteins MCL-1 and BCL2A1 show

more divergence and only possess strong sequence homology in the BH1, BH2, and BH3 regions, however they all protect cells from a wide range of cytotoxic conditions.

The first identified structure of a BCL-2 family member was that of human BCL-X_L as determined by X-ray crystallography and NMR spectroscopy (Muchmore, Sattler et al. 1996). BCL-X_L like all other anti-apoptotic members displays an overall globular folded structure, which consists of eight α -helices connected by loops of varying length. Central are two hydrophobic α -helices surrounded by six amphipathic α -helices- the “BCL-2 core” (Chipuk, Moldoveanu et al.).

The BH1 (portion of α 4- α 5) and BH2 (α 7- α 8) regions reside on one side, whereas the BH3 region (α 2) on the other defines the top of a hydrophobic groove on the surface of the BCL-2 core. The bottom of the groove is formed by α 3 and α 4. This hydrophobic groove represents the binding site for pro-apoptotic BCL-2 family members (Sattler, Liang et al. 1997).

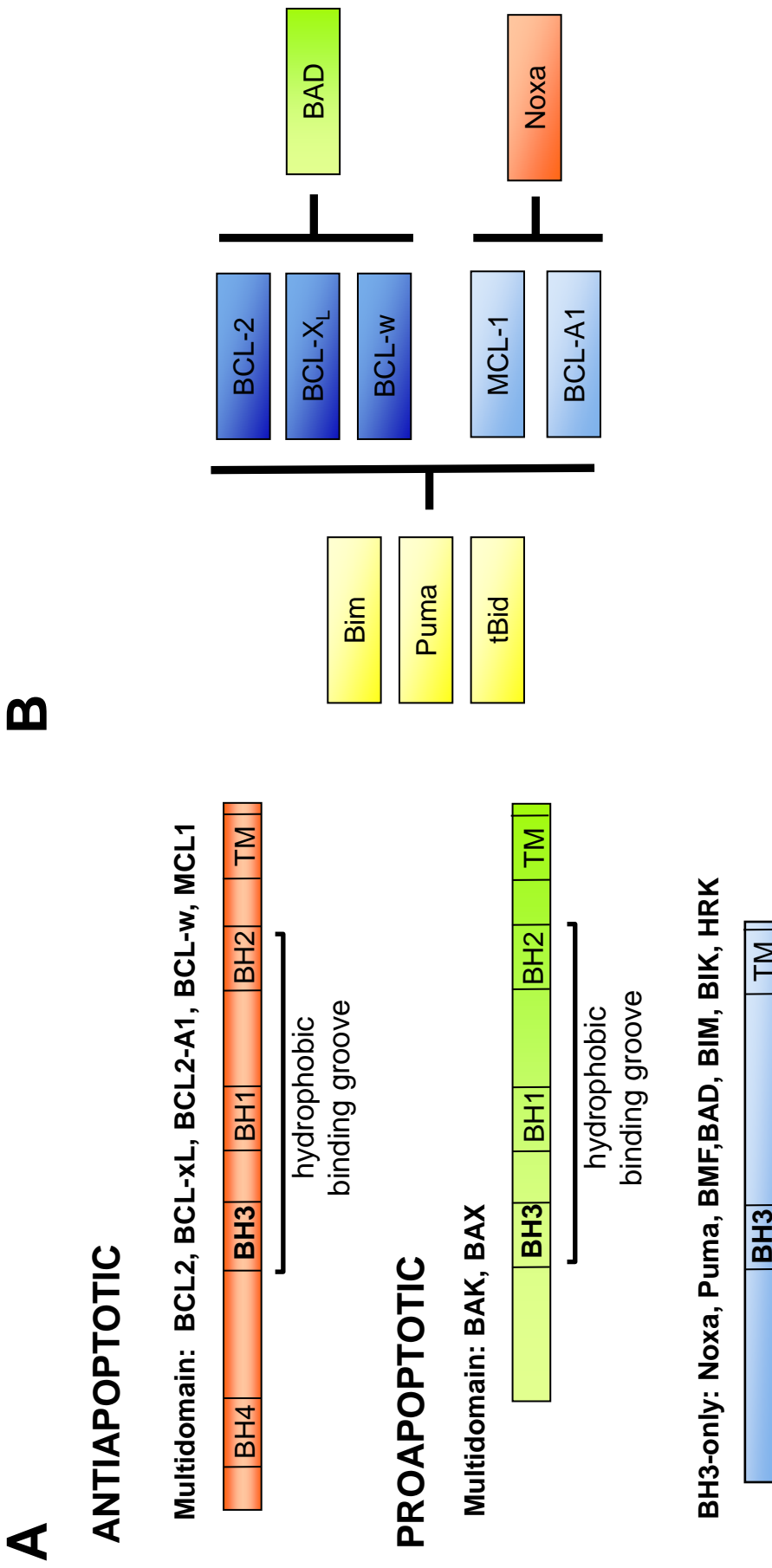


Figure 1.3 Classes of BCL-2 Proteins and their selectivity for each other

(A) Schematic representation of the structural homology of BCL-2 family proteins. Mammalian BCL-2 proteins are categorized into three subclasses based on the presence of *BCL2 homology* (BH) domains: antiapoptotic, proapoptotic multimeric and proapoptotic BH3-only proteins. Most members possess a C-terminal transmembrane domains (TM) which localizes them to the mitochondria / endoplasmatic reticulum. Interactions between family members occur through BH3:groove (BH1-3) interactions. (B) selectivity of BH3-only proteins for specific antiapoptotic BCL-2 proteins. BIM, PUMA and tBID can engage all antiapoptotic BCL-2 proteins, whereby others are more selective.

Differences in the topology and electrostatic character of the hydrophobic binding groove dictate the selectivity for certain BH3 domains of pro-apoptotic proteins.

1.4.2 Pro-apoptotic, multidomain BCL-2 proteins: triggers for death

The multidomain pro-apoptotic family members like BAK and BAX represent the crucial mediators for MOMP and act downstream of the BH3-only proteins and anti-apoptotic proteins (see section 1.3.2). They display sequence homology within BH domains 1-3.

The overall structure of BAX and BAK resembles that of BCL-X_L (Suzuki, Youle et al. 2000), adapting the fold of the BCL-2 core. The transmembrane region which is localized on helix α_9 is occupied in inactive BAX with the hydrophobic binding groove resulting in its cytoplasmic localization. In contrast the BAK helix α_9 is already membrane inserted resulting in its localisation to the mitochondria and endoplasmic reticulum of healthy cells (Wei, Lindsten et al. 2000).

The BH3 domain of BAK was found to be required for heterodimerisation with BCL-X_L (Sattler 1997). The three-dimensional structure of BCL-X_L and the peptide corresponding to the BH3 domain of BAK revealed that the BH3 domain of BAK binds to the hydrophobic groove of BCL-X_L. Four key hydrophobic residues (Val 74, Leu 78, Ile 81, and Ile 85) in BAK point towards the hydrophobic groove of BCL-X_L and are accommodated in four hydrophobic binding pockets along the binding groove of BCL-X_L (Fig. 1.4). The significance of hydrophobic interactions within this association was demonstrated by alanine substitution of Leu 78, which resulted in an 800-fold decrease of binding affinity of the BAK BH3 peptide to BCL-X_L. Interaction is further stabilized by electrostatic interactions, whereby Asp 83 plays an important role by making contact with Arg 139 of BCL-X_L.

Next to the BH3 domain, BAK also displays a hydrophobic binding groove comprising of BH1 and BH2 domains. Mutational analysis revealed that both the BH3 domain as well as the hydrophobic groove are required for BAK pro-apoptotic function (Willis, Chen et al. 2005; Dewson, Kratina et al. 2009). Based on the BH3:groove interface occurring between BAK and BCL-X_L it was proposed that BAK homo-dimerises symmetrically through a reciprocal BH3:groove interaction during activation. This dimer subunit nucleates oligomers leading to pore formation and MOMP (see section 1.7).

The structural similarity of BAX, BCL-X_L and BCL-2 with the membrane inserting, pore-forming domain of diphtheria toxin and bacterial colicins suggests that BAK and BAX may form pores in membranes (Muchmore, Sattler et al. 1996). This would implicate insertion of helices $\alpha 5$ and $\alpha 6$, which are long enough to span a membrane into the mitochondrial outer membrane. In agreement it was shown that BAX inserts the pore domain (helices $\alpha 5$ and $\alpha 6$) into the outer-mitochondrial membrane prior to oligomerisation (Annis, Soucie et al. 2005).

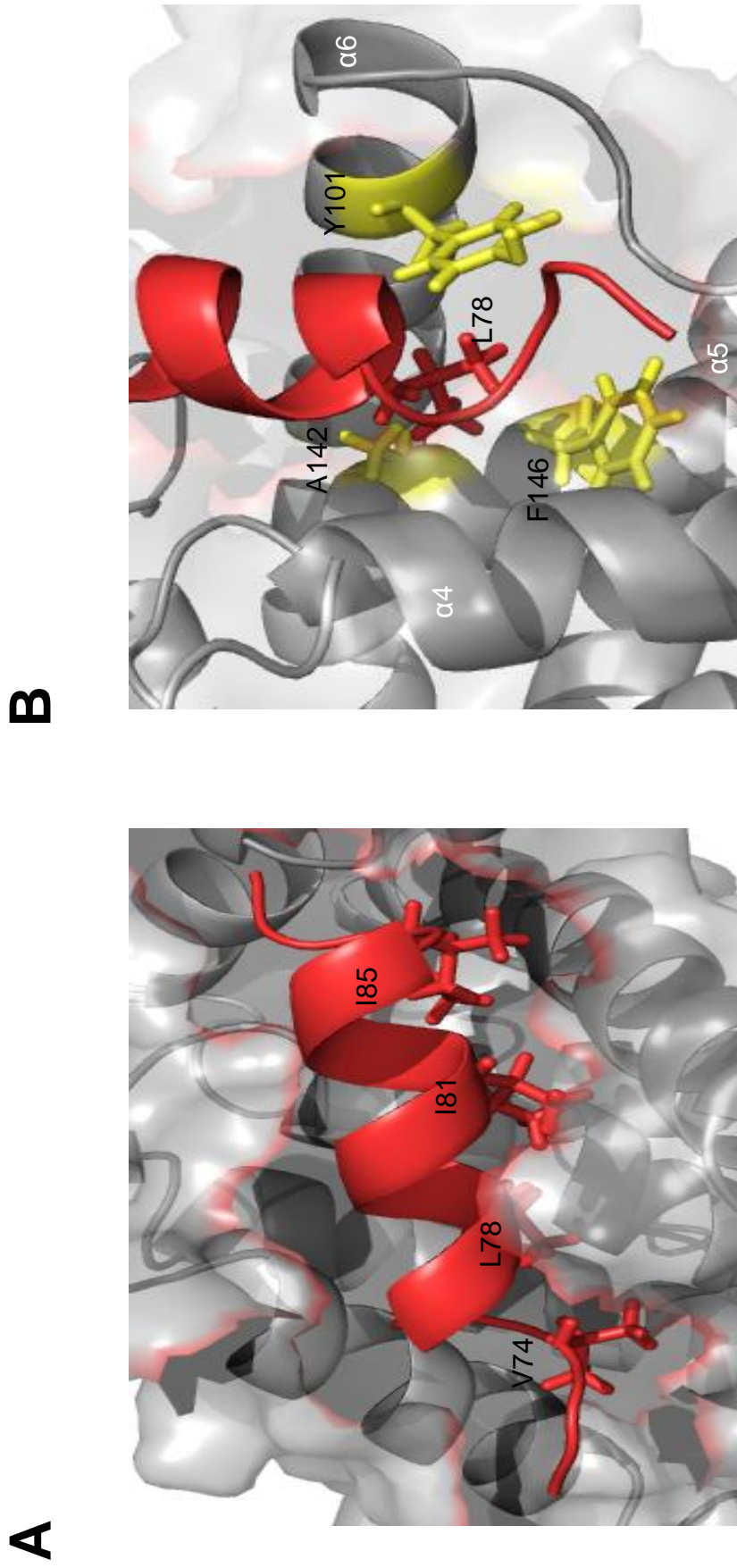


Figure 1.4 BH3:groove interaction

(A) Surface representation of BCL-X_L hydrophobic binding pocket (grey) complexed with BH3 peptide of BAK (red). Side chains of four hydrophobic residues of BAK stabilising association with BCL-X_L are shown. (B) As an example the side chain of BAK L78 (red) inserts into BCL-X_L hydrophobic binding pocket (yellow) build by Y101(helix $\alpha 6$), A 142 and F146 (both helix $\alpha 5$) (Sattler et al, 1997, 1BXL). Figures were produced with PYMOL.

1.4.3 The BH3-only proteins: the cellular damage sensors

Pro-apoptotic BH3-only proteins include at least eight members (Bim, Bid, Bik, Puma, Noxa, Bad, Bmf and Hrk), which share homology in the BH3 domain only and with exception of BID do not adopt the BCL-2 core fold. The BH3-only proteins appear to act as intracellular sensors and monitor stress or damage signals (BIM: Ca flux) as well as cytotoxic signals (BIM: UV radiation). The expression of individual BH3-only proteins may vary according to cell type.

BH3-only proteins are restrained by multiple mechanisms. for example for BIM, NOXA and PUMA are controlled on a transcriptional level. Constitutive expression of other BH3-proteins requires different regulation. For example BIM is controlled by sequestration to microtubule complexes (Puthalakath, Villunger et al. 2001) as well as anti-apoptotic BCL-2 proteins (Harada, Quearry et al. 2004). Post-translational modifications are also described and BIM for example can be phosphorylated, but how this affects its regulation is not understood (reviewed (Ley, Ewings et al. 2005)). BID, in contrast, is regulated by caspase-8 or calpain cleavage which results in production of the active truncated product tBID.

Activated BH3-only proteins can bind through their BH3 domain to the hydrophobic groove of anti-apoptotic family members, where their affinities for anti-apoptotic proteins differ (Chen, Willis et al. 2005; Kuwana, Bouchier-Hayes et al. 2005) (Fig. 1.3 B). BIM, PUMA and tBID can bind all anti-apoptotic proteins, whereas the others can only engage a specific subset. Association with anti-apoptotic BCL-2 proteins may result in the displacement of BAK and BAX leading to their activation and MOMP.

It has also been suggested that the BH3 domain of BIM and tBid in particular can also bind to the hydrophobic groove of BAX inducing its activation. Recently another interface for interaction of BIM with BAX was also described including the back site of BAX (see 1.7). Although the role of BH3-only proteins in apoptosis is not completely understood, it is clear that they act upstream of BAK and BAX as they cannot kill in their absence (Wei, Zhong et al. 2001; Zhong, Lindsten et al. 2001).

1.5 Activation of BAX and BAK: direct vs indirect

The interplay between members of the BCL-2 protein family in order to activate BAK and/or BAX and consequently induce MOMP is not clear. Currently two opposing theories exist to explain how these critical mitochondrial gate keepers are regulated and activated (Leber, Lin et al. 2007).

1.5.1 Direct activation

The critical features of this model are: firstly, BH3-only proteins are classified as sensitizers (derepressors) or activators depending on their multidomain binding partners. Activators can bind both pro- and anti-apoptotic proteins, whereby sensitizers only associate with anti-apoptotic proteins. Secondly, the pro-apoptotic proteins BAK and BAX are activated by direct interaction with activators. To prevent cell death activators are sequestered by anti-apoptotic proteins. During apoptosis activators are displaced from their anti-apoptotic relatives by sensitizer BH3-only proteins, free to activate BAK and/or BAX (Fig. 1.5)(Kuwana, Mackey et al. 2002; Letai, Bassik et al. 2002; Certo, Del Gaizo Moore et al. 2006).

Critical activators are BIM and tBID and a possible activator role has been proposed for PUMA (Cartron, Gallenne et al. 2004; Kim, Tu et al. 2009), however it also has been classed as a sensitizer (Kuwana, Bouchier-Hayes et al. 2005; Certo, Del Gaizo Moore et al. 2006). BH3 peptides derived from BID and BIM induce activation of BAX and MOMP in isolated mitochondria (Letai, Bassik et al. 2002; Cartron, Gallenne et al. 2004; Walensky, Kung et al. 2004; Kuwana, Bouchier-Hayes et al. 2005; Certo, Del Gaizo Moore et al. 2006). Furthermore recombinant tBID can activate recombinant BAX to induce MOMP in isolated mitochondria (Cartron, Gallenne et al. 2004; Kuwana, Bouchier-Hayes et al. 2005).

The mechanism of how these activator proteins activate BAK/BAX depends on the activator per se. In this respect tBID was shown to interact with BAX using *in vitro* translated proteins, which would suggest that this interaction takes place in the cytoplasm (Cartron, Gallenne et al. 2004). However another report suggests that tBID is targeted to the mitochondria, recruiting BAX and inducing its activation (Yethon, Epanand et al. 2003; Lovell, Billen et al. 2008). tBID also induces cytochrome c release from mitochondria by activating and oligomerising BAK (Wei, Lindsten et al. 2000; Ruffolo and Shore 2003).

The role of BIM as a direct activator has not been studied as extensively due to the existence of a number of different isoforms and posttranslational modifications makes it more complex. It has been shown that purified BIM_{EL} can activate recombinant BAX (Terradillos, Montessuit et al. 2002), however interaction with BAX was detected only after the induction of apoptosis (Harada, Quearry et al. 2004). The role of BIM in activation of BAK has not been investigated yet.

The structural basis of the direct interaction model is the classical BH3:groove interaction, whereby the BH3 domain of the direct activator inserts into the hydrophobic binding pocket of BAK and/or BAX. Other interfaces are possible and it has been shown that BIM binds through its BH3 domain to the backside of BAX formed by parts of helix $\alpha 1$ and $\alpha 6$ (Gavathiotis, Suzuki et al. 2008).

1.5.2 Indirect activation displacement model

The critical feature of this model is that pro-apoptotic proteins BAK and BAX are constitutively active. Cell survival therefore requires inhibition of BAK and BAX by their association with anti-apoptotic proteins. During apoptosis BAK and BAX are released by binding of BH3-only proteins to their anti-apoptotic counterparts. Released active BAK and BAX are now free to oligomerise and induce MOMP. This implies that BH3-only proteins can only neutralise anti-apoptotic proteins and do not possess direct activating function (Fig. 1.5) (Willis, Chen et al. 2005; Uren, Dewson et al. 2007; Willis, Fletcher et al. 2007).

In agreement with this model BAK was described to be sequestered by the anti-apoptotic proteins BCL-X_L and MCL-1 in viable cells and this interaction occurs through a BH3:groove interface (Sattler, Liang et al. 1997; Willis, Chen et al. 2005) (see section 1.5). Efficient apoptosis induction requires neutralisation of both anti-apoptotic proteins by BH3-only proteins. Next to BCL-X_L and MCL-1 BCL-2 is also described as possible guardian for constitutively active N-terminal changed BAK (Ruffolo and Shore 2003). An alternative negative regulation of BAK was also proposed to occur through binding to the voltage-dependent anion channel-2 (VDAC2) (Cheng, Sheiko et al. 2003). Recently VDAC2 was found to promote tBID-induced apoptosis by recruiting newly synthesised BAK to the mitochondria (Roy, Ehrlich et al. 2009). Therefore VDAC2 possibly has a role in targeting nascent BAK to the mitochondria and remains associated with BAK after its membrane

insertion. The involvement of specific guardians of BAK and BAX however may vary depending on cell type and neutralisation of all is required to efficiently induce apoptosis.

1.5.3 BAK and BAX: different mechanisms of activation

Both models do not differentiate between BAK and BAX. Both proteins are localized in different cellular compartments and BAX compared to BAK requires an additional activation step including its recruitment to the mitochondria. Therefore both proteins require different mechanisms of activation and are not activated in a redundant parallel fashion. As BAK is constitutively inserted into the membrane interactions with other BCL-2 family members has to occur at the membrane.

The majority of evidence supporting the direct activation model includes BAX, whereby direct interaction with an activator probably induces the C-terminal exposure, its recruitment and insertion into the outer mitochondrial membrane. Therefore it remains difficult to understand how this model accounts for activation of BAK as an already membrane inserted protein. However, BAK immunoprecipitated with tBID in the mitochondrial membrane, whereby tBID is released when BAK/BAX homo-oligomerise as it was not present in BAK aggregates arguing for the transient nature of this interaction (Wei, Lindsten et al. 2000).

In contrast explaining BAX activation by an indirect mechanism remains also difficult as BAX exists as inactive monomer when cells are permeabilised with CHAPS in the cytosol (Hsu and Youle 1997; Antonsson, Montessuit et al. 2001). However evidence exists that BAX can, under certain conditions, associate with BCL-2 (Oltvai, Milliman et al. 1993) and that its BH3 region is required for that association (Zha and Reed 1997). This would argue for a similar regulation also for BAX, whereby constitutive mitochondrial localisation of BAX could be explained by the transformed stage of cells used for these experiments.

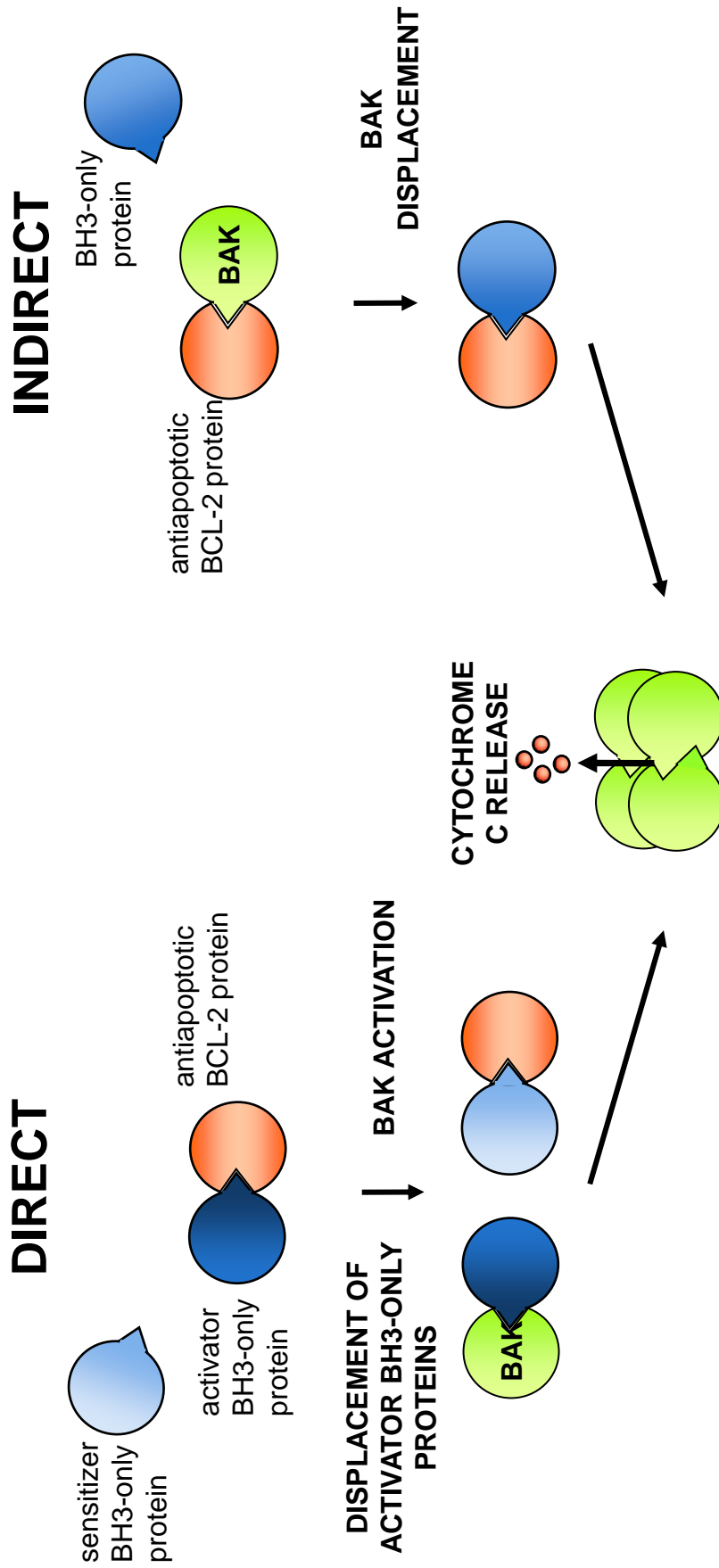


Figure 1.5 Schematic representation of the indirect and direct activation model

Direct activation: to maintain cell survival survival activator BH3 only proteins are sequestered by anti-apoptotic BCL-2 proteins. Stress signals result in displacement of activators by binding of sensitizers to antiapoptotic proteins. Activators then directly activate BAK leading to MOMP. Indirect activation: constitutively active BAK is sequestered by antiapoptotic proteins. During apoptosis BH3 only proteins displace BAK from antiapoptotic proteins leading to its aggregation and subsequently MOMP.

1.6 Conformational changes leading to active BAK and BAX

The transition from inactive monomeric BAK and BAX to pore forming aggregates involves several conformational changes. The common activational steps between BAX and BAK are an N-terminal conformational change and formation of dimers and high molecular weight complexes. BAX as a cytosolic protein further requires additional steps mainly recruitment to the mitochondria and insertion of its transmembrane region into the outer mitochondrial membrane.

1.6.1 Reorganisation of the N-terminal region

A classical feature of BAK and BAX activation is the exposure of the N-terminal region (Griffiths, Dubrez et al. 1999). For BAX it was proposed that this conformational change occurs within the cytoplasm simultaneously with the disengagement of helix $\alpha 9$ and is driven by interaction with activator BH3-only proteins. This open BAX conformation then inserts into the outer mitochondrial membrane. Oligomerisation occurs after further interaction with activator BH3-only proteins (Kim, Tu et al. 2009).

The structure of the N-terminal region in inactive BAK is more complex than in BAX as a long loop including helix $\alpha 2$ overlays and partly restrains helix $\alpha 1$ (Moldoveanu, Liu et al. 2006) (Fig 1.6 A). The first helix contains the epitope for the conformation specific antibody AB-1 as well as a trypsin cleavage site. Both recognition sites are not accessible in inactive BAK (Griffiths, Dubrez et al. 1999; Wei, Lindsten et al. 2000), whereby trypsin cleavage site is faced to the protein core in inactive BAK (Fig 1.6 B). After an apoptotic stimulus the AB-1 epitope and trypsin cleavage sites become accessible (Griffiths, Dubrez et al. 1999; Wei, Lindsten et al. 2000). This would suggest that during activation BAK helix $\alpha 1$ rotates exposing critical residues to the protein surface. To facilitate this the overlaying loop has to swing away first. Therefore N-terminal conformational change, which occurs during apoptosis, represents a reorganisation of the N-terminal region rather than a simple exposure of helix $\alpha 1$ (Kim, Tu et al. 2009).

In terms of the chronology of activation during apoptosis, it was suggested that this N-terminal conformational change occurs before opening of the hydrophobic groove and did not correlate with the observed biochemical changes during apoptosis, suggesting that this change occurs before MOMP (Griffiths, Corfe et al. 2001).

1.6.2 Exposure of the BH3 domain

In BAX the hydrophobic binding groove as well as the BH3 domain is occupied by helix α_9 , which contains the transmembrane region and results in the monomeric soluble character of BAX. By contrast the key hydrophobic residues of the BAK BH3 region (Val 74, Leu 78, Ile 81, and Ile 85) point towards the interior of the protein. Therefore inactive BAK cannot associate with other BCL-2 family members through a BH3:groove interaction. The indirect model proposes that BAK is sequestered by BCL-X_L (see section 1.5.2). This would imply that inactive BAK has to undergo a conformational change to facilitate binding to BCL-X_L, which includes the rotation of helix α_3 (contains the BH3 domain) in order to expose hydrophobic residues to the protein surface. In inactive BAK next to the occluded BH3 domain also the hydrophobic binding groove is sterically hindered by the side chains of R88 and Y89 (Moldoveanu, Liu et al. 2006) (Fig. 1.6 D). Consequently rotation of helix α_3 in order to expose hydrophobic residues of the BH3 domain simultaneously also results in opening of the hydrophobic binding groove. This BAK conformation (exposed BH3 domain and open groove) was referred to as primed BAK (Willis, Fletcher et al. 2007) and is a requirement for the displacement model.

The exposure of the BH3 domain is important for both BAK inhibition by antiapoptotic BCL-2 proteins as well as BAK pro-apoptotic function (Willis, Chen et al. 2005; Dewson, Kratina et al. 2008). Association of BAK into dimers has also been reported to involve the BH3 domain, where the BH3 domain of one BAK molecule inserts into the hydrophobic groove of another and vice-versa (Dewson, Kratina et al. 2008). This association results in formation of a symmetrical homo-dimer with a reciprocal BH3:groove interface. In order to form higher order aggregates these dimer subunits are then linked through another interface including helix α_6 (Dewson, Kratina et al. 2009).

As shown for BAX, full apoptotic activity requires the insertion of helix α_5 and α_6 into the mitochondrial outer membrane (Annis, Soucie et al. 2005). This insertion is promoted by interaction between BAX and tBID. Assuming this occurs in BAK, then only an $\alpha_6:\alpha_6$ associated dimer can interact with a direct activator as membrane insertion of the two central helices would destroy the hydrophobic groove and consequently a BH3:groove associated dimer (Moldoveanu, Liu et al. 2006).

Whether exposure of the BH3 domain occurs simultaneously with the reorganization of the N-terminus or after is not clear yet. The long loop between $\alpha 1$ and $\alpha 3$ could in theory allow both processes to occur independently. However the chronology of these molecular processes remains unclear and it appears that BAK activation is a more complex process than straight forward transformation from inactive to aggregated BAK.

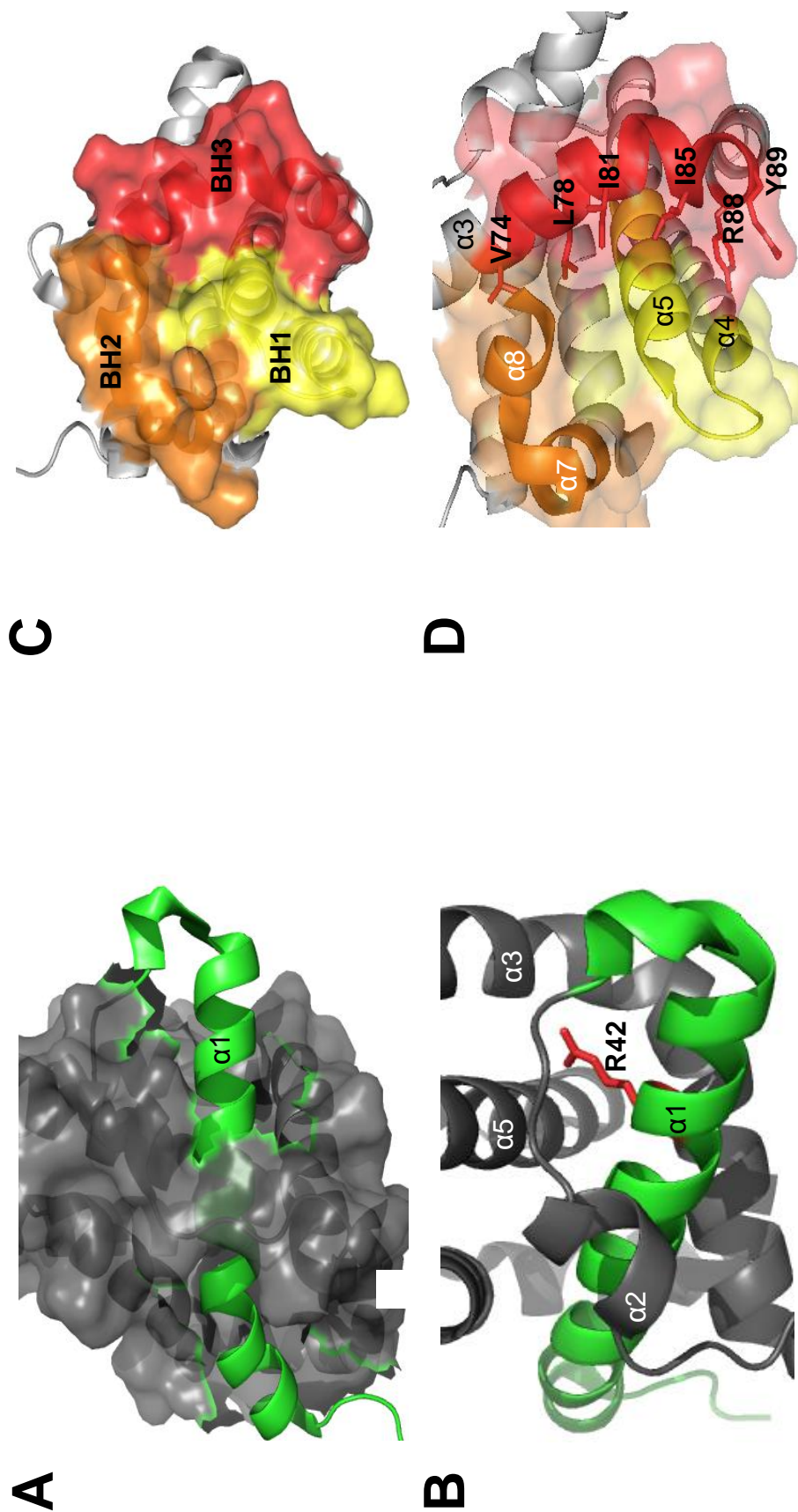


Figure 1.6 Inactive BAK-occluded N-terminus and BH3 domain/groove

(A) Surface diagram of inactive BAK. Helix $\alpha 1$ is shown as cartoon and coloured in green. (B) Ribbon presentation of N-terminal region in inactive BAK, helix $\alpha 1$ coloured green. Side chain of trypsin cleavage site R42 shown in red. Both point to the protein core. (C) Surface representation of inactive BAK. BAK hydrophobic binding groove: the BH1, BH2, and BH3 regions BAK are shown in yellow, orange and red, respectively. (D) Ribbon presentation of hydrophobic groove in inactive BAK colored as (C). Side chains of BH3 domain hydrophobic residues (V47, L78, I84, I85) face protein core and are not available for binding to hydrophobic groove of BCL-2 family members. Side chains of residues R88 and Y89 sterically hinder the hydrophobic groove in BAK (Moldoveanu et al. 2006, 2IMS). Figures were produced with PYMOL.

1.7 BH3 mimetics in cancer therapy

Dysregulation of apoptosis can disrupt the delicate balance between cell proliferation and cell death and represents a critical step towards tumour development as cells are unable to respond to cellular stress and harmful mutations caused by DNA damage. High levels of anti-apoptotic BCL-2 proteins are present to maintain survival and are associated with tumor development and resistance to chemotherapy (Sentman, Shutter et al. 1991; Miyashita and Reed 1993; Hanahan and Weinberg 2000; Adams and Cory 2007).

As the core mitochondrial machinery stays intact, cancer drugs which restore the normal apoptotic pathway are being developed. Anti-apoptotic BCL2 proteins represent an attractive target for treatment of cancer (Fesik 2005), where apoptosis can be promoted by inhibition of anti-apoptotic BCL-2 proteins. This strategy provides an advantage to generate more effective antitumor agents by directly targeting BCL-2 proteins rather than drugs that act further upstream in the apoptotic pathway. It also ensures more selective killing as tumor cells unlike normal cells are highly dependent on aberrations of the apoptotic signaling pathway (e.g. overexpression antiapoptotic BCL-2 proteins) to stay alive.

BCL-2 is overexpressed in 80% of B-cell lymphomas, 30–60% of prostate cancers, 90% of colorectal adenocarcinomas, and a wide variety of other cancers. BCL-X_L is overexpressed in a number of breast and lung cancers. Inhibition of BCL-2 is mediated by the design of agents which mimic the activity of the pro-apoptotic BH3-only proteins. The structure of anti-apoptotic proteins is similar in that they share a hydrophobic groove on their surface which represents the binding site for pro-apoptotic BCL-2 family members (Youle and Strasser 2008). Small molecule inhibitors have been designed to interact with the hydrophobic groove of BCL-2 family proteins to overcome the BCL-2 block in tumor cells.

Using structure based design and high throughput screens several compounds were identified which bind BCL2 proteins in the low micromolar range (Table 1.1) (Zhai, Jin et al. 2006) like the pan-BCL-2 inhibitors chelerythrine (Shing-Leng Chan 2003) and GX15-070 (obatoclax - Gemin X) (Nguyen, Marcellus et al. 2007).

Another pan - BCL-2 inhibitor is gossypol is found in the seed, stem, and root of the cotton plant and is the first compound that demonstrated inhibition of BCL-2, BCL-X_L, and MCL-1 (Kitada, Leone et al. 2003). A gossypol analog, apogossypol (Burnham Institute) targets more

specific BCL-2 and MCL-1 and may decrease the systemic toxicity observed with gossypol (Fig.1.7).

An exception to other BH3 mimetic is ABT-737 which binds to the anti-apoptotic proteins BCL2, BCL-X_L and BCL-w with subnanomolar affinity ($K_i \leq 1\text{nM}$). It was designed by NMR guided, structure based drug design (SAR by NMR: structure-activity relationships by nuclear magnetic resonance) and occupies the same binding site as the BH3-only protein BAD (Oltersdorf, Elmore et al. 2005). ABT-737 showed synergistic cytotoxicity with chemotherapeutic agents or radiation in various cell lines and demonstrated single-agent mechanism-based killing in lymphoma and leukaemia cell lines and primary patient-derived cells (Oltersdorf, Elmore et al. 2005; Certo, Del Gaizo Moore et al. 2006; Konopleva, Contractor et al. 2006).

Next to the pharmacological importance of BCL-2 inhibitors they also provide a potential tool to investigate the induction of the intrinsic mitochondrial apoptotic pathway by directly triggering it at the mitochondria irrespective of any upstream regulation mechanisms.

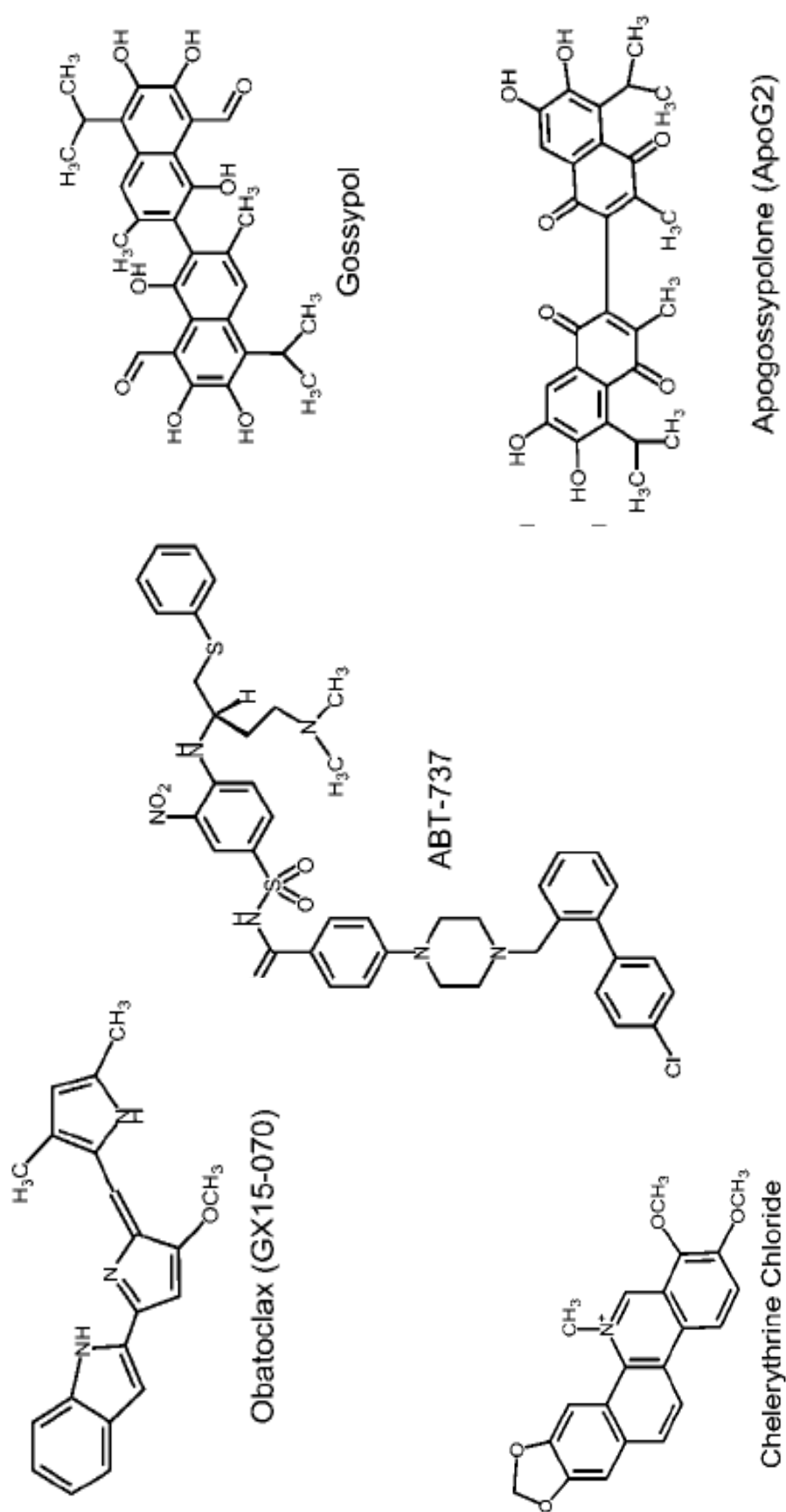


Figure 1.7 Structures of some BCL-2 inhibitors

	K_i (nM)				
	BCL-2	BCL-XL	MCL-1	BCL-W	BCL-B
ABT-737	120	64	> 20 000	24	> 20 000
Gossypol	280	3 030	1 750	1400	> 10 000
Apogossypol	640	2 800	3 350	2100	> 10 000
Obatoclox	1 110	4 690	2 900	7 010	5 000
Chelerythrine	~10 000	~ 10 000	> 10 000	~ 10 000	> 10 000

Table 1.1 Binding affinities (K_i) of different BH3 mimetics for specific antiapoptotic BCL-2 proteins
Adapted from Zhai et al. 2006

1.8 Aims and objectives:

Mitochondrial outer membrane permeabilisation which results in the release of cytochrome *c* from the mitochondrial intermembrane space represents the point of no return during apoptosis. Although BAK plays a crucial role in outer mitochondrial membrane permeabilisation its activation and regulation are still unclear.

The aim of this thesis is to further investigate the activation steps involved in the transition from inactive, monomeric BAK into pore forming oligomers able to permeabilise the mitochondria. The classical characteristics of active BAK are N-terminal conformational change and the formation of dimers and high molecular weight complexes. Increasing evidence suggests that activation of BAK is not a straight forward transition from an inactive state but includes several intermediate conformations. Thus exposure of the BH3 domain of BAK was described to be a characteristic of active BAK. However the relevance and chronology of these events in the commitment of cell death is still unclear.

Members of the BCL-2 protein family are described to regulate the activation of BAK, but their role remains controversial. Antiapoptotic BCL-2 proteins negatively regulate either constitutively active BAK in order to prevent its further activation (indirect model) or activator BH3-only proteins in order to prevent activation of inactive BAK (direct model).

The identification of discrete steps leading to the formation of a BAK pore, their chronology and regulation is essential as every step represents a potential target for therapeutic intervention to either accelerate or inhibit apoptosis.

CHAPTER 2:
Materials and Methods

2.1 Materials

All general laboratory chemicals were supplied by Sigma (Poole, U.K.) and Fisher (Loughborough, UK) and were of analytical grade unless otherwise stated. The poly-caspase inhibitor, Benzyloxycarbonyl-Val-Ala-Asp (Ome) fluoromethylketone (z-VAD.fmk) was from Enzyme Systems (Dublin, CA, U.S.A.). Trypsin was obtained from Calbiochem/Merck Nottingham, UK and Trypsin inhibitor PMSF from Roche, Burgess Hill UK. Fluorescein isothiocyanate (FITC)-conjugated Annexin V was generated by Dr XM Sun, MRC Toxicology Unit, Leicester, UK.

2.2 Cell Biology Techniques

2.2.1 Cell Culture

Medium, Foetal Calf Serum (FCS) and other cell culture-related chemicals were purchased from Invitrogen (Paisley, U.K.). Cell culture plastic ware was from Becton Dickinson (CA, U.S.A.). Jurkat E6.1, Human Embryonic Kidney Fibroblasts (HEK293T) cell lines were obtained from the European Collection of Animal Cell Cultures (ECACC; Porton Down, UK). Mouse embryonic fibroblasts deficient in BAK and BAX were obtained by Drs. A. Strasser and D. Huang (The Walter and Eliza Hall, Institute of Medical Research, Melbourne, Australia). Jurkat JMR cells deficient in caspase-9 and caspase-9 reconstituted were obtained from Dr Schulze-Osthoff, Heidelberg Germany.

Suspension cells were cultured in Roswell Park Memorial Institute (RPMI) medium containing 10 % FCS and 5 % GlutamaxTM (Life Technologies Inc.). Cells were kept at a density of between 0.8 and 1.0×10⁶ cells per ml by routine passage every 3 days. Cells were counted using a CASY 1 cell counter (Scharfe Systems; Reutlingen, Germany), and cell viability was determined before experiments using Annexin V and propidium iodide staining.

Adherent cells were passaged at around 80 % confluency (approximately every 3 days). Cells were washed once with prewarmed Phosphate Buffered Saline (PBS) then incubated at 37 °C for 5 min with trypsin (0.05 %) and EDTA (0.02%) in PBS. Cells were then washed with medium to inactivate the trypsin, collected by centrifugation then resuspended in fresh medium and used to seed further flasks or 6-well culture dishes as required.

All cells were maintained at 37 °C in a humidified 5 % CO₂ incubator. For transfection experiments medium was supplemented with penicillin (100 U/ml) and streptomycin (100 µg/ml) to avoid bacterial growth.

2.2.2 Annexin V and Propidium Iodide Staining

Apoptotic cells were quantified assessed by FITC-labelled Annexin V and propidium iodide (PI) staining (Martin, Reutelingsperger et al. 1995). Annexin V binds to phosphatidylserine, a phospholipid that translocates during apoptosis from the inner to the outer leaflet of the plasma membrane in caspase-dependent process. Conjugation of Annexin V with FITC allows the analysis of apoptotic cells by FACS analysis.

Annexin V was used in combination with the vital dye PI, which is excluded by cells with intact membranes (viable and early apoptotic cells). Therefore this double staining allows the separation of viable cells (AnnexinV and PI negative), early apoptotic cells (AnnexinV positive, PI negative) and late apoptotic or necrotic cells (AnnexinV positive, PI positive).

For non-adherent cells Annexin buffer (10 mM HEPES/NaOH (pH 7.4), 150 mM NaCl, 5 mM KCl, 1 mM MgCl₂, 1.8 mM CaCl₂) supplemented with Annexin V-FITC was added to the cells and incubated for 10 min at RT. Before cell analysis PI (10 µl, 2 µg/ml in PBS) was added to the cells. For adherent cells, floating and trypsinised adherent cells were washed and resuspended in prewarmed DMEM media followed by recovery at 37 °C for 15 min and same staining procedure carried out as for suspension cells. Cells were analysed on a FACS Calibur™ flow cytometer (Becton Dickinson (BD), Oxford, UK) with an excitation/emission wavelength of 488/525 (FITC) and 488/585 (PI) using CellQuest Pro® software (Becton-Dickinson).

2.2.3 Measurement of the Ψ_m

Reduction of Ψ_m was determined by TMRE (Molecular Probes). TMRE is a fluorescent cationic dye that localizes according to the electrochemical gradient across the mitochondrial membrane in on the inner leaflet of the mitochondrial inner membrane in viable cells. During apoptosis the mitochondrial membrane potential collapses resulting in the release of TMRE from the mitochondria into the cytoplasm accompanied by reduced fluorescence. Therefore the percentage of cells with reduced TMRE fluorescence represents cells with a reduced $\Delta\Psi_m$ compared to viable cells.

Suspension cells were incubated at 37 °C for 10 min with 50 nM TMRE (diluted in media). For adherent cells floating and trypsinized adherent cell were resuspended in fresh medium and incubated at 37 °C for 15 min to recover prior to staining. Cells were analysed on a FacsCalibur™ flow cytometer (Becton Dickenson (BD), Oxford, UK) with an excitation/emission wavelength of 488/585 (PI) using CellQuest Pro® software (Becton-Dickinson).

2.2.4 Subcellular fractionation

HM fractions were generated by resuspending 6×10^6 Jurkat cells, HEK293T 0.6×10^6 cells in 200µl mitochondrial isolation buffer (250 mM sucrose, 20 mM Hepes, pH 7.4, 5 mM MgCl₂ and 10 mM KCl) containing 0.01% digitonin). Cells were left on ice for 10 min (Jurkat), 2 min (HEK293T) followed by centrifugation at 13000 rpm for 3 min. Supernatant (cytosolic fraction) and pellets (HM fraction) were analyzed by Western blotting. For preparation of mitochondria enriched fraction $10\text{-}50 \times 10^6$ cells were resuspended in RSB buffer (10mM NaCl, 1.5mM MgCl₂, 10mM Tris-HCl) and left for 10 min on ice. Hypotonic swelling was stopped by addition of MS-Buffer (525mM mannitol, 175mM sucrose, 12.5mM Tris-HCl pH 7.5, 2.5mM EDTA) and cells ruptured by dounce homogenization. After clearing lysates at 2700 rpm for 10 min, mitochondria were pelleted at 13 000 rpm for 15 min and washed in X-link Buffer (100mM sucrose, 20mM HEPES-KOH PH 7.4, 2.5mM MgCl, 50mM KCl)

2.3 Biochemical Techniques

2.3.1 Preparation of Samples for SDS-PAGE

For Western blot analysis appropriate volume of Laemmli sample buffer was added to samples. To enhance solubilisation of CuPhe exposed samples they were also sonicated using an MSE sonicator (5 sec/on, 2 sec off for 5 cycles). Samples were then boiled for 5 min. Once in sample buffer, samples were stored at -80 °C until required.

Laemmli Sample Buffer

(60 mM Tris/HCl (pH 6.8) 2 % (w/v) sodium dodecyl sulphate (SDS), 15 % (v/v) glycerol, 0.05 % (w/v) Bromophenol Blue, 5 % (v/v) β -2-mercaptoethanol (optional)

Resolving Gel Buffer

(1.5 M Tris/HCl (pH 8.8), 0.4% (w/v) SDS)

Stacking Gel Buffer

(0.5 M Tris/HCl (pH 6.8), 0.4 % (w/v) SDS)

	Resolving Gel		Stacking Gel
	<i>13%</i>	<i>10%</i>	<i>4%</i>
Gel Buffer	6.25 ml	6.25 ml	5 ml
30% w/v Acrylamide/ Bisacrylamide mix	10.83 ml	8.33 ml	2.7 ml
Water	7.76 ml	10.26 ml	12.3 ml
10% Ammonium Persulphate	150µl	150µl	150µl
TEMED ¹	20µl	20µl	20µl

¹TEMED: N,N,N',N'-tetramethylethylenediamine

Table 2.1 Recipes for Resolving and Stacking polyacrylamide gels.

The Mini-Protean II gel system (Bio-Rad) was used for gel electrophoresis, and set up according to the manufacturer's instructions. Resolving and stacking gel solutions were made up as indicated in Table 2.1. The gel percentage used depended on the mass of the protein of interest.

2.3.2 Immunostaining of proteins on Nitrocellulose Membranes (Western blotting)

After electrophoresis proteins were transferred to Nitrocellulose membranes: Hybond C (Amersham Pharmacia Biotech) essentially as described (Towbin, Staehelin et al. 1992). After transfer membranes were washed briefly with TBST (20 mM Tris/HCL (pH 7.6), 150 mM NaCl containing 0.1 % Tween-20) then "blocked" for 1 h with TBSMT (TBST

containing 5 % MarvelTM). After a brief wash with TBST, the membranes were incubated with the relevant primary antibody (Table. 2.2) for 1 h followed by a secondary antibody conjugated to horseradish peroxidase (HRP) for 1 h. Membranes were washed with TBSMT then TBST after incubations. Blots were then developed using the enhanced chemiluminescence system (ECL, Amersham) and proteins visualised on X-ray film (Kodak; NY, U.S.A.).

2.3.3 Measurement of Protein Concentration

The Bio-Rad protein assay kit (Bio-Rad), is based on the Bradford method for determination of protein content (Bradford 1976), was used according to the manufacturer's instructions. A standard curve was constructed using known concentrations of a bovine serum albumin (BSA) standard and the $A_{595\text{nm}}$ was measured for each sample and standard in triplicate. Unknown protein concentrations were then calculated from the plotted BSA standard curve.

2.3.4 Antibodies

Antibody	Species	Dilution	Source
BAK NT	rabbit (p)	1/1000	Millipore (Billerica, MA)
BAK AB-1	rabbit (p)	1/1000	Calbiochem, Nottingham, UK
BAK GLY82	rabbit (p)	1/1000	Cell signalling
BCL-X _L	rabbit (p)	1/1000	BD Bioscience
BCL-2	mouse (mAb)	1/1000	Dako (Cambridge, UK)
BIM	rabbit (p)	1/1000	ENZO
Cytochrome <i>c</i>	mouse (Mab)	1/1000	BD Pharmingen (NJ, USA)
Caspase-3	mouse (mAb)	1/500	BD Pharmingen (NJ, USA)
Caspase-9	rabbit (p)	1/2000	Dr. X. Sun (Sun, Bratton et al. 2002)
MCL-1	rabbit (r)	1/500	Santa Cruz Biotechnology (California, USA)
PARP (C-2-10)	mouse (mAb)	1/10,000	Dr. G. Poirier (Laval University, Quebec, Canada)
HSP60	mouse (mAb)	1/500	BD Pharmingen (NJ, USA)
Strep tag	mouse (mAb)	1/1000	Qiagen, (Surrey, U.K)
Flag tag M2	mouse (mAb)	1/1000	Sigma Aldrich (Derset, UK)
Tubulin	mouse (mAb)	1/500	BD Pharmingen (NJ, USA)

mAb - Monoclonal Antibody

p - Polyclonal Antibody

Table 2.2 Sources of Antibodies used in studies.

2.4 Molecular Biology Protocols

2.4.1 Plasmids

pcDNA3.1, 4, 6 and 6-TetR were obtained from Invitrogen (Paisley, UK). Step-tagged BAK, strep-flag double tagged BCL-X_L, untagged BIM_{EL}, myc-tagged MCL-1 and atrep-tagged BCL-2 plasmids were obtained from Dr Nicholas Harper, MRC Toxicology Unit, Leicester UK.

2.4.2 Bacterial Strains and Culture Conditions.

Escherichia Coli strain DH5- α was obtained from Invitrogen and were routinely grown and maintained on Luria agar containing the required antibiotic. For liquid cultures Luria-Bertani (LB) medium (10 g bacto-tryptone, 5 g bacto yeast extract, 10 g NaCl in 1L sterile water) Anachem (Beds, UK) was used and bacteria were grown at 37 °C with shaking.

2.4.3 Transformation of *E.Coli*

DH5 α subcloning efficiency cells (1×10^8 transformants/ μ g DNA) were used for routine transformations. All procedures were carried out under aseptic conditions. DNA (200-500 ng) was added to cells which were then incubated on ice for 30 min prior to heat shock (42 °C, 45 sec). After being allowed to recover on ice for 2 min, 1 ml of SOC medium (Invitrogen) was added and cells grown for 1 h at 37 °C. Cells were then plated onto the appropriate selective medium and grown overnight at 37 °C.

2.4.4 Preparation of Plasmid DNA

Plasmid DNA was prepared using kits supplied by Qiagen Ltd. (Surrey, U.K). Kits used depended on the quantity or quality of DNA required. Mini-preps and maxi-prep kits were carried out according to manufactures protocol. Briefly bacteria were alkaline lysed to denature plasmid DNA, chromosomal DNA as well as cellular protein. Chromosomal DNA and proteins are then “salted out” and removed by centrifugation. Plasmid DNA is then collected from the lysate on a membrane and eluted.

2.4.5 Quantification of DNA

DNA was quantified by first diluting in Milli-Q water then measuring $A_{260\text{nm}}$ using a DNA/RNA calculator (Amersham/PharmaciaBiotech). Double-stranded DNA (dsDNA) concentration was then calculated using the formula:

$$\text{dsDNA concentration } (\mu\text{g/ml}) = (A_{260} \times 100 \text{ (dilution)} \times 50)/1000$$

Purity of isolated DNA could be assessed using the $A_{260\text{nm}}/A_{280\text{nm}}$ ratio. Plasmid DNA has an $A_{260\text{nm}}/A_{280\text{nm}}$ ratio of 1.8.

2.4.6 DNA Electrophoresis on Agarose Gels

Purified and digested plasmid DNA was analysed using agarose gel electrophoresis essentially as described (Sambrook J, 2002). Briefly, agarose (0.5-2% w/v) was dissolved by heating in TAE buffer (40 mM Tris:Acetate (pH 8.5), 2 mM EDTA) and after cooling to ~50 °C ethidium bromide 0.5 $\mu\text{g/ml}$ was added and the gel poured. DNA samples were prepared with 10 \times Orange G loading buffer (0.5% (w/v) Orange G, 25% (w/v) Ficoll-400, 20 mM EDTA) in Milli-Q water and applied directly to wells in the gel. Gels were electrophoresed in TAE buffer at 100 V for 30-60 min.

2.4.7 Mutagenesis

Point mutations were introduced by using Quikchange multi site mutagenesis kit (Agilent Technologies, Berkshire UK) and performed according to manufactures protocol. Primers used for mutagenesis studies are listed in Appendix 1. All constructs were sequenced verified prior to use (PNAACL, Leicester University, Leicester UK).

2.5 Reconstitution of BCL-X_L:BAK complexes

MEF BAK/BAX DKO (transfection reagent Trans LTI (Mirrus Bio, Madison, WI USA) according to manufacturers protocol) or HEK293T cells (transfection reagent: JetPEI, (Polyplus, Illkirch, France) according to manufactures protocol) BAK (pCDNA4) and TETR at a ratio 1:10 and cotransfected with BCL-X_L (1:1 BAK:BCL-X_L). 24 h post transfection BAK expression was induced by 4 $\mu\text{g/ml}$ tetracycline (Calbiochem, Nottingham, UK) for 4 h, followed by exposure to ABT-737 (5 μM for 3 h HEK293T, 3 or 30 μM for 4 h DKO MEF). For reconstitution of BIM BCL-X_L/BCL-2 complexes ratios and procedure were kept constant.

2.6 siRNA transfections

Jurkat cells were transfected using by electroporation using TransfNucleofection system (Amaxa, Köln, Germany), following the manufacturer's instructions. The final concentration of siRNA was 75 nM. Transfected cells were cultured in RPMI supplemented with 20 % FCS and 5 % Glutamax for 48 h (BAK) or 72 h (BIM). Knockdown efficiency was determined by western blotting. For BAK / BIM knockdown, siRNAs were obtained as duplexes in purified and desalted form. For the sense strand of used BAK siRNA see table 2.3. A nonspecific control pool containing four pooled nonspecific siRNA duplexes was used as a negative control.

BAK	Fisher	1		CGACAUCAACCGACGCUAUtt
-pool				
		2		UAUGAGUACUUCACCAAGAtt
		3		GACGGCAGCUCGCCAUCAUtt
		4		AAUCAUGACUCCCAAGGGUtt
BAK	Ambion		sense	GCUUUAGCAAGUGUGCACUtt

Table 2.3 Sense strands of used BAK siRNAs

2.7 Analysis of BAK activation

2.7.1 Intracellular AB-1 staining

To analyse AB-1 exposure Jurkat or HEK293T cells were fixed with 2% paraformaldehyde at room temperature for 10 min, washed with PBS and resuspended in permeabilization buffer (0.1% saponin and 0.5% BSA in PBS) containing 1:100 mouse anti-BAK Ab-1 (Calbiochem, Nottingham, UK) and incubated for 1 h at 4°C on a daisy wheel. Cells were then washed and resuspended in permeabilization buffer diluted into 1:100 goat anti-mouse IgG-Alexa Fluor 488 (Molecular Probes) and incubated for 1 h at 4°C on a daisy wheel. After washing in PBS cells were analyzed with a FACSCalibur (Becton Dickinson).

2.7.2 Immunohistochemistry

To analyse AB-1 exposure and cytochrome *c* release by immunohistochemistry cells were incubated during the last 20 min of exposure to ABT-737 with 10 nM of mitotracker CMX Ros (Invitrogen). Mitotracker CMX Ros passively diffuses through the plasma membrane and

accumulates in mitochondria, where it binds to thiol groups of proteins. This converts it to the corresponding fluorescent mitochondrion-selective probe, which is retained in the mitochondria even after loss of the mitochondrial membrane potential.

Cells were washed and resuspended in PBS and applied to poly-D-lysine coated slides. After incubation for 5 min at room temperature to facilitate immobilization, cells were fixed with paraformaldehyde (2 %) and subsequently incubated with AB-1 or cytochrome *c* (BD, Oxford, UK) antibodies (1:100, diluted in permeabilisation buffer) for 1 h. Cells were washed with permeabilization buffer and incubated with fluorescence labeled secondary antibody (single AB-1 and single cytochrome *c* staining: ALEXA 488- conjugated secondary antibody, double AB-1- cytochrome *c*: mouse IgG2a -ALEXA 488 (AB-1) and 1 IgG1-ALEXA 548 (cytochrome *c*)) (1:100, diluted in permeabilization buffer) followed by 10mg/ml HOECST33324 (Molecular Probes) staining for 10 min. After a final wash in PBS cells were overlaid with VECTASHIELD[®] mounting media (Vector Laboratories, Burlingame, CA, USA), coverslips applied and fixed with nailpolish. Cells were analyzed under a fluorescence confocal microscope (Carl Zeiss Ltd, Welwyn Garden City UK) equipped with an epilluminator and appropriate filters.

2.7.3 Limited Trypsin proteolysis

For limited trypsin proteolysis mitochondria enriched fractions were resuspended in X-Link Buffer and 125µg Trypsin/50µg protein was added and incubated for 20 min on ice trypsin was inhibited by addition of 4 mM Pefabloc SC (AEBSF) (Roche Diagnostics, Basel, Switzerland). Mitochondria enriched fractions were recovered by spinning at 13000 rpm for 15 min Pellets were resuspended in 1x SDS loading dye and subjected to Western blotting (anti-BAK GLY 82, Cell signaling, Hitchin, Herts UK)

2.7.4 Copper(II)(1,10-phenanthroline)₃ (CuPhe)

For formation of BAK high molecular weight complexes mitochondria enriched fractions were exposed to CuPhe (CuPhe was prepared as followed (20 mM 1,10 Phenanthroline (dissolved in 20 % EtOH) and 300 mM CuSO₄ were combined to give a 10mM stock (refers to PHE conc.). 50 µg protein were solved in 200µ X-link Buffer and CuPhe added to final conc of 1 mM. Reaction was quenched by incubation with 100mM EDTA for 15 min on ice. Mitochondria enriched fractions were recovered by spinning at 13 000 rpm for 15 min. Pellets were resuspended in 1 x SDS loading dye without β-ME and analysed by Western blotting under non-denaturing conditions.

2.7.5 Sucrose density centrifugation

Sucrose density gradient allow the separation of proteins and protein complexes to fractions where the buoyancy created by the sucrose is equivalent to their molecular weight. Large proteins/protein complexes migrate to the higher percentage sucrose solution. Mitochondria enriched fractions were lysed in 2 % CHAPS and precleared lysates were layered over a continuous 10-45 % sucrose gradient in a buffering solution (20 mM Tris-HCl pH 7.4, 135 mM NaCl, 1.5 mM MgCl₂, 1 mM EGTA) and centrifuged for 16 h at 35 0000 rpm in a SW60 rotor (Beckmann). 24 200 µl fractions were collected and sucrose content of each fraction was determined with a refractometer and calibrated using Gel Filtration Calibration Kit HMW (Ovalbumin, 40kDa; Ferritin 440 kDa; Aldolase 158 kDa; Thyroglobulin 669 kDa, GE Healthcare, Uppsala, Sweden). Collected fractions were either analysed by Western blotting or pooled and subjected to immunoprecipitations, whereby sucrose content of fraction pools had to be adjusted to 10 % sucrose to minimize unspecific binding to beads.

2.7.6 Immunoprecipitation

For immunoprecipitation Jurkat or MEF cells were lysed in Lysis Buffer (20 mM Tris-HCl pH 7.4, 135 mM NaCl, 1.5 mM MgCl₂, 1 mM EGTA, 10% glycerol) containing 1 % CHAPS or 1 % Triton X-100 and supplemented with protease inhibitor cocktail (Roche Diagnostics, Basel, Switzerland) and incubated on ice for 20 min. Lysates were precleared by centrifugation at 13000 rpm for 15 min. Rabbit anti-BAK Ab (Upstate Biotechnology), mouse anti-BAK AB-1 antibody (Calbiochem, Nottingham, UK), rabbit anti-BCL-X_L antibody (BD Biosciences), hamster anti-BCL-2 antibody (BD Bioscience), rabbit anti-BIM antibody (Cell signaling Technologies) or rabbit anti-MCL-1 antibody (Epitomics, Burlingame, CA) were crosslinked to Protein A-dynabeads using 20 mM dimethylpimelinediimide (Fluka Biochemika, Switzerland). Immunoprecipitations against strep- or flag-tag were carried out using strepavidin coated agarose beads (IBA, Goettingen, Germany) or anti-flag M2 crosslinked agarose beads (Sigma Aldrich, Derset, UK).

Crosslinked antibodies were incubated with 500-1000 µg protein for 12 hours at 4°C. Beads were washed with lysis buffer (0.1 % CHAPS) supplemented with Tween (0.25 %) before elution in sodium dodecyl sulfate (SDS) loading dye and Western blotting.

CHAPTER 3:

Specificity of BH3 mimetics:

ABT-737 as a tool to analyse the activation of BAK

3.1 Introduction

The anti-apoptotic BCL-2 proteins promote cell survival and their overexpression results in impaired apoptosis and is associated with tumor development and resistance to chemotherapy (Sentman, Shutter et al. 1991; Miyashita and Reed 1993; Hanahan and Weinberg 2000; Adams and Cory 2007). Promoting apoptosis by inhibition of BCL2 proteins is therefore a promising strategy for cancer drug development.

The structure of anti-apoptotic proteins is similar in that they share a hydrophobic groove on their surface which forms the binding site for pro-apoptotic BCL-2 family members (Youle and Strasser 2008). To mimic the specificity of pro-apoptotic proteins small molecule inhibitors have been designed to interact with the hydrophobic groove of BCL-2 family proteins to overcome the BCL-2 block in tumor cells. To date several compounds (e.g. Chelerythrine, Gossypol, (Vogler, Dinsdale et al. 2009)) have been developed by structure-based design and discovered through high throughput screening that bind BCL-2 proteins in a low micromolar range (Zhai, Jin et al. 2006).

A more potent BCL-2 inhibitor is ABT-737 which binds to anti-apoptotic proteins with subnanomolar affinity ($K_i \leq 1\text{nM}$) was designed by NMR guided, structure based drug design (SAR by NMR: structure-activity relationships by nuclear magnetic resonance) (Oltersdorf, Elmore et al. 2005). ABT-737 occupies the same binding site as the BH3-only protein BAD and therefore antagonises the anti-apoptotic function of BCL-2, BCL-X_L and BCL-w (Oltersdorf, Elmore et al. 2005). Its ability to induce apoptosis in selected human tumor cell lines, mouse xenograph model and patient-derived primary tumour cells (Oltersdorf, Elmore et al. 2005; Certo, Del Gaizo Moore et al. 2006) demonstrate its potential as innovative anticancer therapeutic.

The central point of the intrinsic apoptotic pathway is the mitochondria and the pro-apoptotic BCL-2 proteins BAX and BAK act as mitochondrial “gate keepers”. Following an apoptotic signal BAK/BAX become activated promoting permeabilisation of the mitochondrial outer membrane (MOMP) resulting in the release of apoptogenic factors into the cytoplasm. Among these is cytochrome *c* which induces the formation of the apoptosome (Green and Kroemer 2004) providing the platform for activation of the initiator caspase, caspase-9. Active caspase-9 then activates downstream executioner caspases orchestrating the direct degradation of a variety of target proteins (Danial and Korsmeyer 2004).

BCL-2 inhibitors also provide a potential tool to investigate the induction of the intrinsic mitochondrial apoptotic pathway by directly triggering it at the mitochondria independently of any upstream regulating mechanisms.

Experiments in this chapter are aimed at examining the specificity of a number of BH3 mimetics. All compounds with the exception of EM20-25 induced apoptosis in mouse embryonic fibroblasts (MEF). However only ABT-737 appears to specifically induce the intrinsic apoptotic pathway with the other compounds causing cell death in the absence of BAK and BAX and caspase-9 suggesting they function to induce cell death independently of BCL-2 inhibition.

3.2 Results

3.2.1 Involvement of BAK/BAX in cell death induced by a variety of BH3 mimetics

To date several BH3 mimetics have been described but proof of their specificity to induce cell death by neutralising anti-apoptotic BCL2 proteins is limited. To investigate the specificity of six different BCL-2 antagonists, MEFs, either wild type (wt) or deficient in both BAX and BAK (double knock out - DKO) were used. Specific BH3 mimetics would require BAK and/or BAX to induce cell death (Wei, Zong et al. 2001; van Delft, Wei et al. 2006), therefore the specificity of the BCL-2 inhibitors can be determined by their cytotoxic activity in BAX/BAK DKO MEFs.

Obatoclax was the most potent compound tested in the MEF cells and induced cell death in a submicromolecular range as determined by PS externalisation (Fig. 3.1,(van Delft, Wei et al. 2006)). However DKO were nearly as sensitive as wt MEFs indicating that BAK and/or BAX and thus neutralisation of BCL-2 proteins were not required for obatoclax induced cell death. Chelerythrine induced cell death in both cell lines to a similar degree, although higher concentration than obatoclax was required.

The two related compounds gossypol and apogossypol induced cell death in a concentration-dependent manner in wt as well as DKO MEFs. Killing appeared to be enhanced in wt MEFs suggesting some involvement of BAK and/or BAX in cell death induction. Exposure to higher concentrations of apogossypol and gossypol also led to cell death in DKO MEFs indicating that higher concentrations of these compounds also induce cell death independent of BCL-2 proteins. EM20-25 had minor effects on cell death induction in wt MEFs. DKO MEFs were completely resistant to exposure to ABT-737, whereby specificity was maintained even at high concentrations.

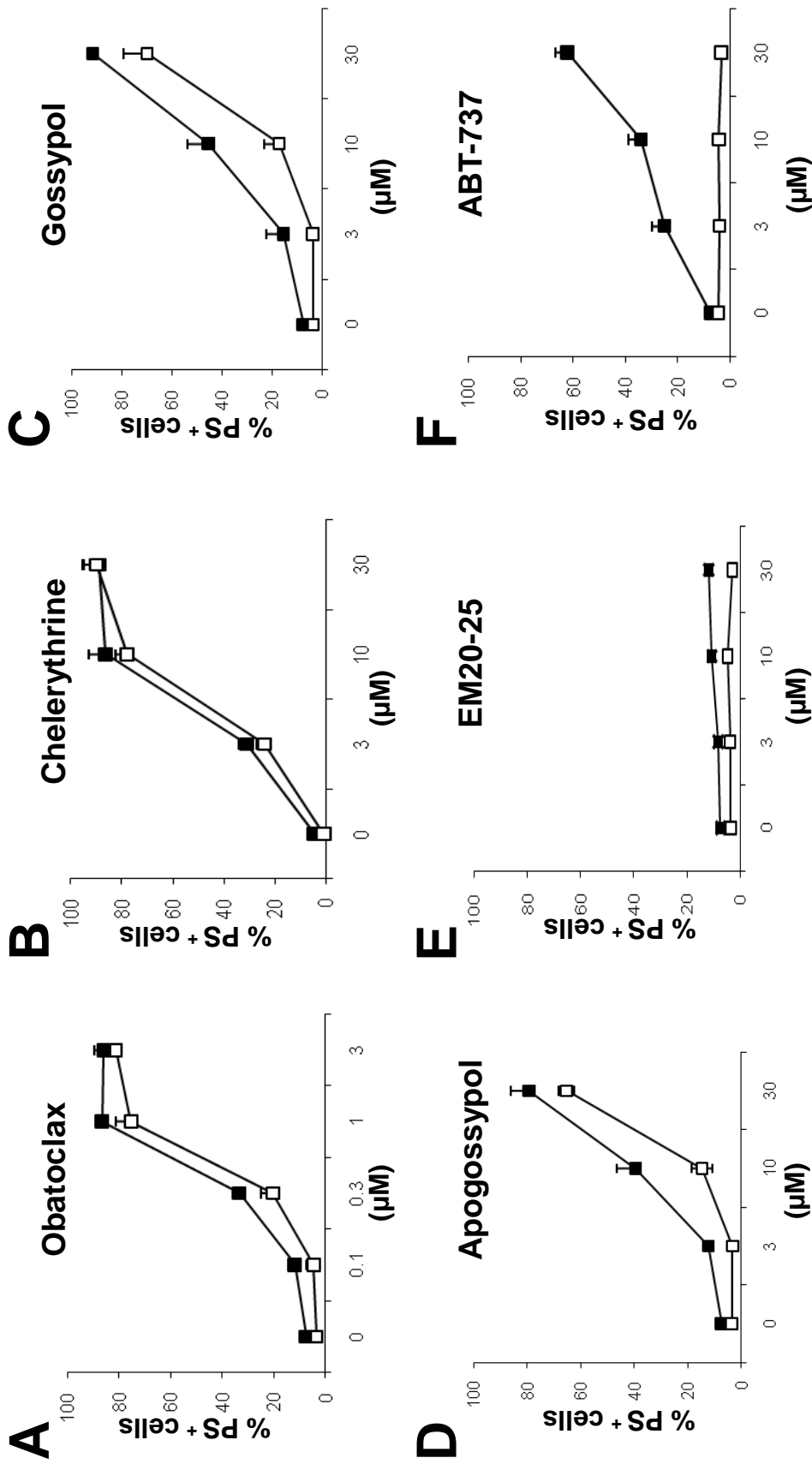


Figure 3.1 Only ABT-737 induces BAX/Bak dependent cell death

Wild type (wt) MEFs (solid fill) or Bax/Bak double knockout (DKO) MEFs (no fill) were exposed to the indicated concentrations of obatoclox, chelerythrine, gossypol, apogossypol, EM20-25 or ABT-737 for 48 h. Cell death was assessed by PS externalization (Annexin-FITC binding) and PI staining (for obatoclox and chelerythrine Annexin-APC was used due to their auto-fluorescence). Data represent the mean S.E.M. of 5–8 experiments.

3.2.2 Involvement of caspase-9 in cell death induced by a variety of BH3 mimetics

Next the specificity of the BH3 mimetics in inducing cell death through the intrinsic apoptotic pathway was assessed in Jurkat T-cells deficient in caspase-9. Neutralisation of anti-apoptotic BCL-2 proteins should result in MOMP, cytochrome *c* release and subsequent activation of caspase-9. Deficiency of caspase-9 will prevent apoptosis induced by neutralisation of BCL-2 proteins and therefore activation of BAK and/or BAX. Cell death was again determined by PS externalisation except for obatoclax. To exclude possible interference of obatoclax auto-fluorescence, apoptosis was assessed by changes in cell scatter properties (FSC/SSC) reflecting changes in cell volume.

Obatoclax, gossypol, apogossypol and chelerythrine showed cytotoxic activity in the caspase-9 deficient cells indicating that these putative BH3 mimetics do not specifically induce the intrinsic apoptotic pathway (Fig. 3.2). EM20-25 (1–30 mM), as in the MEFs, did not induce cell death in Jurkat cells. Again, in contrast to the other compounds, ABT-737 induced cell death in a concentration-dependent manner in cells expressing caspase-9, whereas the caspase-9 deficient cells were resistant confirming that ABT-737 induces cell death specifically through the intrinsic apoptotic pathway.

Collectively these results demonstrate that all tested compounds with the exception of ABT-737 do not solely function as BH3 mimetics as their cell death induction is independent of BAK and/or BAX. However the enhanced sensitivity of wt MEFs to gossypol and apogossypol does suggest some involvement of BAK and/or BAX at least at low concentrations. Thus only ABT-737 specifically induces cell death by neutralising BCL-2 proteins and triggering the intrinsic apoptotic pathway. Importantly, unlike other compounds its specificity was maintained even at higher concentrations. This makes ABT-737 a potentially valuable tool to gain insights into activation of BAK and BAX.

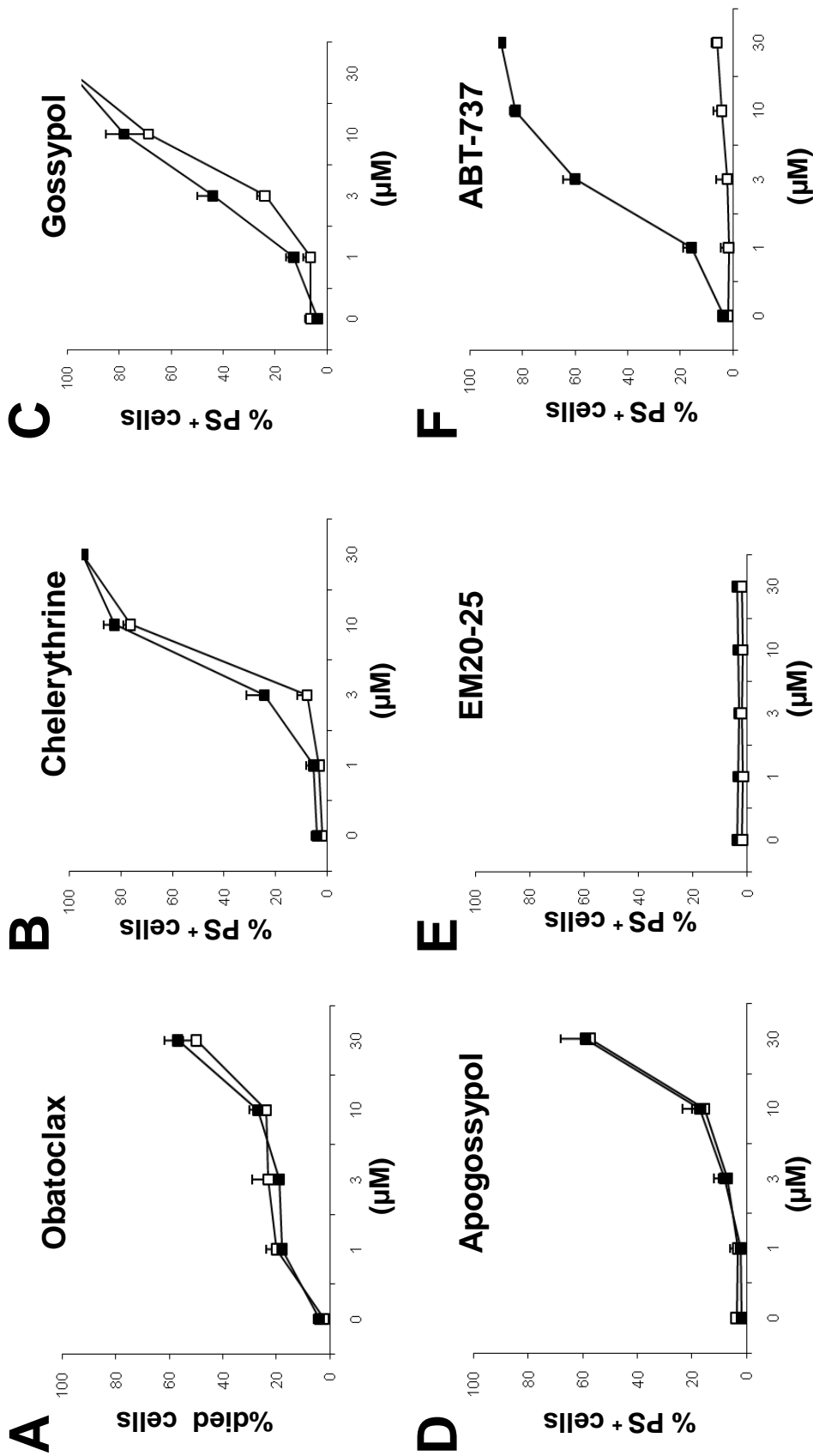


Figure 3.2 Only ABT-737 induces caspase-9 dependent cell death

Jurkat T-cells deficient in caspase-9 (no fill) or reconstituted with caspase-9 (solid fill) were exposed to the indicated concentrations of obatoclox, chelerythrine, gossypol, apogossypol, EM20-25, or ABT-737 for 24 h. Cell death induced by obatoclox was assessed by FSC/SSC analysis and for chelerythrine phosphatidylserine (PS)-exposure by binding of Annexin-APC was used. For all other compounds binding of Annexin-FITC and PI staining was used. Data represent the mean \pm S.E.M. of 4 experiments.

3.2.3 ABT-737 induces the intrinsic apoptotic pathway in a BAX-deficient Jurkat cell line

ABT-737 as an authentic BH3 mimetic requires BAK/BAX to induce apoptosis. It therefore represents a unique tool to investigate activation of BAK and/or BAX. The steps in BAX activation, translocation to the mitochondria, membrane insertion and its oligomerisation has been well studied, less is known about the activation of BAK (Chipuk, Moldoveanu et al.). To further investigate the mechanism of BAK activation during apoptosis I chose ABT-737 as a tool to specifically induce the intrinsic apoptotic pathway. Furthermore to exclude any interference with BAX, Jurkat cells which lack BAX (Shawgo, Shelton et al. 2008) were used.

3.2.3.1 ABT-737 induces PS externalisation and drop of $\Delta\Psi_m$

Sensitivity of Jurkat cells to ABT-737 was determined by exposing cells to 5 μ M ABT-737 for 8 h. ABT-737 efficiently induced cell death as determined by an increase in PS externalisation (Fig. 3.3 A). ABT-737 induced PS positivity in Jurkat cells following 45 min of exposure which increased over time resulting in 60% PS⁺ cells after 8 h of ABT-737 exposure. Within 15 min of ABT-737 exposure mitochondrial membrane potential ($\Delta\Psi_m$) dropped and, after 4 h, nearly 50% of cells showed a reduced $\Delta\Psi_m$ (Fig. 3.3 B). Collectively exposure to 5 μ M ABT-737 induced both externalisation of PS and reduced $\Delta\Psi_m$ in a time-dependent manner in Jurkat T cells. Reduction of $\Delta\Psi_m$ preceded PS externalisation by ~30 min and after ~2 h, the percentages of both the PS⁺ and cells with reduced $\Delta\Psi_m$ converged.

Jurkat cells are type II cells with respect to extrinsic apoptotic signals (e.g. from death receptors such as FAS) and require activation of caspase-8 to occur prior to perturbation of the mitochondria. The reduction of $\Delta\Psi_m$ and cytochrome c release is therefore caspase dependent. A direct activator of the intrinsic apoptotic pathway, such as ABT-737, would be expected to cause reduction of $\Delta\Psi_m$ upstream of any caspase activation. Jurkat cells were therefore exposed to the broad spectrum caspase inhibitor z-VAD.fmk prior to ABT-737 exposure (Fig. 3.3 C). Although z-VAD.fmk blocked ABT-737 induced PS externalisation (a known caspase-dependent process), it did not alter the percentage of low $\Delta\Psi_m$ cells compared to control. This indicates that the perturbation of the mitochondria occurs upstream of the activation of the caspase providing further evidence for the specific activation of the intrinsic pathway following ABT-737 exposure.

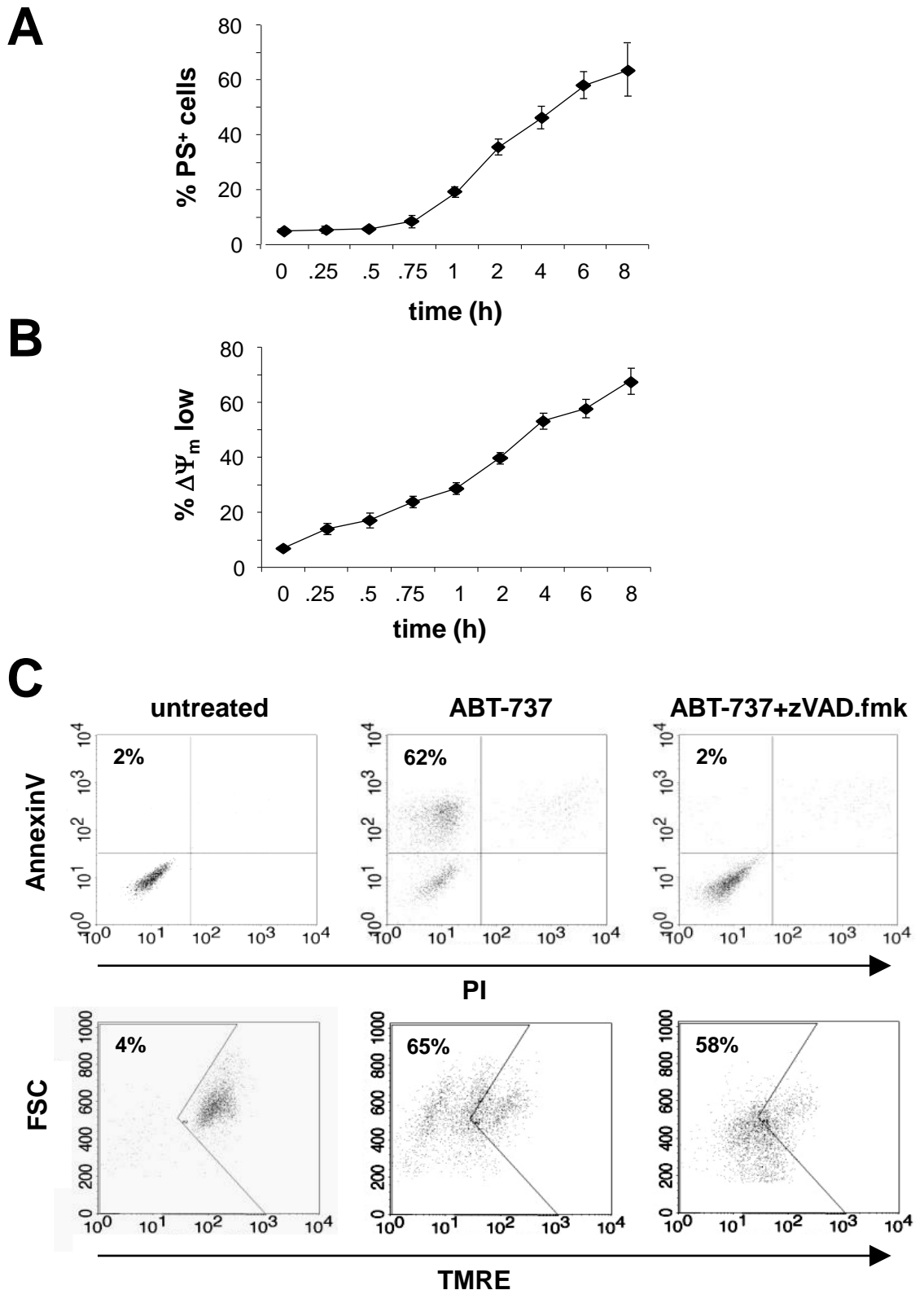
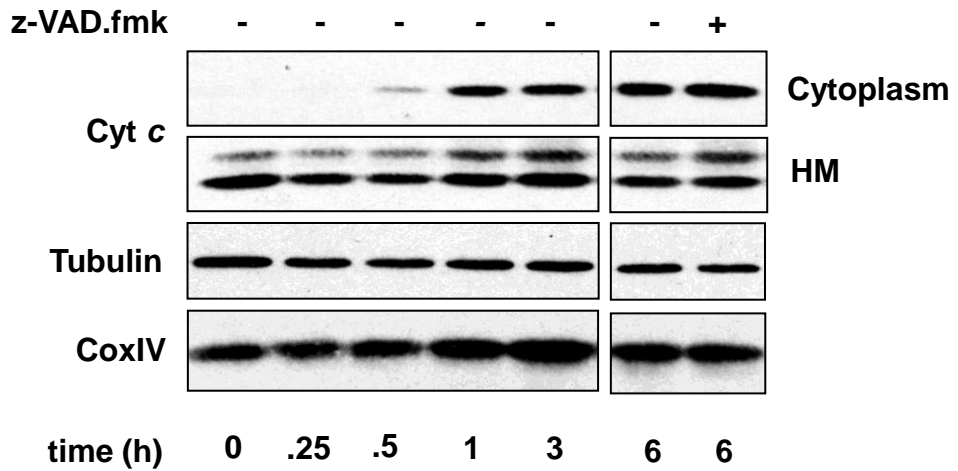
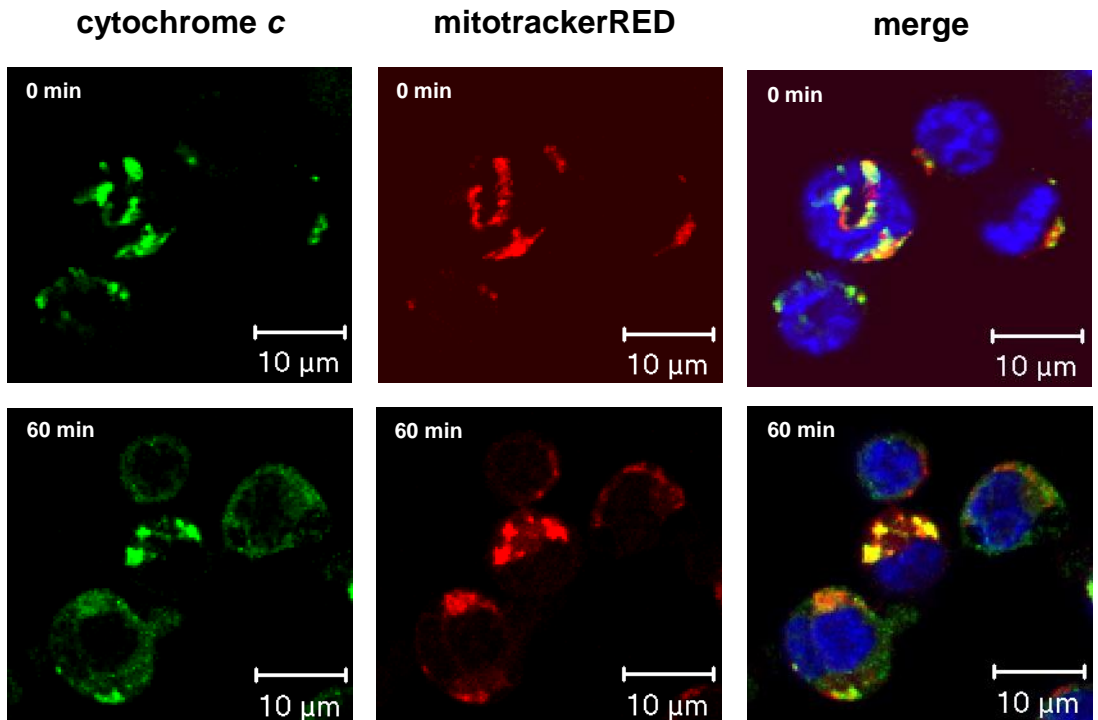


Figure 3.3 ABT-737 induces PS externalisation and reduction in $\Delta\Psi_m$

(A) Jurkat cells were exposed to 5 μM ABT-737 for indicated times and cell death determined by externalisation of PS (AnnexinV positive cells) and (B) reduced $\Delta\Psi_m$ (TMRE negative cells). Data points represent the Mean \pm standard error of the mean (SEM) of five different experiments. (C) Jurkat cells were exposed to 50 μM z-VAD.fmk for 1 h prior to 5 μM ABT-737 exposure for 6 h and the effect on ABT-737 induced reduction of $\Delta\Psi_m$ was determined. As positive control PS externalisation was analysed.

3.2.3.2 ABT-737 induces cytochrome *c* release from the mitochondria upstream of caspase activation

A classical hallmark of the intrinsic apoptotic pathway is the release of cytochrome *c* from the mitochondria into the cytoplasm, where it induces formation of the Apaf-1 apoptosome, which functions as an activation platform for procaspase-9 (Green and Kroemer 2004). To investigate if ABT-737 induces the release of cytochrome *c*, a mitochondria-containing heavy membrane (HM) and a cytosolic fraction from ABT-737 exposed and control Jurkat cells were analysed. Cytochrome *c* was released by ABT-737 as soon as 0.5 h after exposure and this increased in a time-dependent manner (Fig. 3.4 A). However even after 6 h of ABT-737 exposure, cytochrome *c* release was not complete. z-VAD.fmk did not alter cytochrome *c* release indicating that this process occurs upstream of the activation of caspases. To confirm these results on a single cell level, I performed immunofluorescence using anti-cytochrome *c*. In control cells, cytochrome *c* staining is punctated reflecting mitochondrial localized cytochrome *c* as it overlapped with the mitochondrial marker dye MitotrackerRED (Fig. 3.4 B). Following ABT-737 exposure the cytochrome *c* staining became diffuse which confirmed the release of cytochrome *c* from the mitochondria into the cytoplasm. Furthermore it seemed that in some cells the cytochrome *c* was only partial released as both punctated and diffuse staining occurred within the same cells. These results suggest that ABT-737 induced caspase-independent rapid cytochrome *c* release from the mitochondria into the cytoplasm in Jurkat cells.

A**B****Figure 3.4 ABT-737 induces cytochrome *c* release**

(A) Heavy membrane and cytoplasmic fractions from control or ABT-737 exposed Jurkat cells were prepared by lysing in 0.01% Digitonin. Release of cytochrome *c* was determined by Western blotting of the cytosolic as well as HM fractions. Cytochrome *c* oxidase subunit 4 (Cox IV) was used as a control for the integrity of the mitochondrial fraction and tubulin as loading control. (B) Jurkat T cells were exposed to 5 μ M ABT-737, fixed and immunostained with anti-cytochrome *c* antibody (secondary antibody ALEXA 488 labelled), MitotrackerRed and Hoechst33342 and analysed by fluorescence microscopy.

3.2.3.3 ABT-737 induces activation of caspases

Released cytochrome *c* induces the formation of the apoptosome. This leads to activation of initiator caspase-9. Once activated it activates effector caspases-3 and 7, which are responsible for the degradation of multiple cellular substrates such as the classical caspase substrate, Poly (ADP-ribose) polymerase PARP-1 (Kaufmann, Desnoyers et al. 1993; Lazebnik, Kaufmann et al. 1994).

To investigate the activation of caspases Jurkat cells were exposed to ABT-737 for 6 h and cell lysates analysed for caspase processing by Western blotting. Caspase-9 was processed in a time dependent manner and the active 37 kDa and 35 kDa fragments were detected as soon as 0.5 h (Fig. 3.5). However, the caspase-9 proform was still detectable following 6 h of ABT-737 exposure indicating that not all procaspase-9 was activated following ABT-737 exposure. Active caspase-9 then processes caspase-3 which was determined by the detection of the p19 cleavage fragment. This fragment coincided with the appearance of the processed caspase-9 fragment. To provide further evidence for the activation of caspase-3, cleavage of PARP was analysed. Apoptotic cleavage of PARP results in the detection of an 89 kDa fragment, which correlated with the detection of the caspase-3 19 kDa fragment. PARP was fully processed after 2 h indicating that partial activation of caspase-3 at this time point is sufficient to fully degrade its substrate. The processing of both caspases and the cleavage of PARP were blocked by z-VAD.fmk. Collectively these results show that, ABT-737 exposure results in the activation of the caspase cascade and processing of apoptotic substrates.

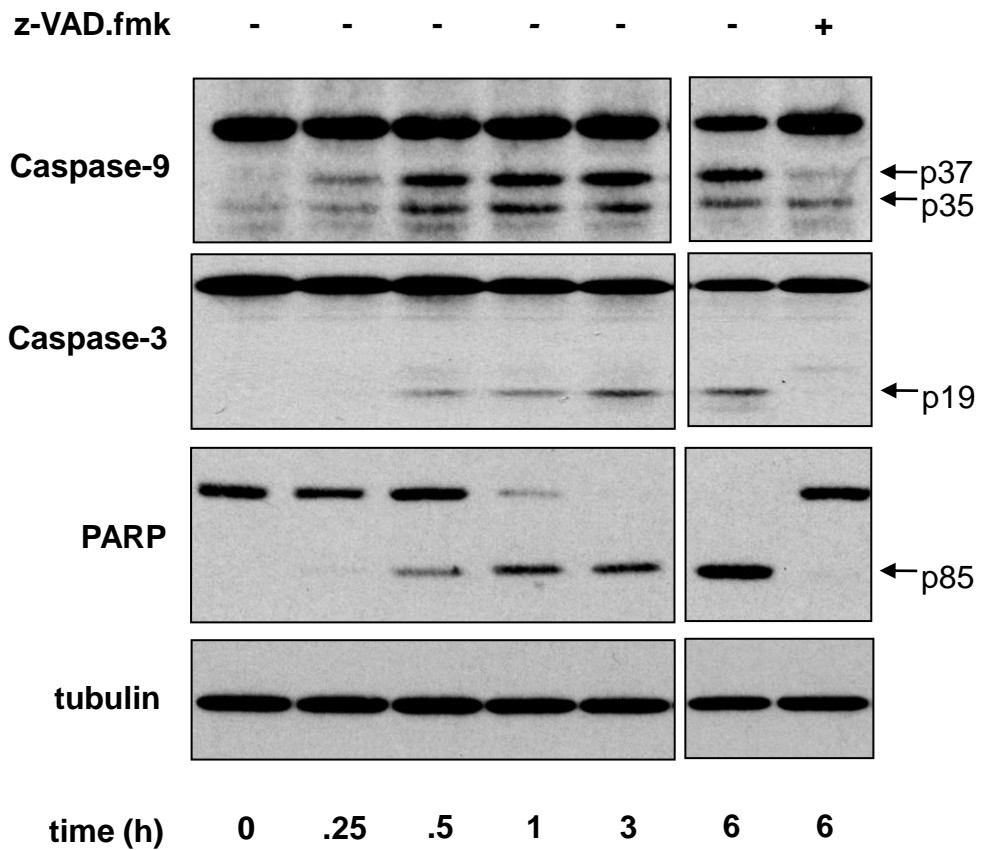


Figure 3.5 ABT-737 initiates the caspase cascade

Jurkat cells were exposed to 5 μ M ABT-737 for 0.25 h - 6 h. z-VAD.fmk (50 μ M) was used as a 1 h pre-exposure where indicated. Processing of caspase-3, and -9 and PARP was analysed by Western blotting. Expression of tubulin served as an internal loading control.

3.2.4 ABT-737 induced apoptosis requires BAK in BAX-deficient Jurkat cell line

As shown in Fig. 3.1, ABT-737 induces apoptosis in a BAK and/or BAX dependent manner (van Delft, Wei et al. 2006; Vogler, Weber et al. 2009). To investigate if BAK is required for ABT-737 induced apoptosis in the Jurkat cells BAK expression was suppressed using siRNA. Both a single BAK siRNA and a pool of BAK siRNAs resulted in a decrease in PS externalisation as well as reduced $\Delta\Psi_m$ low compared to control siRNA following ABT-737 exposure (Fig 3.6 A and B). Knock down of BAK also reduced cytochrome *c* release from the mitochondria into the cytosol following ABT-737 exposure (Fig. 3.6 C). As a consequence of inhibited cytochrome *c* release activation of the caspase cascade was abrogated following ABT-737 exposure as determined by inhibition in generation of caspase-3 p19 fragment (Figure 3.6 C).

This suggests that ABT-737 induces apoptosis in a BAK-dependent manner also in Jurkat cells. In contrast to the marked decrease in apoptosis, BAK protein levels were only modestly reduced by the siRNAs. (Fig. 3.6 D). Therefore only a discrete reduction in BAK protein levels appeared to be sufficient to decrease sensitivity to ABT-737.

The moderate suppression of BAK protein levels reflects low transfection efficiency, which could be determined by fluorescence labelled siRNA. Another explanation would be that only a discrete portion of total cellular BAK is involved in apoptosis induction by ABT-737. This discrete portion could correlate with primed BAK complexed with BCL-X_L. Primed BAK does not represent a different transcriptional/splice isoform, but converts from inactive BAK by exposing its BH3 domain. Consequently primed BAK would need to have a higher turnover rate compared to inactive BAK which could be mediated by e.g. modifications like phosphorylation of primed BAK.

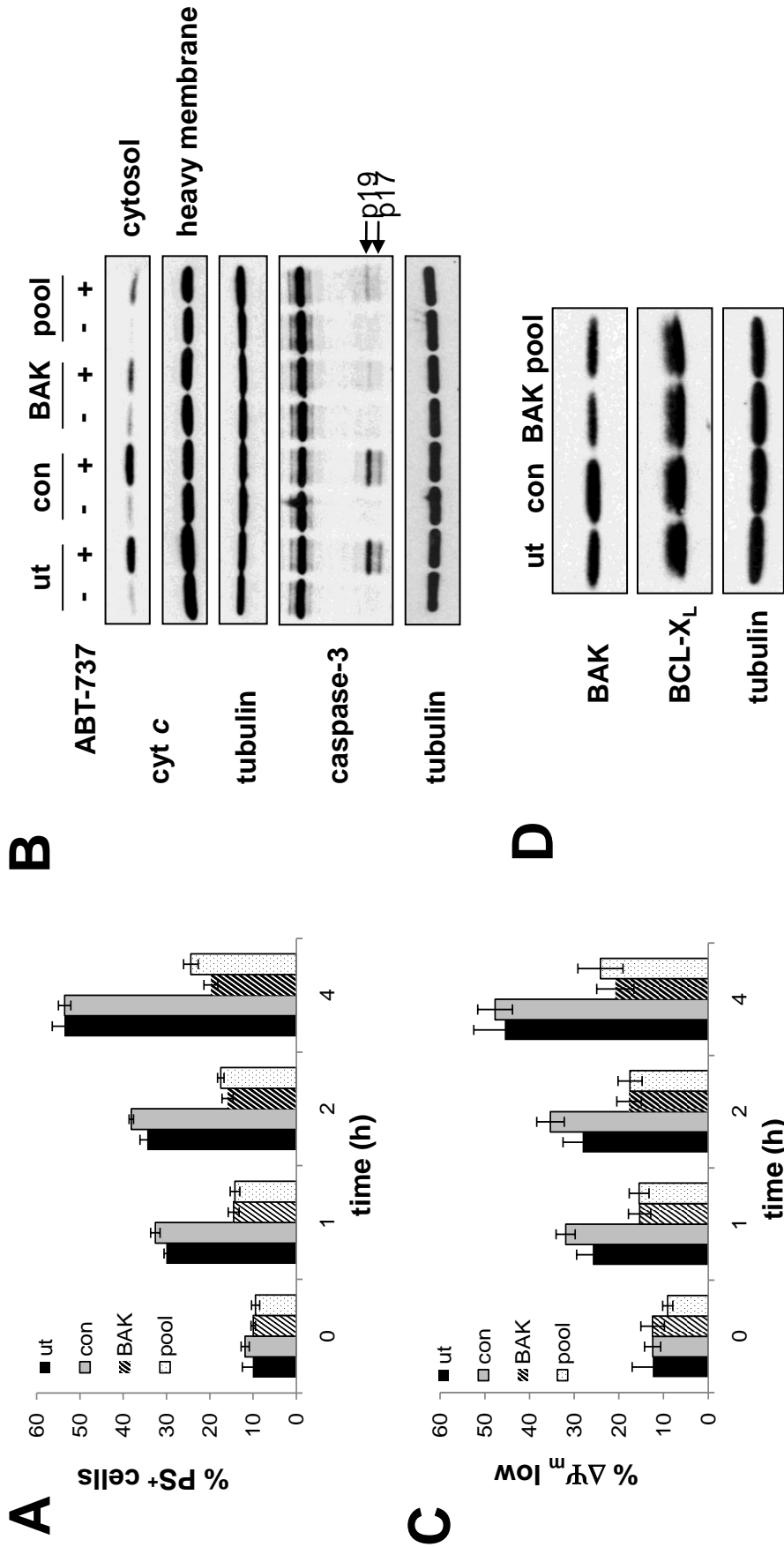


Figure 3.6 ABT-737 requires BAK to induce apoptosis in Jurkat cells

(A) Jurkat cells were transiently transfected with a BAK specific siRNA (BAK), a pool of BAK specific siRNAs (pool), or control siRNA (con). 48 h after transfection cell death following ABT-737 exposure for the indicated times was analysed by PS externalisation or (B) reduced $\Delta\Psi_m$. Data points represent the Mean standard error of the mean (SEM) of five different experiments. (C) Cytochrome *c* release as well as activation of the caspase cascade as accompanied by the processing of caspase-3 following ABT-737 exposure (2 h) was analysed from BAK siRNA and control by Western blotting. (D) Protein levels of BAK and BCL-X_L were determined by Western blotting.

3.3 Discussion

Upregulation of anti-apoptotic BCL-2 proteins has been observed in a number of primary tumors and correlates with resistance to chemotherapy (Hanahan and Weinberg 2000; Adams and Cory 2007). An attractive strategy to overcome this resistance of tumor cells is to directly activate the normal cell death machinery by targeting anti-apoptotic BCL-2 proteins. Several BH3 mimetics that mimic BH3-only proteins have been reported and their specificity can be determined through activation of their essential downstream effectors BAK and BAX (Wei, Zong et al. 2001; van Delft, Wei et al. 2006). Out of the six putative BH3 mimetics tested five killed cells independently of BAK and/or BAX and only ABT-737 act as an authentic BH3 mimetic as cells deficient in BAK and/or BAX were resistant (Fig. 3.1). Similar results have been reported earlier for obatoclax and chelerythrine with comparable results (van Delft, Wei et al. 2006). BAK and BAX deficient MEFs did show a slight resistance to gossypol and apogossypol indicating a possible contribution of BAK and/or BAX to the observed toxicity of these compounds. However off target effects of these compounds are more pronounced (Fig. 3.1). These putative BH3 mimetics could therefore be useful as leads in the development of higher affinity compounds, solely depending on BAK and/or BAX. The cytotoxic activity did not decrease in the absence of caspase-9 for all tested compounds except ABT-737 (Fig. 3.2). Inducing cell death by neutralisation of anti-apoptotic BCL-2 proteins requires the activation of BAK and BAX leading to the release of cytochrome *c* from the mitochondria into the cytoplasm, where it promotes formation of the Apaf-1 apoptosome and subsequent activation of caspases. Inhibition of cell death in the absence of caspase-9 was only observed following ABT-737 exposure indicating its caspase-dependency, whereas obatoclax induced cell death was not blocked by zVAD.fmk (Zhang, Liu et al. 2007; Balakrishnan, Wierda et al. 2008).

The observed differences in specificity of the compounds may in part be explained by their relative affinities for their anti-apoptotic targets. ABT-737 binds with comparable affinity as a BAD-derived BH3 peptide to BCL-X_L, BCL-2 and BCL-w (nM range), whereas all other tested compounds display a lower affinity for their targets (μM range) (Zhai, Jin et al. 2006). Therefore lower affinity could promote off target effects outside of the BCL-2 resulting in the nonspecific toxicity observed. Accordingly it was shown that gossypol induces the generation of reactive oxygen species which may be responsible for cell death (Ko, Shen et al. 2007).

The results presented in this chapter demonstrate that ABT-737 acts as an authentic BH3 mimetic requiring BAK and/or BAX as well as caspase-9 the key components of the intrinsic apoptotic machinery. By neutralising anti-apoptotic BCL-2 proteins, ABT-737 acts as a specific apoptosis inducing agent providing a unique tool to explore the mechanism of activation of the intrinsic apoptotic pathway, specifically the activation of BAK and/or BAX. ABT-737 as an authentic BH3 mimetic should overcome the resistance mechanism and resensitise tumour cells to apoptosis by neutralising over-expressed, anti-apoptotic BCL-2 proteins and thereby specifically inducing the intrinsic apoptotic pathway.

Out of six tested compounds only ABT-737 specifically triggered the intrinsic apoptotic pathway (Fig. 3.1 and 3.2) by induction of the classical biochemical markers (reduction of $\Delta\Psi_m$, cytochrome *c* release, activation of the caspase cascade and PS externalisation) (Fig. 3.3, 3.4 and 3.5). Therefore ABT-737 represents a valuable tool to investigate the mechanism of BAK activation.

CHAPTER 4:

**A discrete pool of cellular BAK is sequestered by BCL-X_L
and can be displaced by ABT-737**

4.1 Introduction

The point of no return during apoptotic cell death is the permeabilisation of the outer mitochondrial membrane which promotes the release of a number of apoptogenic proteins from the mitochondrial intermembrane space (Youle and Strasser 2008). Permeabilisation is mediated by BAK and BAX, however the mechanism how these proteins lead to MOMP is still unclear. Currently two opposing theories exist to explain how these critical mitochondrial gate keepers are regulated and activated (Leber, Lin et al. 2007) (see section 1.5). BAK is suggested to be activated according to the “indirect activation” model. This model postulates that BAK is constitutively active and exists in a primed conformation. Therefore in viable cells it must be sequestered by anti-apoptotic BCL-2 family members to prevent MOMP. During apoptosis BH3-only proteins bind to anti-apoptotic BCL-2 proteins resulting in displacement of BAK. Free BAK then oligomerises into multimeric pores, which facilitate MOMP (Willis, Chen et al. 2005; Uren, Dewson et al. 2007; Willis, Fletcher et al. 2007). In support of this model, BAK has been shown to be sequestered by the anti-apoptotic proteins BCL-X_L and MCL-1 and efficient induction of apoptosis requires neutralisation of both anti-apoptotic proteins (Willis, Chen et al. 2005).

BAK activation is controlled by the tight balance between members of the BCL-2 protein family specifically through sequestration by anti-apoptotic proteins. Heterodimerisation between anti- and pro-apoptotic BCL-2 family members is mediated by BH3:groove interactions, where four hydrophobic residues of the BH3 domain of the pro-apoptotic protein bind into four hydrophobic pockets along the hydrophobic binding groove of its anti-apoptotic binding partner (Sattler, Liang et al. 1997). To facilitate this BCL-X_L:BAK association inactive BAK has to undergo a conformational change in order to expose critical hydrophobic BH3 residues on the protein surface (Moldoveanu, Liu et al. 2006). This conformational change co-incidentally induces the rotation of R88 and Y89 resulting in opening of the hydrophobic binding groove of BAK. The resultant BAK conformation is referred to as “primed”(Willis, Chen et al. 2005).

Experiments in this chapter are aimed at investigating the indirect activation of BAK by ABT-737. A discrete proportion of BAK was found to be sequestered by BCL-X_L and displaced by ABT-737. Introduction of a BCL-X_L:BAK complex into BAK and BAX DKO MEFs sensitised them to ABT-737 suggesting that the distinct proportion of primed BAK is sufficient to initiate apoptosis. Additionally BCL-2 had no role in guarding primed BAK,

whereas MCL-1 sequestered primed BAK but could not be neutralised by ABT-737. Another feature of the indirect model is that BAK has to be constitutively active to bind BCL-X_L through a BH3:groove interface. In support I found that the BAK BH3 domain mediates its association with BCL-X_L by inserting the BH3 domain into the hydrophobic groove of BCL-X_L.

4.2 Results

4.2.1 A distinct proportion of total cellular BAK is associated with BCL-X_L and displaced by ABT-737

BAK has been described to be associated with the anti-apoptotic BCL-2 proteins BCL-X_L and MCL-1 in viable cells and efficient induction of apoptosis requires neutralisation of both (Willis, Chen et al. 2005). According to the indirect model of BAK activation, ABT-737 should induce apoptosis by antagonising BCL-X_L resulting in the displacement and further activation of BAK.

To further examine this hypothesis, the binding of BAK to BCL-X_L was assessed by immunoprecipitating BCL-X_L. BAK was associated with BCL-X_L in control cells and exposure to ABT-737 resulted in its displacement (Fig. 4.1 A, upper panel). These data were reproduced by the reciprocal immunoprecipitation using the BAK NT antibody (Fig. 4.1 A, lower panel). The portion of BAK complexed with BCL-X_L is below the 10 % input band raising the possibility of an artifact. However the displacement of BAK from BCL-X_L by ABT-737 demonstrates the integrity of the existence of an BCL-X_L:BAK complex in these cells. The discrete portion of total cellular BAK which co-immunoprecipitated with BCL-X_L may not reflect the endogenous situation. Cell lysis and immunoprecipitation conditions result in an expanded volume, which could increase the off-rate of BAK from BCL-X_L. Consequently BCL-X_L:BAK complexes would dissociate due to the experimental procedure.

Further analysis of the supernatants of the BAK and BCL-X_L immunoprecipitations showed that although the targeted protein was completely depleted from the supernatant an overall reduction in its co-precipitated binding partner was not detected (Fig. 4.1, box).

These data indicate that BAK is sequestered by BCL-X_L in control cells. The relative levels of depletion of binding partners compared to the targeted protein in post immunoprecipitation lysates suggest that only a discrete portion of the total cellular BAK exists in complex with BCL-X_L.

To analyse the distribution of BCL-X_L:BAK complexes in relation to the residual protein enriched mitochondrial preparations were fractionated on sucrose density gradients (10 - 45 % sucrose). BAK and BCL-X_L co-eluted in a series of protein complexes ranging from ~ 44 to 700 kDa (Fig. 4.2 A). The wide distribution of in particular BAK is in contrast to earlier

findings (Kim et al, 2009), raising the possibility that sucrose like for example nonionic detergents induced conformational changes which could result in the unspecific aggregation of BAK and BCL-X_L.

To ensure the integrity of the gradients, fractions were blotted for TOM20 (20kDa), which is a component of receptor complex in the outer mitochondrial membrane (around 600 kDa). Together with TOM22, TOM20 interacts with the N-terminal sequences of precursor proteins, which are synthesized in the cytoplasm and destined for the mitochondrial matrix and inner membrane. The detection of both monomeric as well as receptor complexed TOM20 in distinct fractions demonstrate that sucrose did not induce artefactual aggregation of TOM20. Consequently, sucrose mediated aggregation of BAK or BCL-X_L appears to be unlikely.

Co-elution does not necessarily infer a direct interaction, therefore immunoprecipitations using a BCL-X_L antibody were performed to analyse BCL-X_L:BAK complexes in pooled gradient fractions. I confirmed that BAK was associated with BCL-X_L but found that this complex was localised predominantly to fraction pool B, corresponding to ~150 kDa (Fig. 4.2 B). Therefore despite the apparent wide range of co-eluting BAK and BCL-X_L the localisation of a specific BCL-X_L:BAK complex was more discrete and the majority of BCL-X_L and BAK although co-eluting were not associated. This again suggested that only a distinct proportion of total cellular BAK resides in a complex with BCL-X_L.

Taken together these results suggest that ABT-737 induces apoptosis in Jurkat cells by displacing BAK from BCL-X_L. In control cells only a discrete pool of BAK is complexed with BCL-X_L and it is this form of BAK which is targeted by ABT-737.

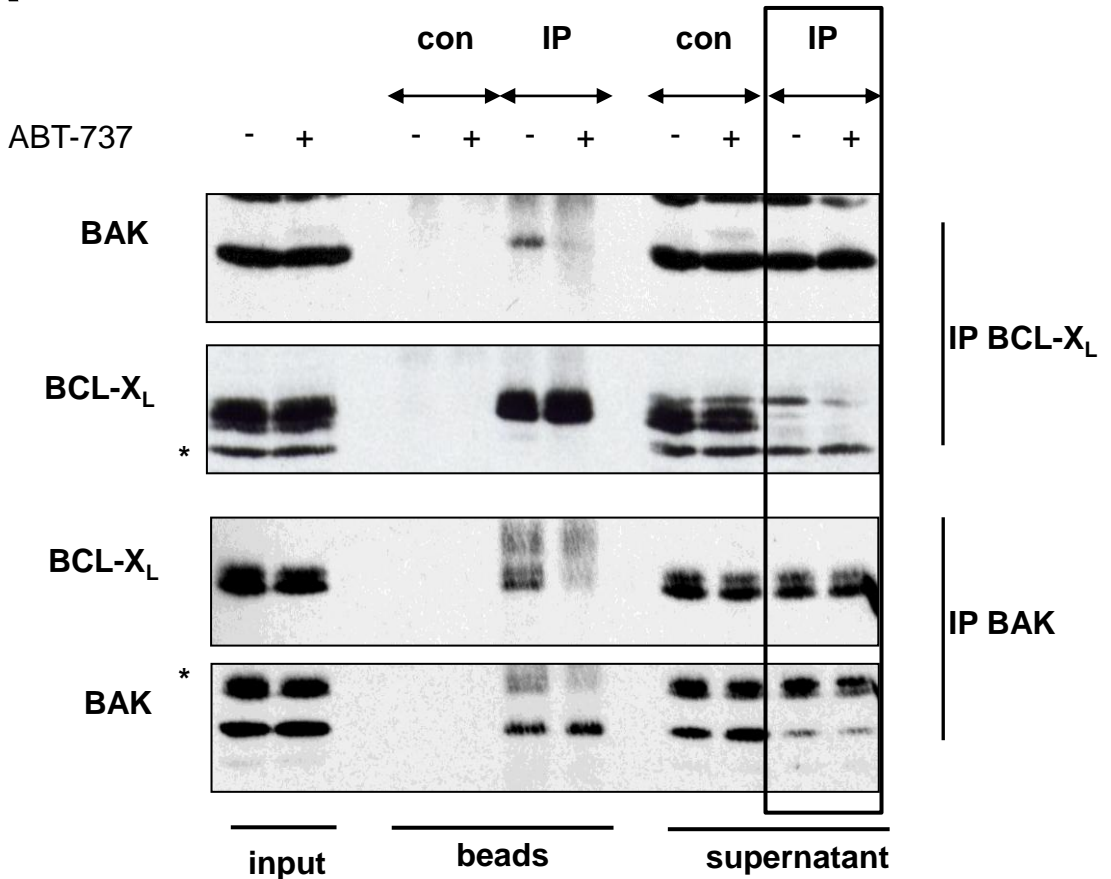
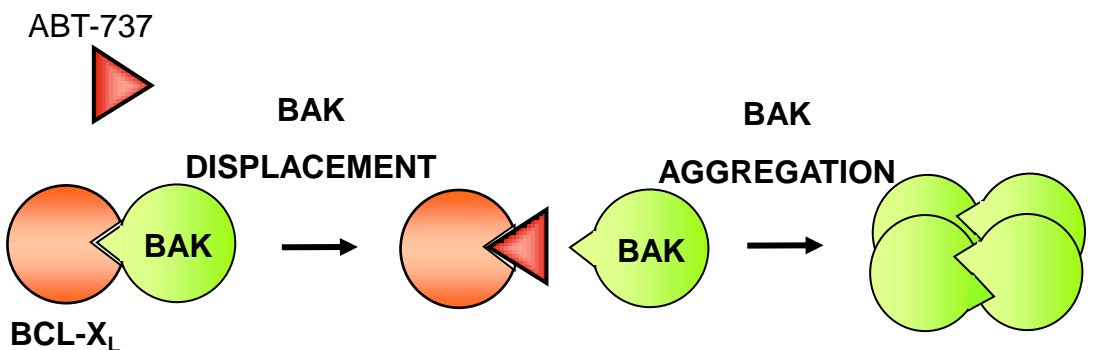
A**B**

Figure 4.1 BAK is bound to BCL-X_L and can be displaced by ABT-737

(A) Jurkat cells were exposed to ABT-737 (5 μM) for 4 h then lysed in 1% CHAPS and subjected to immunoprecipitation using either BCL-X_L (upper panel) or BAK (lower panel) antibodies. Supernatants and immunoprecipitates were analyzed for interaction partners by Western blotting. Asterisk denotes residual BAK signal after reprobing. (B) According to the indirect activation model ABT-737 displaces primed BAK from BCL-X_L promoting aggregation of BAK.

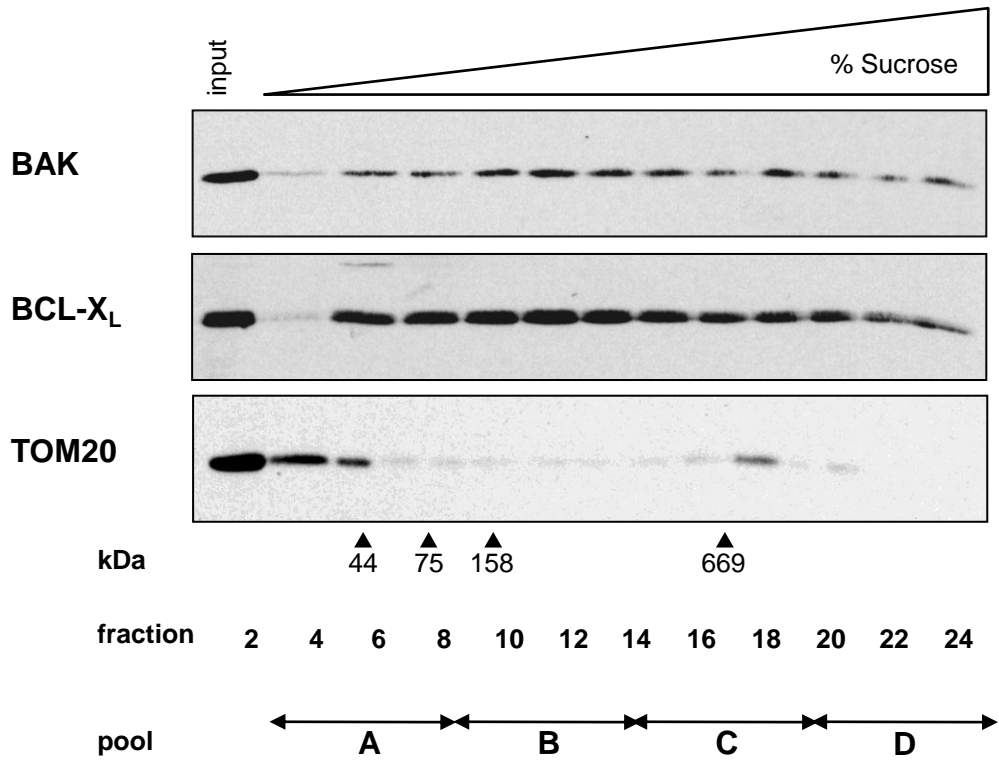
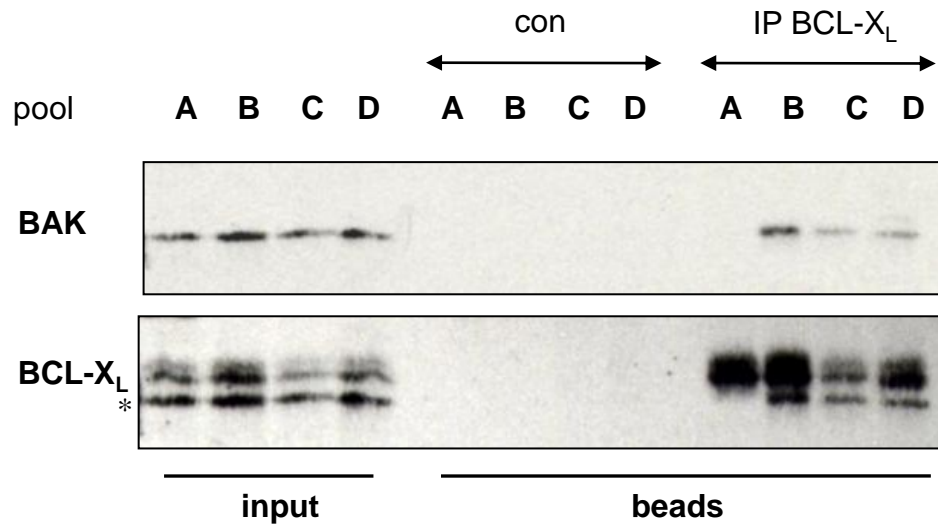
A**B**

Figure 4.2 A distinct proportion of total cellular BAK is associated with BCL-X_L

(A) Mitochondria were isolated by Dounce homogenisation and lysed in 2 % CHAPS. Cleared lysates were separated by sucrose density gradient centrifugation (10 – 45 % Sucrose) and fractions were either Western blotted to analyse the distribution of BAK and BCL-X_L (control: TOM 20) or (B) pooled as indicated (pool A: fractions # 2, 4, 6; pool B: # 8, 10, 12; pool C: # 14, 16, 18; pool D: # 20, 22, 24) and subjected to immunoprecipitation using anti-BCL-X_L antibody. Interaction of BCL-X_L with BAK was analysed by Western blotting. Asterisk denotes residual BAK signal after reprobing.

4.2.2 Reconstitution of a BCL-X_L:BAK complex sensitises resistant cells to ABT-737

If the distinct proportion of primed BAK in the Jurkat cells is sufficient to initiate ABT-737 induced apoptosis then introducing primed BAK into a resistant cell should sensitise cells to ABT-737. To test this hypothesis BAK and BAX DKO MEF cells were used to exclude interference of reconstituted BAK with endogenous BAK or BAX. BAK is known as the gatekeeper of mitochondrial integrity and its over-expression resulted in auto-activation and apoptosis in a DNA concentration dependent manner (Fig. 6.3 A). Primed BAK represents an activation state of BAK, which should be blocked from further activation by association with BCL-X_L. Therefore to achieve a block in BAK activation by BCL-X_L BAK was expressed under the control of a tetracycline inducible vector. After 24 h of constitutive BCL-X_L expression BAK was induced for 4-8 h with tetracycline. Induced cells were still viable presumably due to a block in BAK activation by BCL-X_L (Fig. 4.3 A).

To investigate if the ABT-737 resistance of MEFs could be modulated by reconstituting the BCL-X_L:BAK complex control and reconstituted cells were exposed to different ABT-737 concentrations and after 4 h apoptosis was assessed by both PS externalisation and reduction of $\Delta\Psi_m$. Reconstituted cells became sensitive to ABT-737, whereas untransfected cells remained resistant (Fig. 4.3 B and C). To provide further evidence that in this reconstitution model the intrinsic mitochondrial pathway was being triggered caspase-9 cleavage was assessed in control and reconstituted cells. The caspase-9 cleavage fragments p37 and p35 were only detected following ABT-737 exposure in reconstituted cells (Fig. 4.3 D).

According to its mechanism of action, ABT-737, as a BH3 mimetic, should disrupt the reconstituted BCL-X_L:BAK complex. Released primed BAK would then get further activated resulting in the perturbation of the mitochondria and execution of apoptosis. To examine if in the reconstituted cells BAK and BCL-X_L formed a complex, immunoprecipitation using BCL-X_L antibody was performed. BAK was associated with overexpressed BCL-X_L and was completely depleted from the cell lysate indicating that all the induced BAK was complexed with BCL-X_L (Fig. 4.4). Following ABT-737 exposure BAK was displaced from BCL-X_L supporting that this association occurs through a BH3:groove interaction. Furthermore complex formation of BAK with BCL-X_L as well as its displacement by ABT-737 reflects the endogenous situation in the Jurkat cells.

Collectively these results demonstrate that the discrete proportion of primed BAK is sufficient to execute ABT-737 induced apoptosis.

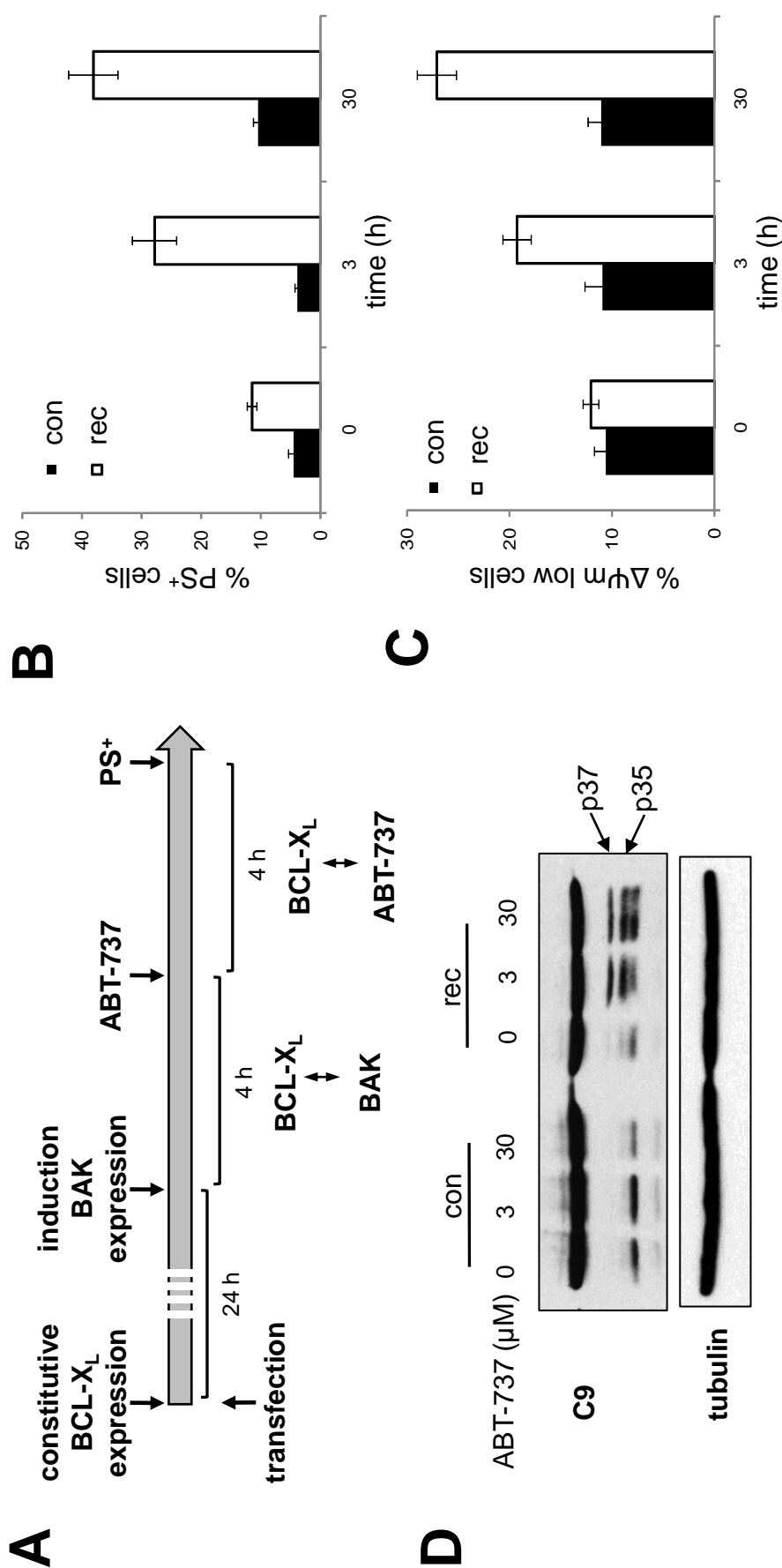


Figure 4.3 Discrete proportion of primed BAK is sufficient to launch apoptosis

(A) Schematic representation of the reconstitution of the BCL-X_L:BAK complex. In order to generate primed BAK⁺, BAK and BAX DKO MEF cells were transiently transfected with N-terminal strep-flag-double tagged BCL-X_L (constitutively expressed), N-terminal strep-tagged BAK (under the control of tetracycline inducible vector) and TETrepressor (TETR) (recon) or left untransfected (con). After 24 h constitutive BCL-X_L expression, BAK was induced for 4 h with tetracycline and induced BAK associates with over-expressed BCL-X_L. Exposure to ABT-737 should result in displacement of BAK, which is then free to get further activated and induce the intrinsic pathway of apoptosis. (B) Analysis of PS externalization or (C) loss of ΔΨ_m following ABT-737 exposure (3 and 30 μM) for 4 h of reconstituted (recon) and control (con) cells. Data points represent the Mean SEM of 5 different experiments. (D) Analysis of caspase-9 cleavage of reconstituted and control cells after exposure to 3 or 30 μM ABT-737 for 4 h by Western blotting. Asterisk denotes unspecific band.

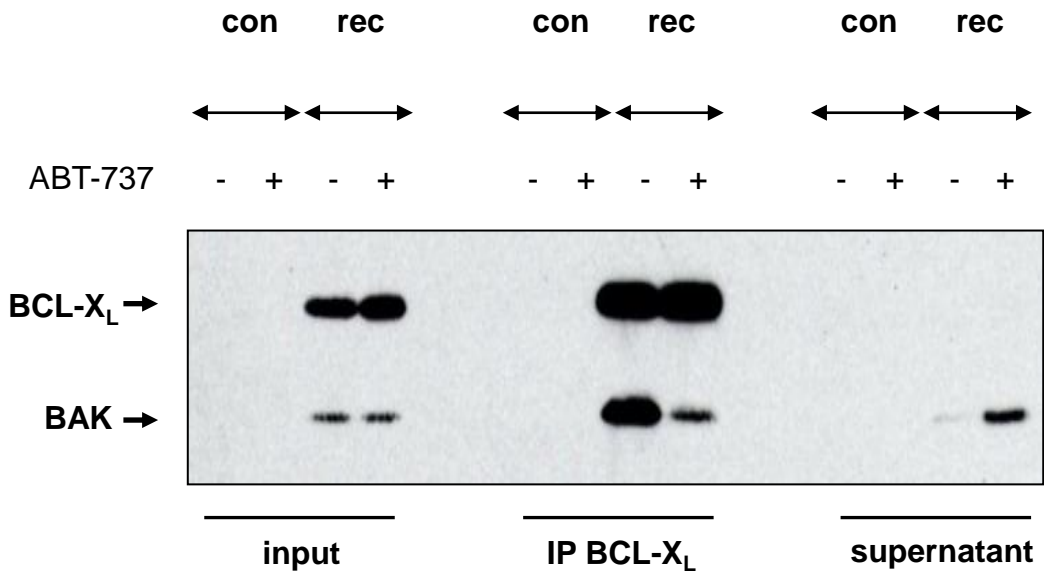


Figure 4.4 Reconstituted BCL-X_L:BAK complex is disrupted by ABT-737

BCL-X_L (strep-flag double tagged):BAK (strep-tagged) reconstituted (rec) and control (con) MEF DKO cells were exposed to ABT-737 (3 μM) for 4 h, lysed in 1% CHAPS and immunoprecipitated using BCL-X_L antibody. Interaction with BAK was determined by Western blotting using anti-strep.

4.2.3 Role of MCL-1 and BCL-2 as inhibitors of BAK

Besides BCL-X_L, MCL-1 is also reported to sequester BAK (Willis, Chen et al. 2005). However the potency of ABT-737 as single agent in the Jurkat cells (Fig. 3.3) does not suggest a major role for neutralisation of MCL-1 in apoptosis induction. The failure of MCL-1 to co-precipitate with BAK in control cells also supports an exclusive role for BCL-X_L in ABT-737 induced apoptosis in the Jurkat cells. However, ABT-737 did induce binding of BAK to MCL-1 (Fig. 4.5 A). This association probably did not represent an endogenous interaction of both proteins as the intensity of the BAK band is largely reduced compared to the 10 % input band. In addition to MCL-1, BCL-2 is also described as a possible guardian of BAK (Ruffolo and Shore 2003). Although the Jurkat cells also express BCL-2 an interaction between BCL-2 and BAK was not observed, both in the presence or absence of ABT-737 (Fig. 4.5 B). Therefore in Jurkat cells ABT-737 induced apoptosis appears to be mediated solely by displacement of BAK from BCL-X_L.

To further investigate a potential role for BCL-2 and MCL-1 in binding primed BAK, BCL-X_L was replaced in the reconstitution system by BCL-2 and MCL-1. Cell death was determined by PS externalisation following exposure to ABT-737 (Fig. 4.6 A). Reconstitution with BCL-2 resulted after induction of BAK in a high background cell death, which did not increase following ABT-737 exposure. This suggests that BCL-2 cannot block BAK auto-activation in this system. Indeed I found by immunoprecipitation that BCL-2 was not able to bind to BAK in transfected cells (Fig. 4.6 B).

In contrast MCL-1 protected cells from BAK induction but reconstitution of a MCL-1:BAK complex failed to sensitise cells to ABT-737 (Fig. 4.6 A). Immunoprecipitating BAK demonstrated that MCL-1 can bind to BAK correlating with earlier data (Fig. 4.5 A). However, according to the binding profile of ABT-737 this complex cannot be disrupted thereby explaining the resistance of these cells to ABT-737 (Fig. 4.6 B).

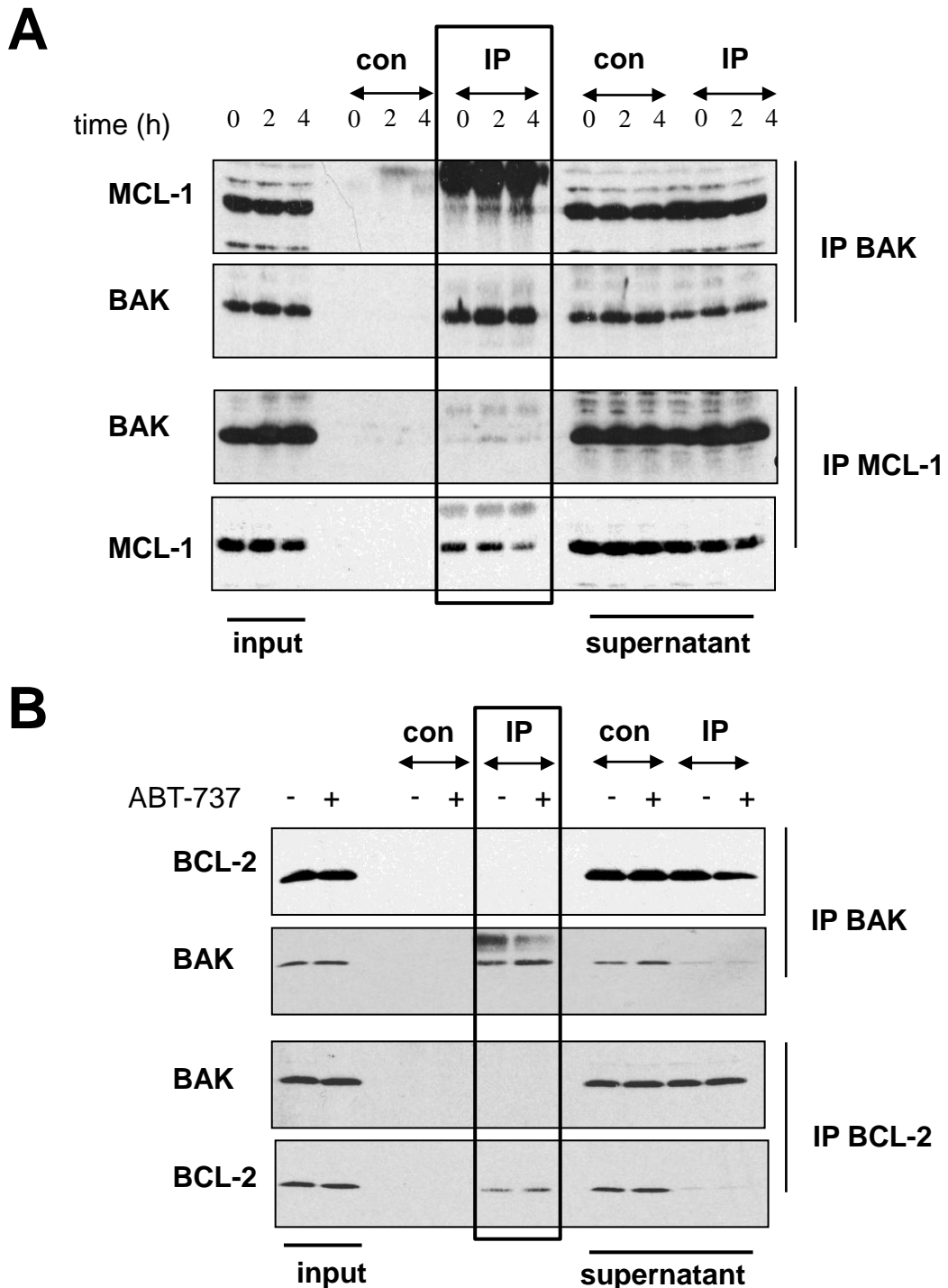


Figure 4.5 BAK is sequestered by MCL-1 but not by BCL-2

(A) Jurkat cells were exposed to ABT-737 for the indicated time periods then lysed in 1% CHAPS and subjected to immunoprecipitation using either anti-BAK (upper panel) or anti-MCL1 (lower panel). Supernatants and immunoprecipitates were analyzed for interaction partners by Western blotting. (B) Jurkat cells were exposed to ABT-737 for 4 h, lysed in 1% CHAPS and immunoprecipitation anti-BAK (upper panel) or anti-BCL2 (lower panel) were performed. Supernatants and immunoprecipitates were analysed for interaction partners by Western blotting. Asterisk in (A) denote IgH band and in (B) unspecific band.

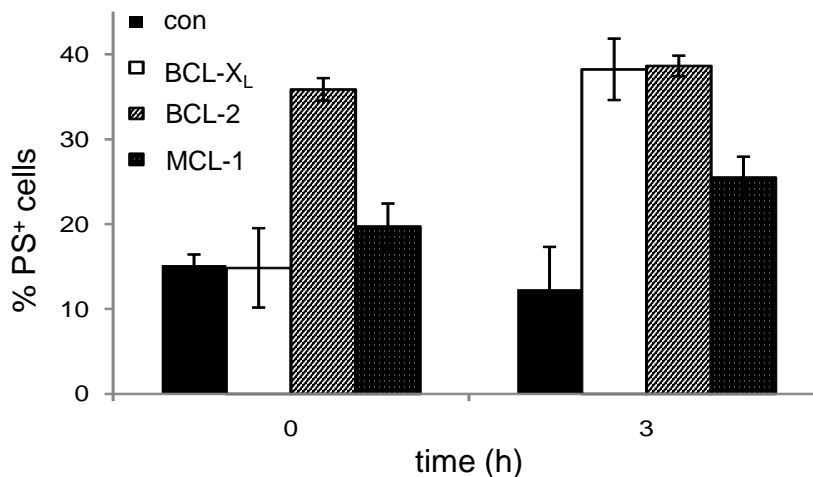
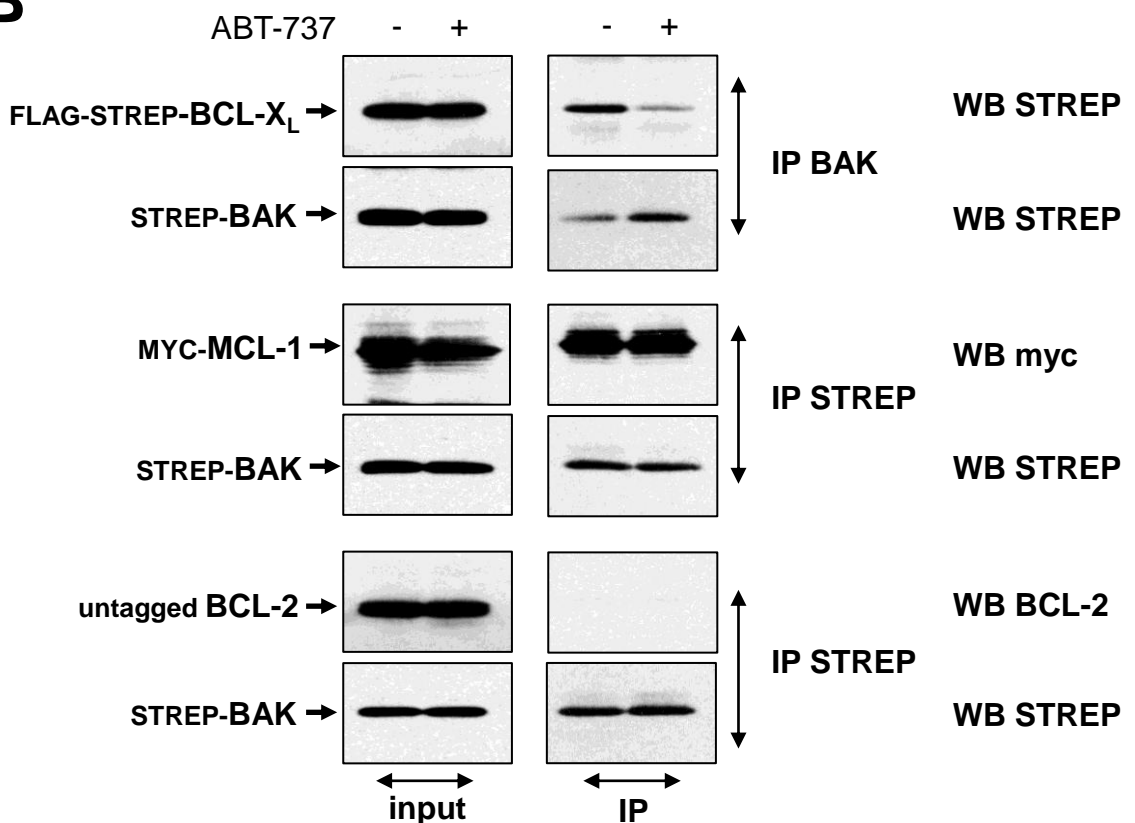
A**B**

Figure 4.6 Failure to reconstitute a BCL-2:BAK complex, MCL-1 associates with BAK but is not targeted by ABT-737

HEK293T cells were reconstituted with flag-strep double tagged BCL-X_L, untagged BCL-2 or myc-tagged MCL-1 and strep-tagged BAK or left untransfected. Externalisation of PS was determined from ABT-737 (5 μ M) exposed and control cells after 3 h. Data represent the mean S.E.M. of 4 experiments. (B) Interaction between anti-apoptotic BCL-2 proteins and BAK from control and ABT-737 exposed cells was analysed by immunoprecipitation using anti-strep (MCL-1 and BCL-2) or anti-BAK antibody (BCL-X_L). Interaction with antiapoptotic proteins was determined by Western blotting.

4.2.4 The BAK BH3 domain mediates interaction with BCL-X_L

The reconstitution system allows us to further investigate the role of the BAK BH3 domain in binding to BCL-X_L. If the BH3 domain of BAK is essential in binding to BCL-X_L then mutation of key residues should abolish binding. To explore this I generated two different BAK BH3 mutants L78A and D83A (Sattler, Liang et al. 1997; Willis, Chen et al. 2005). L78 points into the hydrophobic cleft of the BCL-X_L binding pocket and extensively interacts with several hydrophobic residues in BCL-X_L explaining the 800-fold decrease in binding affinity when substituted with alanine (Sattler, Liang et al. 1997). Complex formation is further stabilized by electrostatic interactions involving D83 which interacts with R139 of BCL-X_L and its substitution with alanine results in a 120-fold decrease in binding affinity (Sattler, Liang et al. 1997). Therefore both amino acids are required for heterodimerisation of BAK with BCL-X_L. Furthermore these residues are also implicated in mediating homodimerisation and thus promote BAK pro-apoptotic function (Willis, Chen et al. 2005; Dewson, Kratina et al. 2008).

To first determine if the BAK mutants L78A and D83A associate with BCL-X_L they were introduced into the reconstitution system (Fig. 4.7 B). After induction of BAK no cell death was observed with the L78A mutant, whereas cell death was observed with the D83A mutant. Exposure to ABT-737 did not induce cell death with both mutants when compared to wt BAK (Figure 4.7 B). Considering the decrease in binding affinity of both mutants to BCL-X_L this result would suggest that they can no longer associate with BCL-X_L. Therefore ABT-737 would have no effect as no primed BAK is bound to BCL-X_L.

To address this I immunoprecipitated BCL-X_L from BAK wt, L78A and D83A reconstituted cells (Fig. 4.7 C). Analysis of the supernatant revealed that the BH3 mutant L78A was like wt BAK nearly completely depleted from the supernatant of this immunoprecipitation indicating that all induced BAK L78A is complexed with BCL-X_L. Exposure to ABT-737 resulted in the detection of wt as well as L78A BAK in the supernatant, indicating that ABT-737 displaced wt and L78A BAK from BCL-X_L. In contrast BAK D83A was present in the supernatant of the immunoprecipitation in the control situation. This indicates that this mutant cannot associate as efficiently as wt BAK. These results confirm earlier reports that BAK associates with BCL-X_L through a BH3:groove interaction (Sattler, Liang et al. 1997; Willis, Chen et al. 2005). However, in contrast, to the decreased binding affinities for BAK BH3 mutants to

BCL-X_L, substitution of L78 with an alanine did not prevent association with BCL-X_L (Sattler, Liang et al. 1997). This result suggests that L78 is not solely required for association with BCL-X_L but plays an exclusive role for BAK pro-apoptotic function as this mutant did not induce cell death after its displacement from BCL-X_L by ABT-737.

Collectively these results demonstrate that ABT-737 induces apoptosis by displacing primed BAK from BCL-X_L. This pool of primed BAK (BH3 domain exposed) seems to be distinct and does not represent the majority of cellular BAK. Furthermore the BH3 domain of BAK is required to facilitate binding to BCL-X_L and the proportion of primed BAK bound appears sufficient to induce apoptosis as shown by the reconstitution of a BCL-X_L:BAK complex.

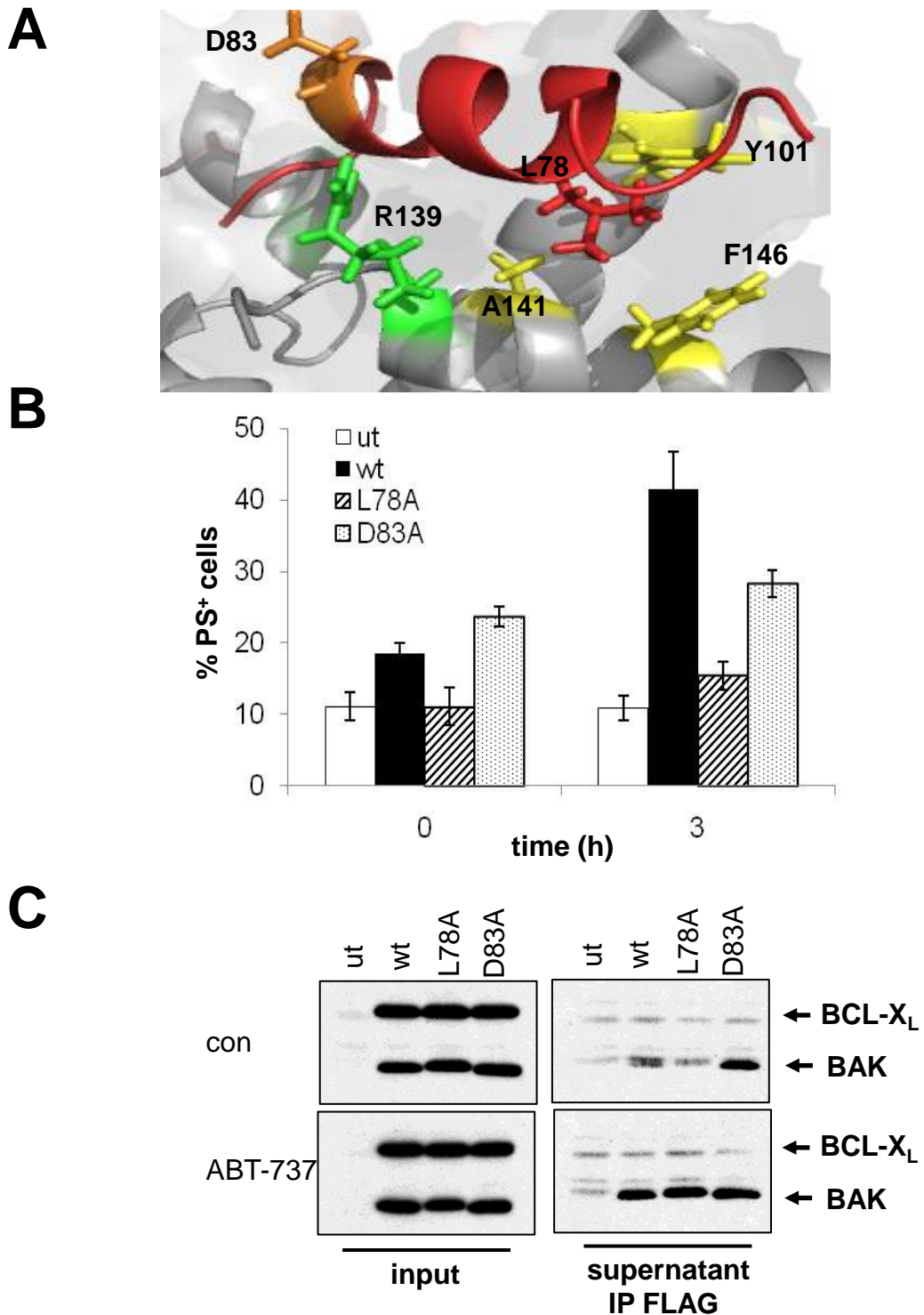


Figure 4.7 The BAK BH3 domain mediates interaction with BCL-X_L

(A) Ribbon presentation of BAK BH3 peptide (red) and BCL-X_L (grey). Side chains of BAK L78 (red) point into BCL-X_L hydrophobic binding pocket (yellow). BAK D83 (orange) interacts with BCL-X_L R139 (green). Figure was produced with PYMOL (2IMS, Sattler et. al 1997). (B) N-terminal strep-tagged BAK BH3 mutants L78A and D83A were introduced into the BCL-X_L reconstitution system into HEK293T cells and exposed to 5 μM ABT-737 for 3 h. Cell death was determined by PS externalization or (C) lysed in 1 % CHAPS and subjected to immunoprecipitation using FLAG beads to immunoprecipitate BCL-X_L. Interactions were determined by Western blotting using anti-BCL-X_L and anti BAK.

4.3 Discussion

BCL-2 family members associate through BH3:groove interactions and differences in both the sequence and structure of the BH3 domain and the groove result in distinct binding profiles. BAK has been described to be exclusively regulated by direct interaction with BCL-X_L and MCL-1 (Willis, Chen et al. 2005). However in Jurkat cells I found BAK was sequestered only by BCL-X_L, although exposure to ABT-737 did induce binding of BAK to MCL-1 (Fig. 4.1 and 4.5). Therefore in Jurkat cells neutralisation of BCL-X_L was sufficient to induce BAK-mediated apoptosis and no neutralisation of MCL-1 was required (Fig. 4.6). This specific subset of anti-apoptotic BCL-2 proteins involved in the negative regulation of BAK may vary depending on cell type. Contrary to an earlier report there was no evidence that primed BAK associates with BCL-2 (Fig. 4.6) (Ruffolo and Shore 2003). Reconstitution of a BCL-2:BAK complex was not possible as both binding partners did not appear to interact and BCL-2 was not able to protect cells from BAK induced cell death. Thus BCL-2 does not appear to be a direct inhibitor of BAK agreeing with earlier studies (Willis, Chen et al. 2005).

Association of anti- and pro-apoptotic BCL-2 proteins into heterodimers was described to occur through a BH3:groove interface, where the BH3 domain of pro-apoptotic BAK inserts into the hydrophobic groove of anti-apoptotic BCL-X_L (Sattler, Liang et al. 1997; Willis, Chen et al. 2005). Using the BH3 mimetic ABT-737 I provide further evidence that BAK associates with BCL-X_L through a BH3:groove interface as ABT-737 can displace BAK by competing for the hydrophobic groove of BCL-X_L (Fig. 4.1 D). Furthermore introducing a BAK D83A mutant into the reconstitution system revealed that substitution of D83A with alanine decreased interaction with BCL-X_L (Fig. 4.7). This provides evidence that the BH3 domain of BAK is required for association with BCL-X_L. In contrast substitution of L78 with alanine did not alter binding affinity to BCL-X_L. These results suggest that either other hydrophobic residues within the BAK BH3 domain can compensate for L78A mutation or electrostatic interactions dominate over hydrophobic ones in heterodimer stabilization (Sattler, Liang et al. 1997). The discrepancy of these results to the earlier defined binding affinities for these BAK mutants may be explained by the use of BAK BH3 peptides rather than the full length protein (Sattler, Liang et al. 1997).

CHAPTER 5:

**BAK undergoes an N-terminal conformational change
and oligomerizes during apoptosis-
both do not represent the point of no return**

5.1 Introduction

BAK activation is characterised by an N-terminal conformational change and oligomerisation into pores which induce the permeabilisation of the outer mitochondrial membrane. Despite intense study the precise mechanism and chronology of steps leading to an active BAK pore and how this then facilitates release of cytochrome *c* from the intermembrane space remains unknown.

Biochemical analysis has revealed that during apoptosis the N-terminal region of BAK repositions as assessed by exposure of a BAK antibody - AB-1 epitope, which exact epitope is not known, or increased trypsin sensitivity (Griffiths, Dubrez et al. 1999; Wei, Lindsten et al. 2000). The AB-1 epitope as well as the trypsin cleavage site must be occluded in inactive BAK. The trypsin cleavage site (R42) is localized in the middle of helix $\alpha 1$ and faces the protein core explaining the trypsin resistance of inactive BAK (Moldoveanu, Liu et al. 2006). Access of this cleavage site to trypsin during apoptosis requires the rotation of helix $\alpha 1$ in order to expose R42 on the protein surface. Rotation of helix $\alpha 1$ is inhibited in inactive BAK by the overlying helix $\alpha 2$. Therefore in order to expose the trypsin cleavage site, helix $\alpha 2$ first has to swing open, which releases and allows repositioning of helix $\alpha 1$. The N-terminal conformational change therefore represents a reorganisation rather than the simple exposure of helix $\alpha 1$.

Whether the N-terminal conformational change occurs simultaneously or subsequent to exposure of the BH3 domain is still unclear. Consequently it is not known if BCL-X_L-complexed BAK, which by inference must have an exposed BH3 domain, is N-terminally changed. In theory the flexible loop between helix $\alpha 1$ and $\alpha 3$ (containing the BH3 domain) could allow each conformational change to occur independently. It has been suggested that the AB-1 epitope is occluded in BAK complexed with BCL-X_L and can be released after an apoptotic stimulus while BAK is still bound to BCL-X_L (Griffiths, Corfe et al. 2001).

Another consistent feature observed during apoptosis is the formation of BAK dimers and high molecular weight complexes, which are proposed to release cytochrome *c* by forming pores in the outer mitochondrial membrane. The BAK pore complexes remain poorly defined in terms of composition, size, and structure. It has been proposed that formation of BAK oligomers is initiated by homo-dimer formation through a reciprocal BH3:groove interface involving the front site of BAK (Dewson, Kratina et al. 2008). This front:front/BH3:groove

BAK dimer represents the smallest subunit and association into oligomers requires a second interface represented by helix α_6 , the rear site of BAK (Dewson, Kratina et al. 2009).

Reorganisation of the N-terminus and oligomerisation of BAK occur early, before the detection of morphological and biochemical changes typical of apoptosis. Consequently they do not indicate the execution phase per se (Griffiths, Dubrez et al. 1999; Griffiths, Corfe et al. 2001; Makin, Corfe et al. 2001).

Experiments in this chapter are aimed at investigating N-terminal conformational change and formation of dimers and high molecular weight complexes during ABT-737 induced apoptosis. The N-terminal conformational change in BAK was found to occur after its displacement from BCL-X_L. Therefore primed BAK, which is complexed to BCL-X_L, is not yet N-terminally changed indicating that exposure of the BH3 domain and the N-terminal conformational change occur independently of each other. BAK dimers and high molecular weight complexes were detectable after ABT-737 exposure and therefore occurred after displacement of BAK from BCL-X_L. Although both N-terminal conformational change and BAK oligomerisation are detectable after 15 min of ABT-737 exposure they do not seem to represent the point of no return in BAK activation.

5.2 Results

5.2.1 BAK unmask the N-terminal region during apoptosis

One classical feature during the activation of BAK is the N-terminal conformational change which commonly is analysed by the exposure of the AB-1 epitope or increased trypsin sensitivity (Griffiths, Dubrez et al. 1999).

To assess if ABT-737 induces the N-terminal conformational change in BAK, cells were labelled with the BAK AB-1 antibody and analysed for AB-1-associated fluorescence by flow cytometry (Fig. 5.1 A). No AB-1 associated fluorescence was detected in control cells indicating that BAK was not N-terminal conformationally changed or that the AB-1 epitope was being masked by another protein. AB-1 associated fluorescence of the entire cell population increased following 15 min of ABT-737 exposure indicating that every cell contained N-terminal conformationally changed BAK. The increase in AB-1 associated fluorescence remained constant up to 3 h (Fig. 5.1 A).

Exposure of the AB-1 epitope can be also induced by cellular stress. To demonstrate that the observed N-terminal conformational change was a direct effect of neutralisation of BCL-X_L by ABT-737 and not a general stress response, cells were exposed to the inactive ABT-737 enantiomer (Fig. 5.1 A). Even after 3 h of enantiomer exposure no AB-1 associated fluorescence was detectable demonstrating that the exposure of the AB-1 epitope required displacement of BAK from BCL-X_L to occur.

The AB-1 staining demonstrates that ABT-737 induces exposure of the AB-1 epitope in every cell. However this method represents a qualitative measurement and therefore no conclusion can be drawn about the percentage of total cellular BAK this actually represents. To examine if the total cellular BAK underwent this change, limited trypsin proteolysis was performed. BAK becomes trypsin-sensitive at R42 only after N-terminal conformational change this leads to the generation of a 19 kDa fragment detectable with the Gly82 antibody (epitope within the BH3 domain, Fig. 5.4 A) (Wei, Lindsten et al. 2000). The p19 fragment was not detectable in control cells demonstrating that this trypsin cleavage site is occluded (Fig. 5.1 B). Following exposure to ABT-737 a p19 fragment was detected with the BAK Gly82 antibody and this could be blocked by inclusion of the protease inhibitor Pefabloc. However even after 3 h, trypsin-sensitive BAK represented only a discrete portion of the total BAK pool as the full

length protein was still detectable (Fig. 5.1 B). This indicates that following ABT-737 exposure only a discrete portion of BAK exposes the AB-1 epitope and becomes trypsin-sensitive. Additionally, the immunoreactivity of the NT and AB-1 antibodies on the Western blots decreased only slightly, presumably due to loss of their epitopes indicating that both epitopes must reside within the first 42 amino acids of BAK (Fig. 5.1 B).

To further confirm BAK conformational change following ABT-737 exposure AB-1 binding was analysed at single cell level by immunofluorescence staining. In control cells no AB-1 associated fluorescence was observed (Fig. 5.1 C). Within 15 min of ABT-737 exposure a punctated staining was detectable, which colocalised with mitotrackerRED-stained mitochondria (Figure 5.1 C, right panel). BAK staining occurred in most of the cells within 15 min and again it appeared that all cells show the presence of AB-1 positive BAK after only a short period of ABT-737 exposure.

Collectively these results demonstrate that ABT-737 induces exposure of the AB-1 epitope and accessibility of R42 to trypsin resulting in the generation of the p19 fragment. Both events occur as early as 15 min after ABT-737 exposure. However no conclusion about the conformational state of the N-terminus in primed BAK complexed with BCL-X_L can be drawn.

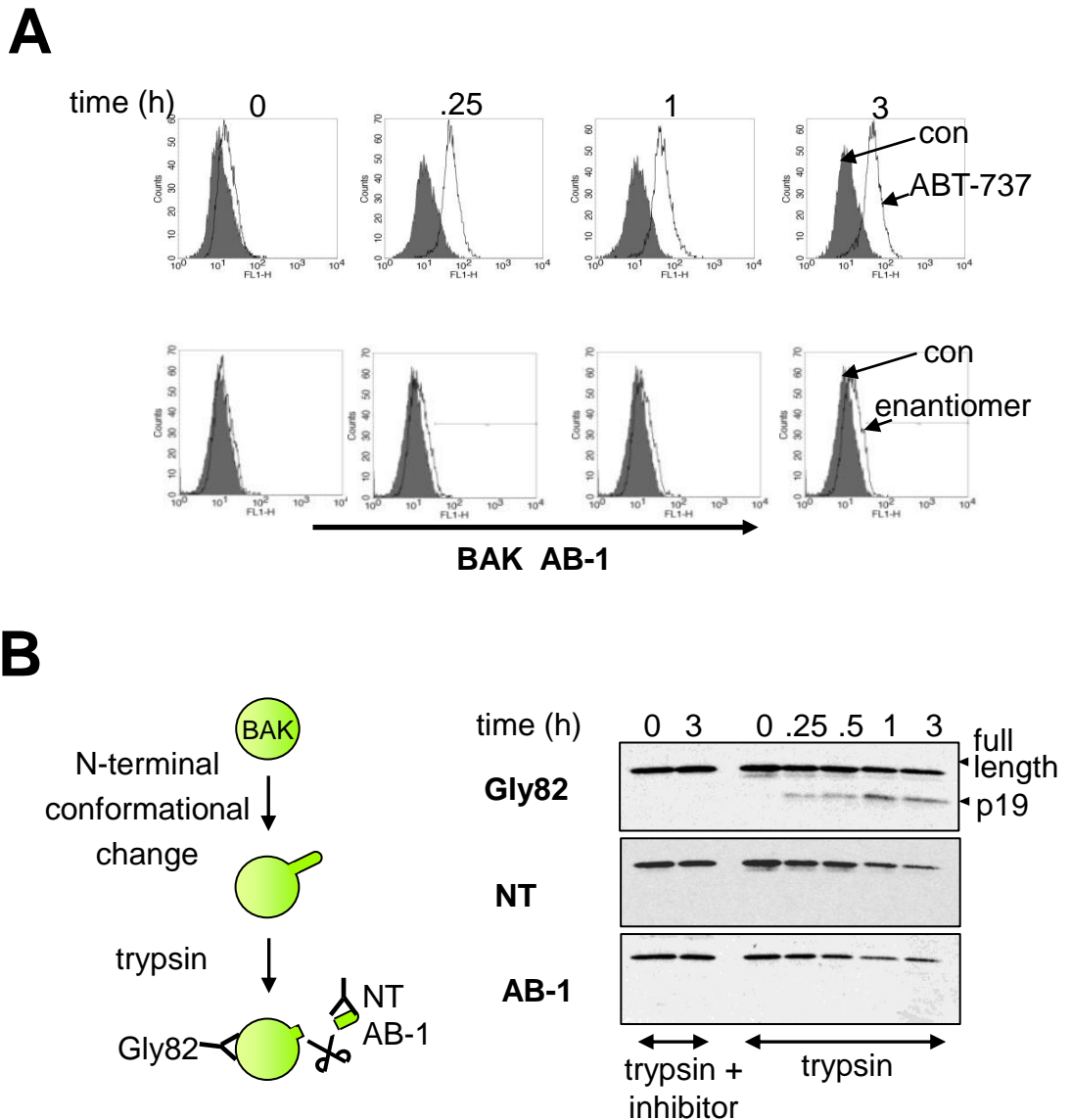


Figure 5.1 BAK undergoes an N-terminal conformational change during apoptosis

(A) Jurkat cells exposed to ABT-737 (5 μ M) or its inactive enantiomer (5 μ M) were intracellularly labelled with BAK AB-1 together with an ALEXA488 labeled secondary antibody. Cells were analysed by flow cytometry at the indicated time points (open histogram). Control (con), secondary antibody only (filled histogram) (B) left panel schematic representation of limited trypsin proteolysis. Right panel mitochondria enriched fractions from ABT-737 exposed or control cells were subjected to limited trypsin proteolysis or as control to trypsin in combination with the trypsin inhibitor Pefabloc. Trypsin cleavage of BAK was analysed using Gly82, NT or AB-1 antibodies.

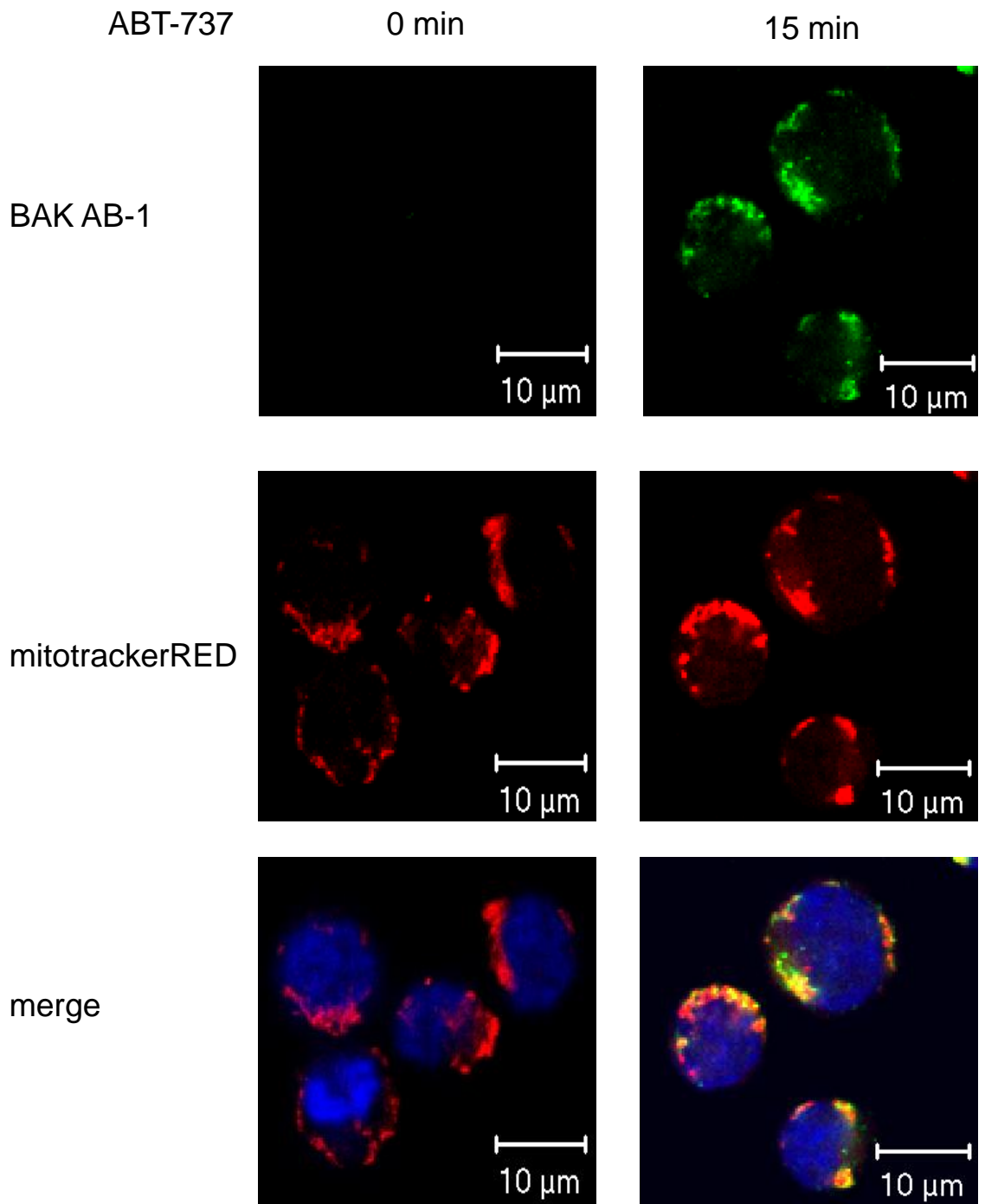
C

Figure 5.1 BAK undergoes an N-terminal conformational change during apoptosis

(C) ABT-737 exposed or con Jurkat cells were stained with the AB-1 antibody and ALEXA 488 labelled secondary antibody (green). Mitochondria were visualised by MitotrackerRED staining and Nuclei by HOECHST33342. Cells were analysed by confocal microscopy.

5.2.2 Primed BAK exposes the AB-1 epitope after displacement from BCL-X_L

To determine if the discrete pool of BAK which becomes trypsin sensitive/AB-1 exposed represents primed BAK after its displacement from BCL-X_L, I performed a double immunoprecipitation procedure (Fig. 5.2 A). N-terminal conformational changed BAK was immunoprecipitated from Jurkat cell lysates using the AB-1 antibody. The supernatant of this immunoprecipitation was then subjected to a second immunoprecipitation for BCL-X_L.

Based on my earlier results in control cells total cellular BAK, which includes BCL-X_L complexed primed BAK, should not expose the AB-1 epitope (Fig. 5.1). Therefore AB-1 should not precipitate any BAK as its epitope is buried. Consequently the BCL-X_L:BAK complex should reside in the supernatant of the AB-1 immunoprecipitation and should be isolated using the BCL-X_L antibody (Fig. 5.2 A a). In control Jurkat cells, BAK was not immunoprecipitated by the AB-1 antibody and no BCL-X_L co-precipitated (Fig. 5.2 B, middle panel, box). As AB-1 did not deplete any BAK, the BAK:BCL-X_L complex was localized to the supernatant of the AB-1 immunoprecipitation (Fig. 5.2 B, lower panel, box) This confirms my earlier finding that in control cells the AB-1 epitope is not exposed (Fig. 5.1). Consequently BCL-X_L complexed primed BAK does not expose the AB-1 epitope.

Exposure to ABT-737 resulted in an exposure of the AB-1 epitope (Fig. 5.1) and it was suggested that this conformational change occurs while BAK is still bound to BCL-X_L after exposure to an apoptotic stimulus (Griffiths, Corfe et al. 2001). If ABT-737 induces exposure of the AB-1 epitope while BAK is bound to BCL-X_L then BCL-X_L should co-immunoprecipitate with BAK using AB-1. Consequently no BCL-X_L:BAK complex should be present in the supernatant of the AB-1 immunoprecipitation (Fig 5.2 A b). Exposure to ABT-737 for 15 min resulted in the immunoprecipitation of BAK by AB-1, but BCL-X_L did not co-precipitate (Fig. 5.2 B, middle panel). Furthermore very little BAK was found complexed with BCL-X_L in the supernatant of the AB-1 immunoprecipitation. (Fig. 5.2 B, lower panel). This suggests that the exposure of the AB-1 epitope does not occur while BAK is sequestered by BCL-X_L. In addition after 15 min of ABT-737 exposure the discrete proportion of primed BAK was displaced from BCL-X_L and a discrete proportion of BAK is N-terminal changed. This reinforces the idea that the distinct proportion of primed BAK exposes after its displacement from BCL-X_L the AB-1 epitope demonstrating the correlation between both distinct pools.

As a positive control immunoprecipitations were repeated in the presence of Triton X-100, which artificially induces BAK N-terminal conformational change (Dewson, Kratina et al. 2008). Under these conditions, BAK could be immunoprecipitated by AB-1 from control cells (Fig. 5.2 B, middle panel). Furthermore BCL-X_L co-immunoprecipitated with BAK indicating that Triton X-100 induced exposure of the AB-1 epitope while primed BAK is still bound to BCL-X_L. Analysis of the second anti-BCL-X_L immunoprecipitation revealed that the BCL-X_L:BAK complex was also present in the supernatant of the AB-1 immunoprecipitation (Fig. 5.2 B, lower panel). Therefore this concentration of Triton X-100 did not induce the N-terminal conformational change in all primed BAK complexed with BCL-X_L resulting in a heterogeneous population of N-terminal changed and occluded primed BAK complexed with BCL-X_L.

Collectively these results demonstrate that BCL-X_L complexed, primed BAK exposes the AB-1 epitope after its displacement from BCL-X_L. Therefore both distinct portions correlate and ABT-737 does not induce the exposure of the AB-1 epitope while primed BAK is bound to BCL-X_L.

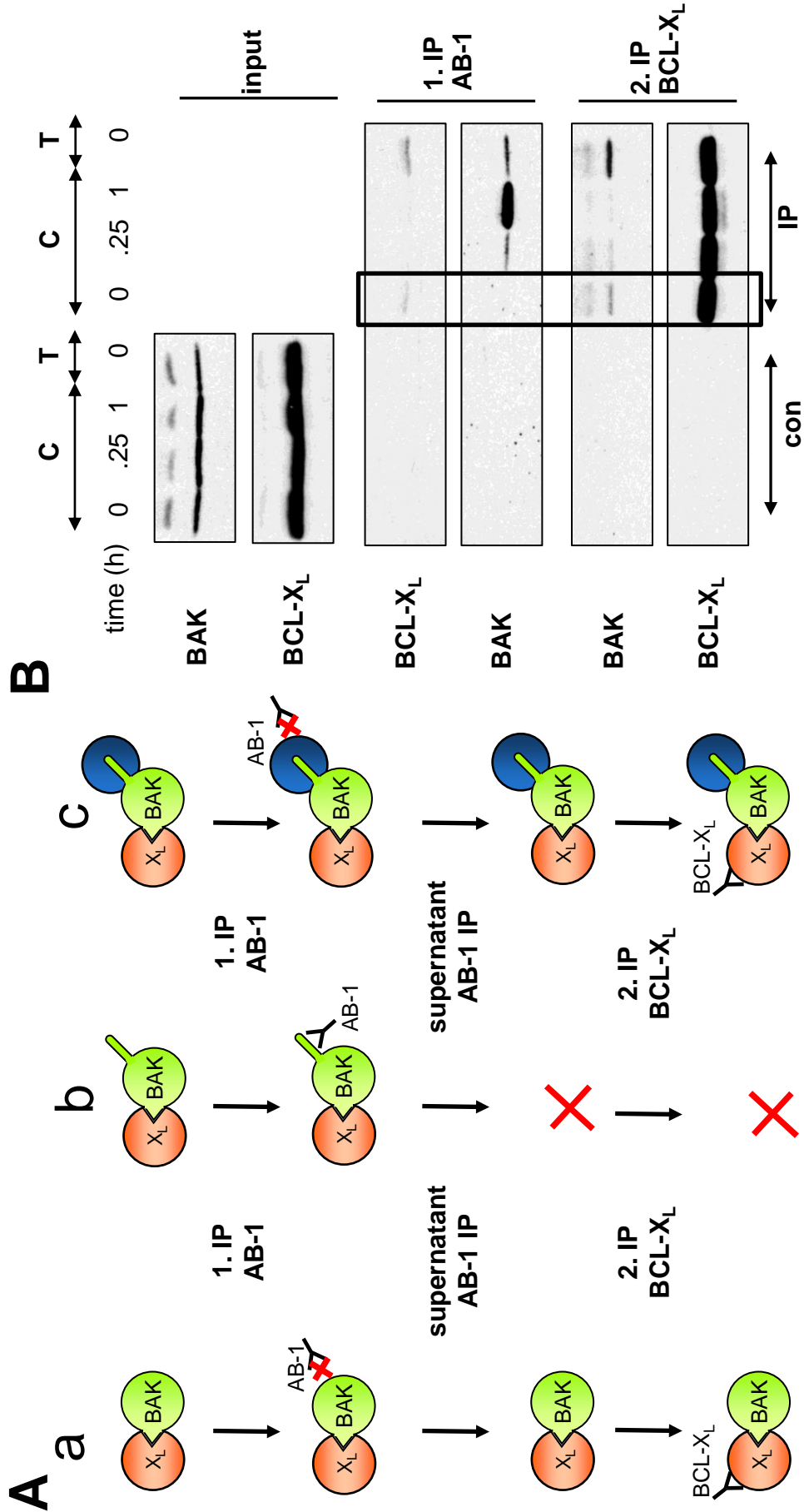


Figure 5.2 Exposure of the AB-1 epitope occurs after displacement of primed BAK from BCL- X_L .

(A) Schematic representation for double AB-1 / BCL- X_L immunoprecipitation. The three possibilities for primed BAK are shown: a N-terminus is not exposed, b N-terminus is exposed, c N-terminus is exposed but mask by another protein (blue circle) (B) Control and ABT-737 exposed Jurkat cells were either lysed in 1% CHAPS (C) or in CHAPS supplemented with 1% Triton X-100 (T) when indicated and subjected to immunoprecipitation using AB-1 (middle panel). BCL- X_L was immunoprecipitated from the supernatant of AB-1 immunoprecipitation (lower panel). Interactions between BAK and BCL- X_L were determined by Western blotting.

5.2.3 Primed BAK is not N-terminally changed

Primed BAK complexed with BCL-X_L does not expose the AB-1 epitope leading to two possible explanations: either primed BAK has not yet undergone the N-terminal change or secondly the N-terminus is changed, but the recognition sites for AB-1 is masked by a protein(s), which is released by the more stringent detergent Triton X-100 or by displacement from BCL-X_L (Fig. 5.2 A c).

To further investigate if the AB-1 epitope is exposed but masked in primed BAK complexed with BCL-X_L I switched to the BCL-X_L:BAK reconstitution system and again performed the double immunoprecipitations (Fig. 5.2 A). In control cell BAK was immunoprecipitated by AB-1 and BCL-X_L co-precipitated (Fig. 5.3 A). This result confirms that the exposure of the AB-1 epitope can occur while bound to BCL-X_L and reflects the result obtained with Triton X-100 (Fig. 5.2 B, middle panel). Not all primed BAK was N-terminal conformationally changed as the BCL-X_L:BAK complex was also immunoprecipitated from the AB-1 supernatant detected by anti-BCL-X_L immunoprecipitation (Fig. 5.3 A). Therefore in the BCL-X_L:BAK reconstitution system induced BAK is present as a heterogeneous population including N-terminal conformationally changed and N-terminal occluded forms.

Furthermore these results demonstrate that masking of the N-terminus by another protein in a detergent dependent manner is rather unlikely. The detergent used for this double immunoprecipitation was CHAPS. Therefore if the stringency of CHAPS is not sufficient to remove proteins masking the AB-1 epitope in primed BAK then no N-terminally changed BAK should be detectable in control cells.

Another argument is that the nature of the reconstitution system requires the overexpression of BAK. Therefore any protein(s) that would mask the AB-1 epitope would not be present in a sufficient cellular concentration to mask all N-terminal conformationally changed BAK resulting in the detected heterogeneous population of BCL-X_L complexed, primed BAK. However this seems unlikely as the expression levels of induced BAK correlate well with the endogenous levels in wt MEFs (Fig. 5.3 B). This result reinforces the idea that endogenous primed BAK is not yet N-terminal conformationally changed.

Collectively, these results demonstrate that primed BAK complexed with BCL-X_L is not yet N-terminal conformationally changed and thus possible masking of AB-1 epitope in primed

BAK is excluded. Therefore the N-terminal conformational change occurs independently and downstream from the exposure of the BH3 domain.

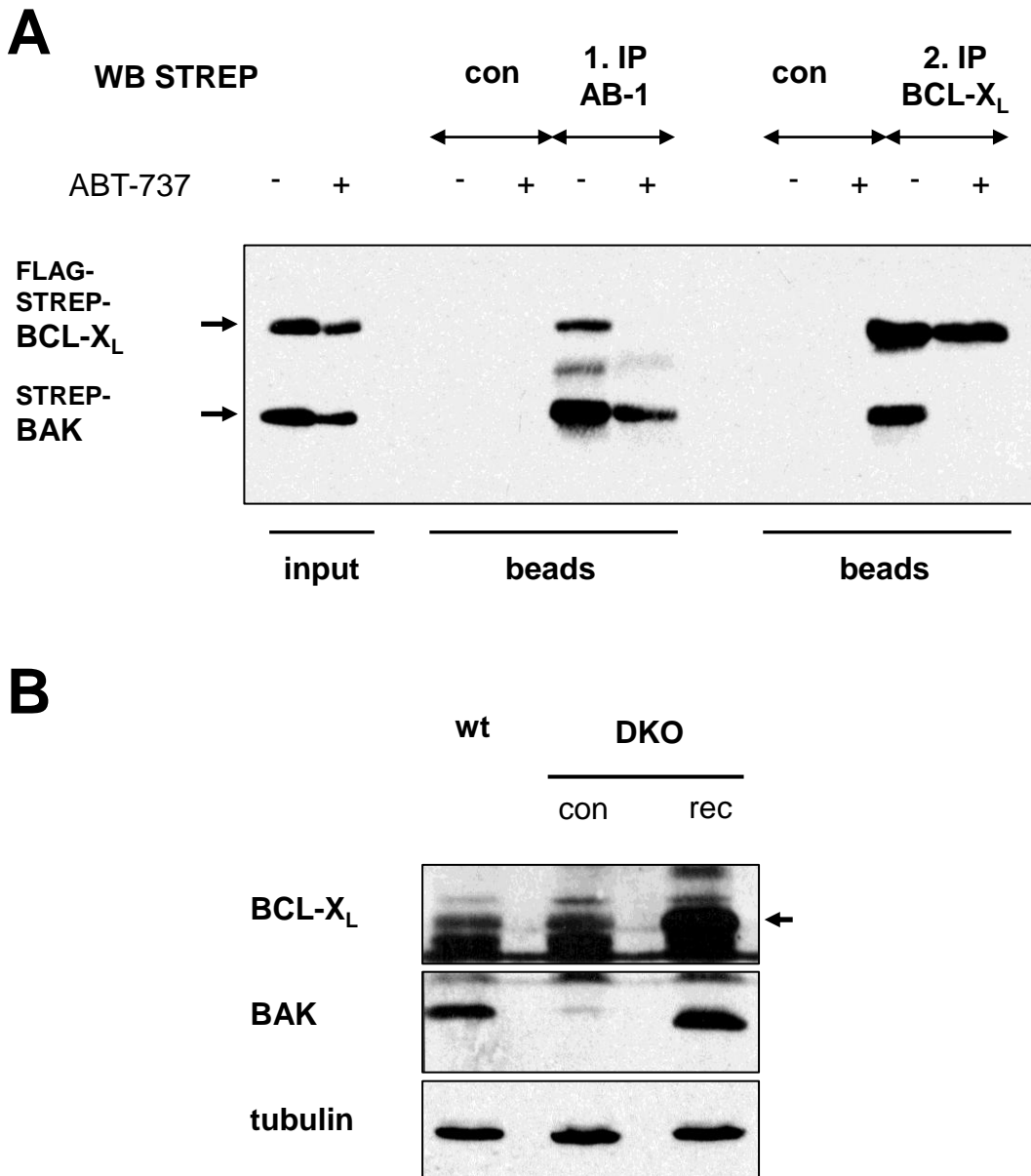


Figure 5.3 N-terminus is not exposed in primed BAK

(A) BCL-X_L:BAK reconstituted and control DKO MEF cells were exposed to 30 μ M ABT-737 for 4 h and lysed in 1 % CHAPS. Lysates were subjected to immunoprecipitation using AB-1. BCL-X_L was immunoprecipitated from the supernatant of the AB-1 immunoprecipitation by anti-BCL-X_L. Interaction of BAK with BCL-X_L was analysed by Western blotting using anti-strep. (B) wt MEF and control (con) or BCL-X_L:BAK reconstituted (rec) DKO MEF cells were lysed in 1 % CHAPS and protein levels were determined by Western blotting using anti-strep.

5.2.4 The N-terminal conformational change: a reorganisation of the N-terminal region

The N-terminal conformational change results in trypsin sensitivity and exposure of the AB-1 epitope. To expose the relevant trypsin cleavage site (R42) on the protein surface in order to allow trypsin access helix $\alpha 1$ has to rotate. To facilitate this the overlaying helix $\alpha 2$ has to be repositioned first. The N-terminal conformational change therefore represents a reorganisation rather than the simple exposure of helix $\alpha 1$.

To further investigate the changes represented by the N-terminal conformational change I mapped the epitope of the AB-1 antibody, which was not known exactly. My results suggest that the epitope resides within the first 42 amino acids of BAK as it cannot recognize the p19 trypsin cleavage fragment (Fig. 5.1 B). To analyse this BAK was truncated up to amino acid 42 to mimic the p19 fragment. BAK Δ N42 failed to bind AB-1 antibody demonstrating that the epitope resides within the first 42 amino acids of BAK (Fig. 5.4 C).

In order to map the epitope more precisely different mutations (T31R, F35A and Y38R) which reside within helix $\alpha 1$ were generated (Fig. 5.4 C). These mutants were originally designed to construct a constitutively N-terminal conformational changed BAK (Fig. 5.8 C). Substitution of Y38 with an arginine, abolished binding of AB-1 as analysed by Western blotting, whereas immunoreactivity was not altered with a T31R or F35A mutant. This suggests that the AB-1 epitope centres around amino acid 38 (Fig 5.4 C). To confirm this I reconstituted a BCL-X_L:BAKY38R complex (Fig. 4.3) followed by AB-1 staining (Fig. 5.4 D). In comparison to reconstituted wt BAK and the T31R mutant no increase in AB-1 associated fluorescence was detectable when Y38R mutant was introduced into the reconstitution system. To exclude that this result is not a consequence of the mutant affecting N-terminal conformational change, reconstituted BCL-X_L:BAK mutant complexes were subjected to limited trypsin proteolysis (Fig. 5.4 E). Both of the reconstituted BAK mutants as well as wt BAK showed the characteristic p19 trypsin cleavage fragment. These results demonstrate that BAK Y38R exposes its N-terminus analogous to wt BAK but cannot be recognised by the AB-1 antibody.

Consequently the epitope of AB-1 maps around amino acid 38 near the trypsin cleavage site and downstream of overlaying helix $\alpha 2$ (Fig. 5.4 B). To expose the AB-1 epitope the same conformational changes are required as for exposing the trypsin cleavage site: helix $\alpha 2$

requires repositioning to allow the rotation of helix $\alpha 1$ in order to expose these residues to the protein surface. Therefore the N-terminal conformational change represents a reorganisation of the N-terminal region rather than a simple exposure of helix $\alpha 1$ (Kim, Tu et al. 2009).

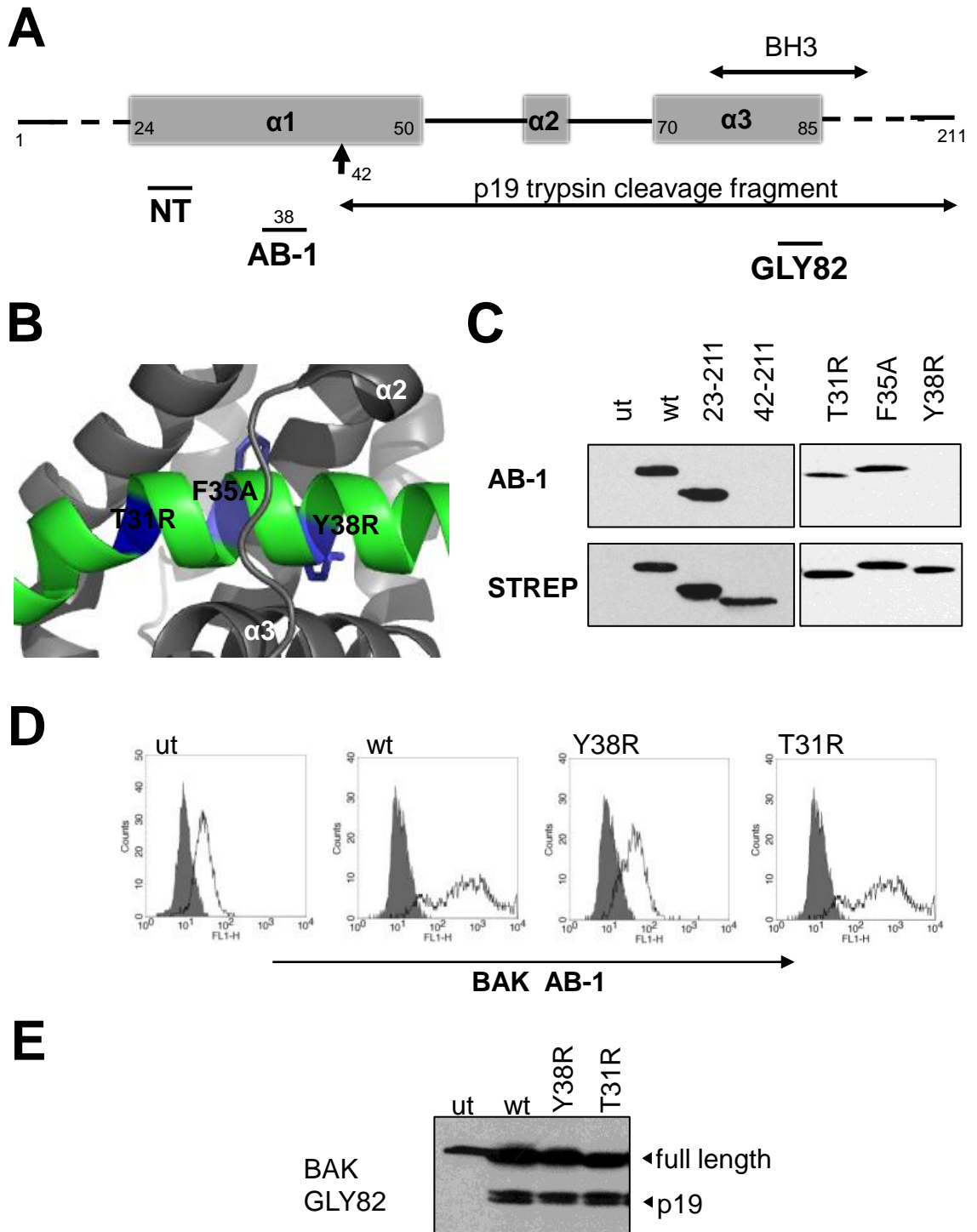


Figure 5.4 The epitopes of the AB-1 antibody reside on helix $\alpha 1$

(A) Schematic representation of BAK and location of NT, AB-1 and Gly82 epitopes. Trypsin cleavage site relevant for limited trypsin proteolysis is marked by arrows and the resulting p19 fragment is shown. (B) Ribbon diagram showing the localisation of BAK mutants T31R, F35A and Y38R (blue) on helix $\alpha 1$ (green). (C) BAK mutants or BAK truncations were transiently transfected into HEK293T cells. Detection of BAK mutants by AB-1 antibody was determined by Western blotting. (D) BAK N-terminal mutants were introduced into the BCL- X_L reconstitution system. Detection by AB-1 was determined by flow cytometry using AB-1 in combination with secondary ALEXA 488 intracellularly stained cells. (E) Exposure of N-terminus was verified by limited trypsin proteolysis and generation of the p19 trypsin cleavage fragment was determined by Western blotting.

5.2.5 BAK forms dimers and high molecular weight complexes during apoptosis

Aggregation of BAK into dimers and high molecular weight complexes is a characteristic of its activation and can be assessed by introducing disulphide bonds into BAK using the redox catalyst CuPhe (Falke, Dernburg et al. 1988; Dewson, Kratina et al. 2008). In control cells CuPhe induces the formation of an intramolecular disulphide bond in BAK between the N-terminal Cys14 and C-terminal Cys166 residues resulting in a faster migrating band on SDS PAGE termed M_X (Fig. 5.5 A, (Wei, Lindsten et al. 2000). Addition of CuPhe to mitochondria from control cells revealed that all BAK was present in the M_X conformation (Fig. 5.4). In agreement with my earlier results (Fig. 5.1 and 5.2) this indicates that total cellular BAK which also includes BCL- X_L complexed BAK is not N-terminal conformationally changed as the N-terminal C14 must be constrained near helix α_6 located C166.

Exposure to ABT-737 results in the N-terminal conformational change of BAK (Fig. 5.1 and 5.2). Consequently C14 and C166 lose proximity and cannot be disulphide linked anymore resulting in the loss of the M_X band. Indeed ABT-737 exposure resulted in the decrease of the M_X band and this was accompanied by the detection of BAK dimers (D) and high molecular weight complexes (D^X). Correlating with detection of the N-terminal conformational change, BAK aggregates were obtained as soon as 15 min after ABT-737 exposure and increased over time (see Fig. 5.1, 5.2 and 5.5). However at this time point the M_X conformation was also detectable. This demonstrates that after 15 min of ABT-737 exposure a distinct portion of BAK oligomerises apparently correlating with the portion of N-terminal conformationally changed BAK. This would suggest that the initial oligomerised BAK represents the portion of BAK which is N-terminal conformationally changed at 15 min of ABT-737 exposure. Therefore as soon as BAK is N-terminal conformationally changed it oligomerises.

All higher molecular weight complexes as well as the M_X form were no longer apparent under reducing conditions demonstrating that the immunoreactivity observed was not an artefact but in fact represented different species of BAK (Fig. 5.5).

5.2.7 Auto-activation

It is suggested that oligomerised BAK can potentially induce oligomerisation of inactive/monomeric BAK causing a cascade of BAK auto-activation (Ruffolo and Shore 2003).

Supporting this I found that generation of the trypsin cleavage fragment p19 increased over time (Fig. 5.1 B) together with the increased accessibility of the AB-1 epitope (Fig. 5.2 B). As primed BAK is displaced from BCL-X_L after 15 min of ABT-737 exposure this increase in N-terminal conformationally changed BAK can be explained by a feed forward loop. Thus the initial N-terminal conformationally changed portion of primed BAK present after 15 min of ABT-737 exposure can induce the N-terminal conformational change in N-terminal occluded BAK. Also the formation of dimers and high molecular weight complexes and consequently the loss of the M_X conformation increase over time (Fig. 5.5). This indicates that initial oligomerised BAK can induce oligomerisation of monomeric BAK.

Therefore not only the N-terminal conformational change seems to feed forward but also oligomerisation resulting in an auto-activation loop.

5.2.8 N-terminal conformational change occurs before BAK oligomerisation

Both the N-terminal conformational change and formation of BAK oligomers were detectable within 15 min of ABT-737 exposure suggesting that both events occur coincidentally. To investigate the relationship of both events N-terminal conformational change was inhibited prior to BAK activation.

Inhibition of the N-terminal conformational change was achieved by introduction of the intramolecular disulfide bond in inactive BAK using CuPhe. This leaves BAK trapped in the M_X conformation and therefore unable to undergo the N-terminal conformational change during its activation. This required a cell free system and in order to activate BAK a mitochondrial enriched fraction was incubated at 42°C (Pagliari, Kuwana et al. 2005). Incubation at 42 °C induced BAK oligomerisation as judged by the formation of dimers and other high molecular species (Fig 5.6 A). However when BAK was restrained in the M_X conformation prior to heat activation no dimers or high molecular weight complexes were detected (Fig 5.6 A). This indicates that the N-terminal conformational change occurs before the formation of dimers and high molecular weight complexes and is required for BAK oligomerisation.

Formation of BAK oligomers is associated with MOMP and consequently cytochrome *c* release. The observed block in the formation of BAK aggregates when BAK N-terminal conformational change was inhibited should therefore result in a decrease in cytochrome *c* release (Fig 5.6 B). Incubation of mitochondrial fractions at 42°C induced cytochrome *c* release which correlated with heat induced BAK oligomerisation. However when the N-terminal conformational change was inhibited with CuPhe and no BAK oligomers were detectable, cytochrome *c* release was also reduced in a CuPhe concentration dependent manner (Fig 5.6 B). These results suggest that N-terminal conformational change has to precede BAK oligomerisation.

These results also demonstrate that the initial N-terminal conformationally changed proportion of BAK detectable after 15 min of ABT-737 exposure (Fig. 5.1 B and 5.2 B) represents the same portion of BAK which is oligomerised at this time point (Fig.5.5) as oligomerisation cannot occur without N-terminal conformational change.

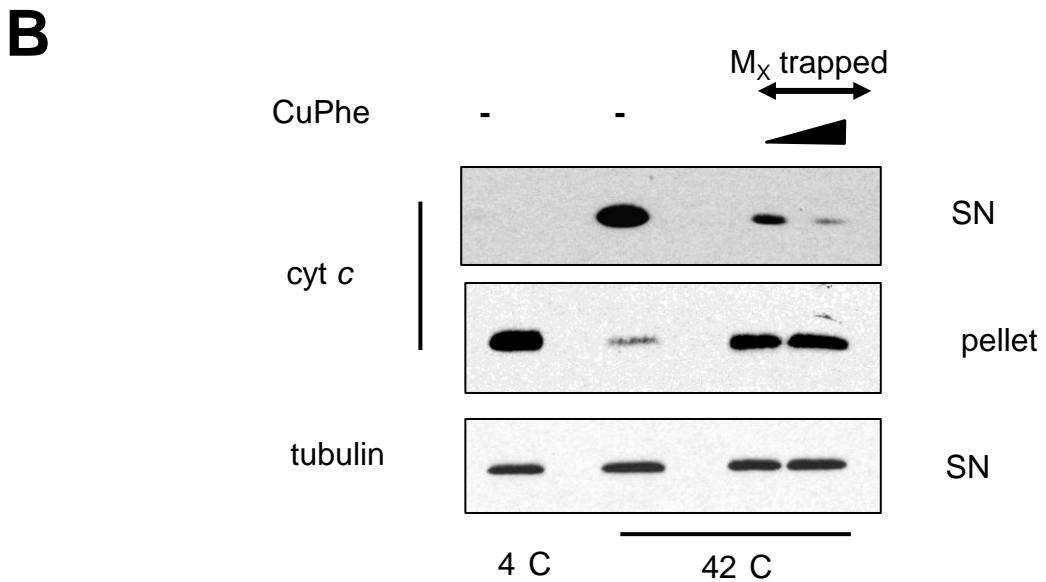
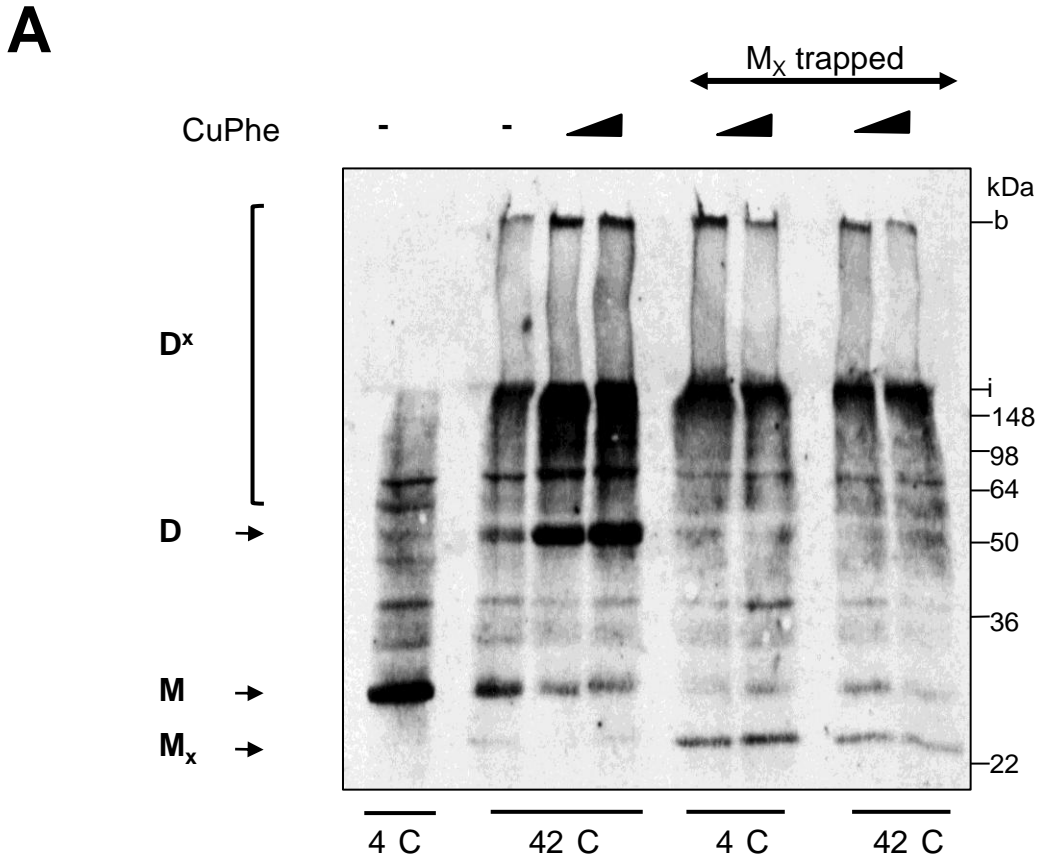


Figure 5.6 N-terminal conformational change is required for BAK proapoptotic function

(A) Mitochondria enriched fractions from control Jurkat cells were exposed to increasing concentrations of CuPhe prior to heat incubation. Disulphide stabilised dimers were incubated at 42 C for 30 min or left at 4 C and heat induced dimer formation was analysed by exposure to CuPhe and Western blotting under non-reducing conditions. (B) Cytochrome *c* release under these conditions was determined by Western blotting.

5.2.9 N-terminal conformational change as well as aggregation of BAK are not sufficient for the commitment to apoptosis

It has been proposed that N-terminal conformational change of BAK and BAX as well as oligomerisation occur before the detection of morphological and biochemical changes typical of apoptosis and are therefore not indicative of the execution phase per se (Griffiths, Dubrez et al. 1999; Makin, Corfe et al. 2001). Correlating with this my results show that the N-terminal conformational change as well as formation of dimers and high molecular weight complexes occur as soon as 15 min after ABT-737 exposure, preceding cytochrome *c* release and PS externalisation (Fig. 3.3 A and 3.4).

To further investigate the chronology N-terminal conformational change was analysed together with cytochrome *c* release as indicator for MOMP in individual cells by confocal microscopy. ABT-737 exposed cells were co-stained with AB-1 (green fluorescence) and cytochrome *c* (red fluorescence) antibodies. No AB-1 associated fluorescence was detectable in control cells and cytochrome *c* staining was punctate indicating intact mitochondria (Fig. 5.7). Exposure to ABT-737 for 15 min resulted in the detection of AB-1 associated immunofluorescence indicative of a BAK N-terminal conformational change. However no release of cytochrome *c* was detected at this time point as staining was still punctate. After 1 h, cytochrome *c* staining became diffuse suggesting release into the cytoplasm indicating the perturbation of mitochondria.

These results demonstrate that BAK N-terminal conformational change precedes the perturbation of mitochondria and concomitant cytochrome *c* release. This provides the possibility that the N-terminal conformational change is not sufficient to transform primed BAK into a “killer” protein.

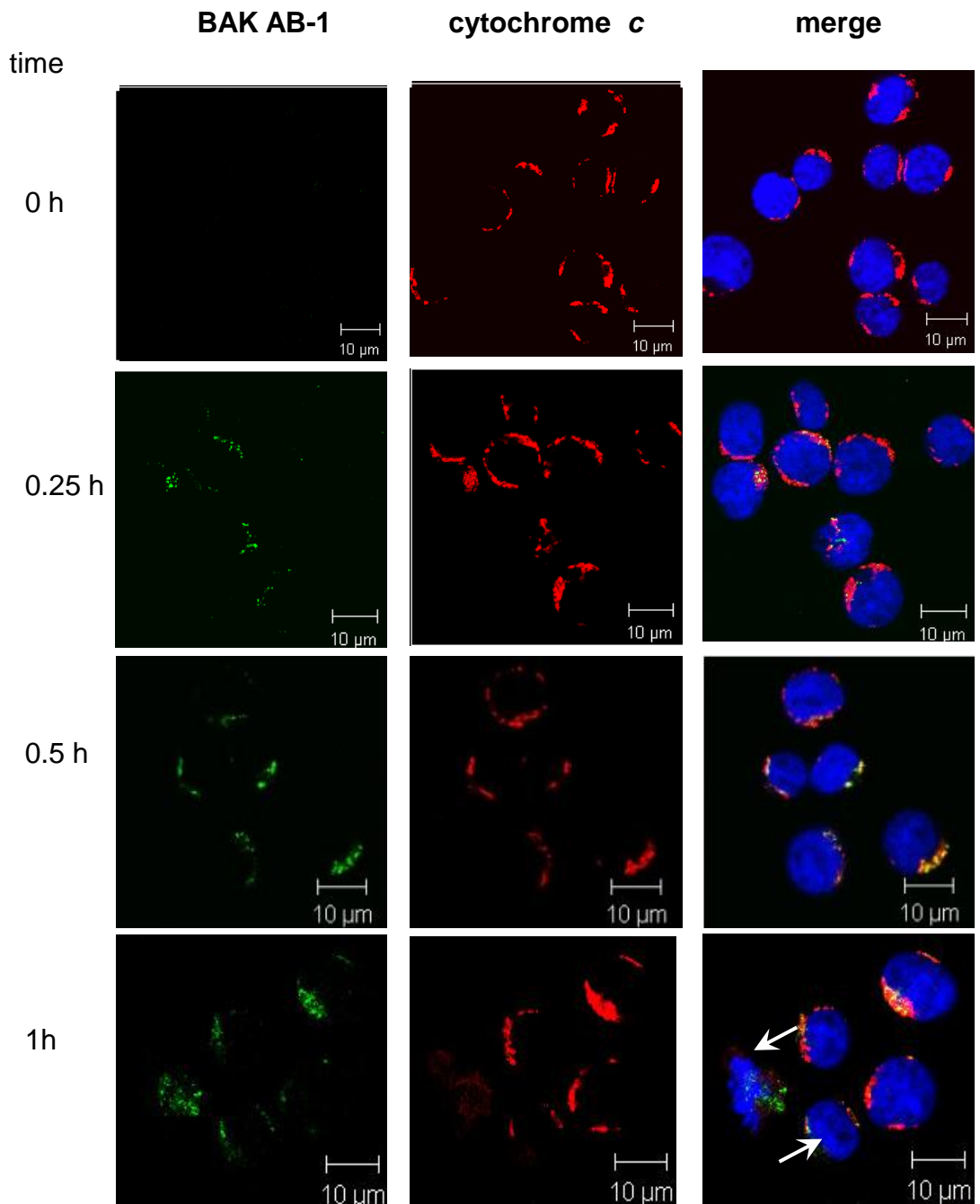


Figure 5.7 N-terminal conformational change precedes cytochrome c release
 Jurkat cells were exposed to ABT-737 for indicated times and intracellularly co-stained with anti-AB-1 (secondary antibody ALEXA 488 labelled) and cytochrome c (secondary anti-body 548 labelled). Nuclei were stained with HOECHST33342. Cell were analysed by confocal microscopy.

Although the N-terminal conformational change was required for BAK pro-apoptotic function as its inhibition blocked MOMP (Fig. 5.6) it is unclear whether it represents the point of no return in BAK activation. If the N-terminal conformational change is the crucial step to commit apoptosis then deletion of the N-terminal region should result in “super-active” BAK with enhanced killing activity compared to wt BAK. To analyse this I constructed a number of different N-terminal strep-tagged BAK truncations (Fig. 5.8 A).

Deletions included the predicted unstructured N-terminal region of BAK, $\Delta N23$ misses the region before helix $\alpha 1$, $\Delta N42$ lacks part of helix $\alpha 1$, $\Delta N69$ begins in the loop region between helix $\alpha 1$ and $\alpha 2$. BAK $\Delta N82$ was generated as positive control as it lacks the first part of the BH3 domain. Therefore it should not display any BAK pro-apoptotic function as the BH3 domain is necessary for the formation of BAK oligomers (Dewson, Kratina et al. 2008). Analysis of the killing activity of these BAK truncations by transient transfection into BAK/BAX DKO MEF cells revealed that all mutants except BAK $\Delta N82$ displayed killing activity comparable to wt BAK (Fig. 5.8 B). As expected BAK $\Delta N82$ did not show killing activity reinforcing the idea that the BH3 domain is required for BAK pro-apoptotic function. This demonstrates that the N-terminal region of BAK up to amino acid 69 is dispensable for its pro-apoptotic function. Furthermore deletion up to amino acid 69 did not lead to a “super-active” BAK indicating that the N-terminal conformational change is not the point of no return in BAK activation (Fig. 5.8 B).

To further confirm that the N-terminal conformational change did not represent the commitment step in BAK activation, mutations which restrict the N-terminal region were generated. All the BAK mutants were designed to prevent correct folding of the N-terminal region and as a result possibly mimic N-terminal conformationally changed BAK. Mutants T31R and Y38R reside within helix $\alpha 1$ and M60A and L63R are positioned within the loop region between helix $\alpha 1$ and $\alpha 2$. All the mutants retained killing activity (Fig. 5.8 C), however by destabilizing the N-terminal region, no enhanced killing of these mutants, compared to wt BAK, was observed (Fig. 5.8 C). These results further confirmed that the N-terminal conformational change does not represent the point of no return in the activation of BAK.

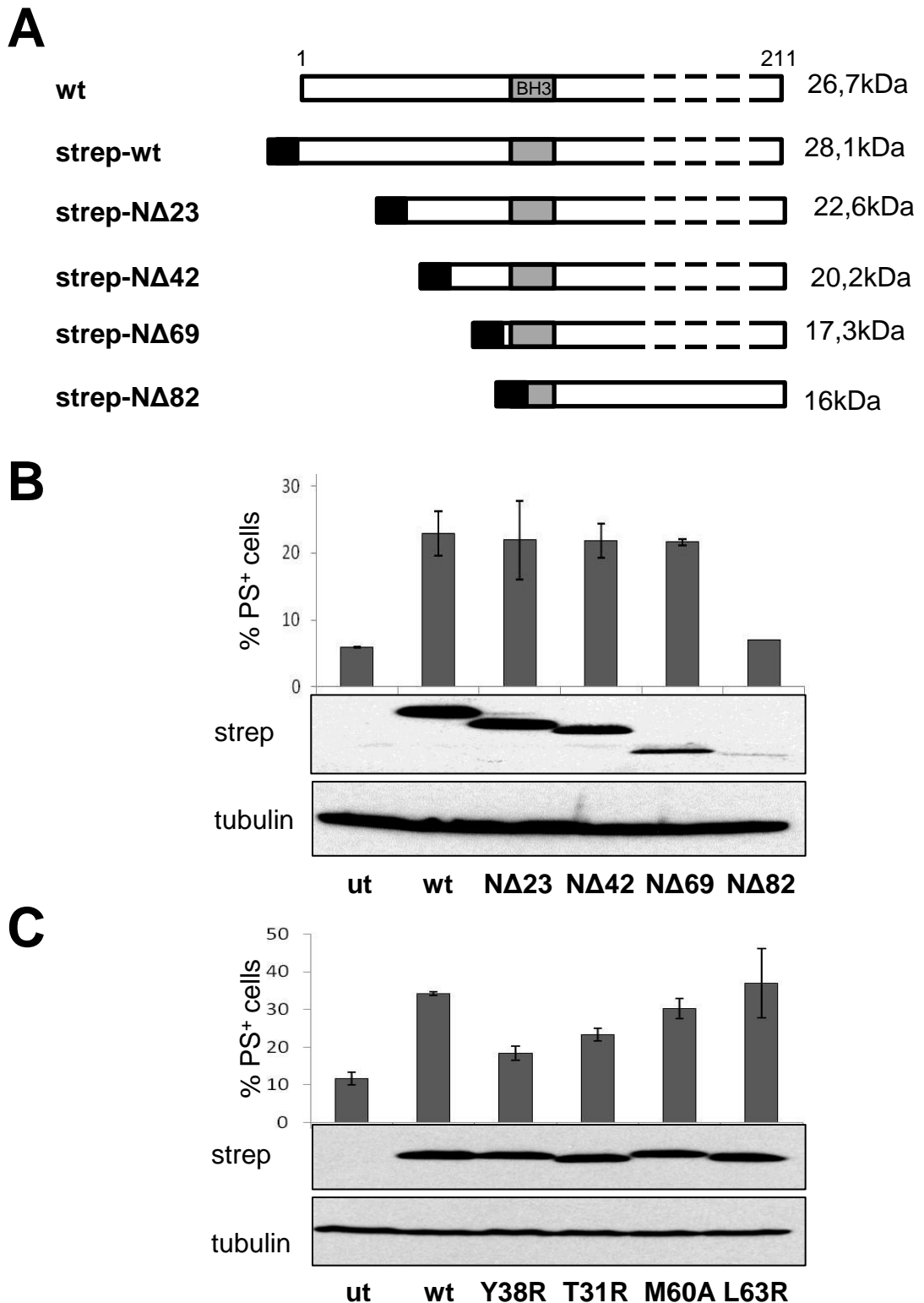


Figure 5.8 N-terminal change does not represent the point of no return in BAK activation
 (A) Schematic representation of generated strep-tagged BAK truncations. BH3 domain is indicated.
 (B) BAK truncations were transiently transfected into DKO MEFs. PS externalisation was analysed 24 h post transfection and protein levels determined by Western blotting. Data represent the mean S.E.M. of 4 experiments.
 (C) Strep-tagged mutants were transiently transfected into DKO MEFs. PS externalisation was analysed 24 h after transfection and expression levels were determined by Western blotting. Data represent the mean S.E.M. of 4 experiments.

This raises the question whether the formation of BAK dimers and high molecular weight complexes is the final step to commit apoptosis. The BAK BH3 mutant L78A did not show pro-apoptotic function when introduced into the BCL-X_L reconstitution system (Fig. 4.7). To further investigate the pro-apoptotic function of these BAK BH3 mutants, BAKL78A and D83A were transiently transfected into BAK and BAX DKO MEFs (Fig. 5.9 A). BAK pro-apoptotic activity was abolished with the L78A mutant, whereas the D83A mutant in contrast to earlier reports displayed no altered killing activity (Fig. 5.9 A) (Dewson, Kratina et al. 2008). Exposure to etoposide further enhanced cell death, but the differences in cell death between the mutations and wt BAK were similar. This result at least demonstrates that L78 is critical for BAK pro-apoptotic function.

As the L78A mutant lost its pro-apoptotic function it was not expected to oligomerise. However exposure to CuPhe revealed the L78A mutant still formed dimers and high molecular weight complexes at least as effectively as wt BAK (Fig. 5.9 B). This result indicates that the formation of dimers and high molecular weight complexes do not represent the final commitment step during BAK activation.

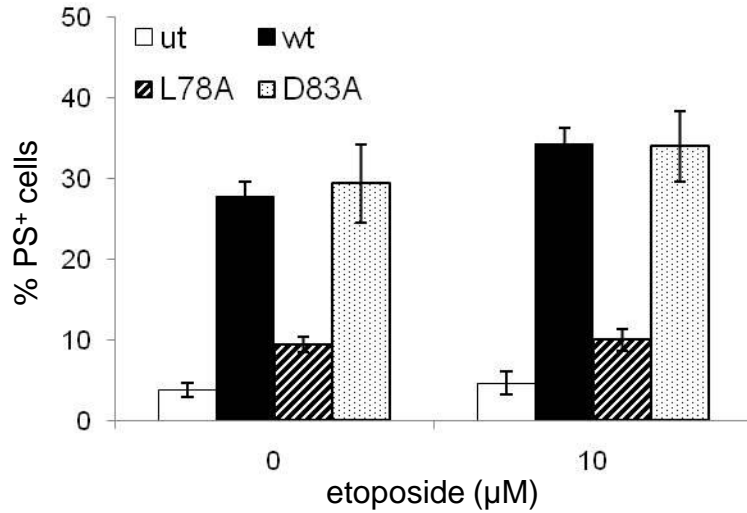
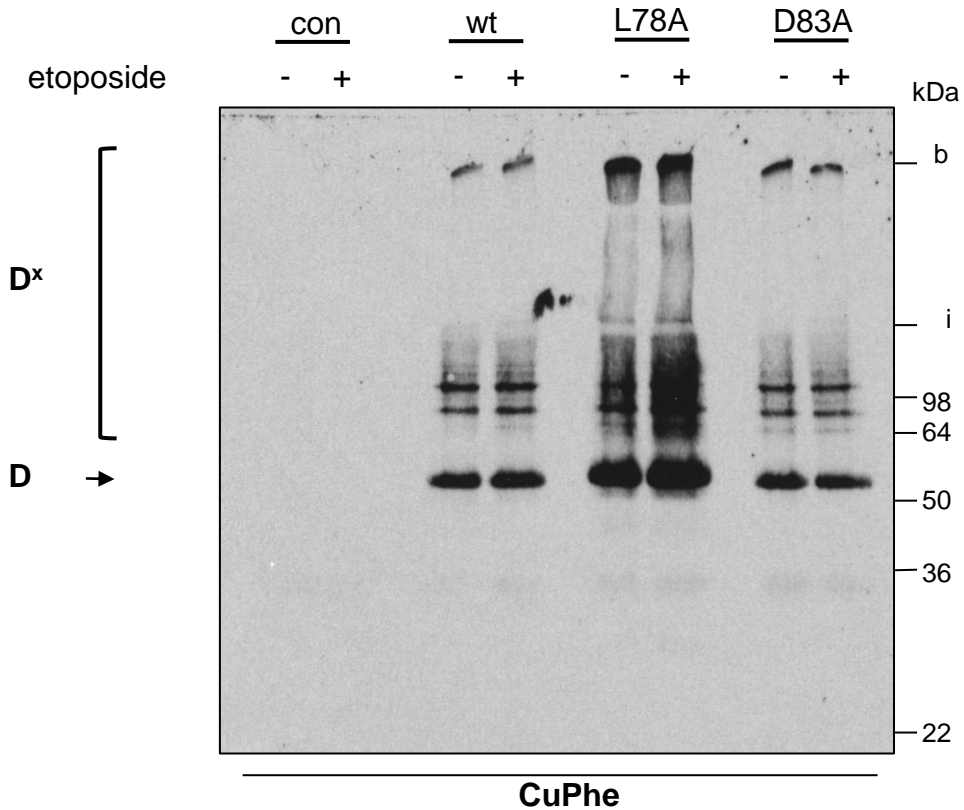
A**B**

Figure 5.9 Formation of BAK oligomers does not represent the point of no return in BAK activation

(A) BAK BH3 mutants were transiently transfected into DKO MEFs and 24 h after transfection exposed to 10 μ M etoposide for a further 8 h. Cell death was analysed by PS externalisation (data represent the mean S.E.M. of 4 experiments) or (B) exposed to CuPhe. Formation of dimers and high molecular weight complexes was analysed by Western blotting under non-denaturing conditions. D: dimeric BAK, stabilized by an intermolecular disulfide bond, D^x: BAK high molecular weight complexes, i: interface between stacking and running gel, b: bottom of well.

5.3 Discussion

A characteristic of BAK activation is the N-terminal conformational change commonly determined by exposure of the epitope of the AB-1 antibody or increased trypsin sensitivity (Griffiths, Dubrez et al. 1999; Wei, Lindsten et al. 2000). After 15 min of ABT-737 exposure AB-1 associated fluorescence as well as the p19 trypsin cleavage fragment were detected (Fig. 5.1). Two interpretations of these results are possible first the N-terminus is not exposed in primed BAK or the N-terminus is changed but the AB-1 epitope and trypsin cleavage sites are masked by another protein (Griffiths, Corfe et al. 2001). This would imply that the N-terminal conformational change occurs before binding of primed BAK to BCL-X_L providing the possibility that it occurs concurrently with the exposure of the BH3 domain. I demonstrate that primed BAK complexed with BCL-X_L is not N-terminally conformational changed in the endogenous situation in the Jurkat cells (Fig. 5.2). Therefore the exposure of the BH3 domain occurs independently and downstream of the N-terminal conformational change.

However in the BCL-X_L:BAK reconstitution system BAK complexed with BCL-X_L represents a heterogeneous population of N-terminal conformationally changed and N-terminal occluded BAK. This probably reflects the autoactivation of induced BAK by undergoing subsequently the exposure of the BH3 domain and the N-terminal conformational change. BCL-X_L interferes with this autoactivation process on several levels resulting in the sequestration of N-terminal conformationally changed as well as occluded BAK.

It has been proposed that primed BAK exposes the AB-1 epitope after apoptotic stimulation while BAK is still bound to BCL-X_L (Griffiths, Corfe et al. 2001). I demonstrate that only a discrete proportion of BAK undergoes the N-terminal conformational change after 15 min of ABT-737 exposure (Fig. 5.1 B and 5.2 B). Furthermore I show by double immunoprecipitations that primed BAK is displaced from BCL-X_L within 15 min of ABT-737 exposure which then undergoes the N-terminal conformational change (Fig. 5.2 B). Therefore the discrete pool of primed BAK complexed with BCL-X_L represents that which undergoes the N-terminal conformational change after 15 min of ABT-737 exposure.

The second characteristic of activated BAK is its formation of dimers and high molecular weight complexes. Correlating with the N-terminal conformational change BAK oligomers were detected as soon as 15 min, when again only a small portion of BAK was oligomerised (Fig. 5.5). This provides the possibility that the portion of BAK which is N-terminal

conformationally changed represents the proportion of BAK which is oligomerised and both events directly correlate.

Which of these activation steps occurs first? By trapping BAK in the M_X conformation thus inhibiting the N-terminal conformational change, a block in BAK oligomerisation and cytochrome *c* release was detected (Fig. 5.6). This demonstrates that the N-terminal conformational change has to occur before oligomerisation of BAK and the proportion of oligomerised BAK must represent that which is N-terminal conformationally changed. Furthermore formation of BAK dimers and high molecular weight complexes is important for induction of MOMP.

Active BAK can activate inactive BAK (Ruffolo and Shore 2003) and supporting this I found that initial N-terminal conformationally changed, oligomerised BAK seems to activate to N-terminal occluded, monomeric BAK (Fig. 5.1, 5.3 and 5.5). This results in a feed forward loop inducing N-terminal conformational change and oligomerisation of the inactive BAK pool(s).

The transition from inactive cytosolic BAX to a membrane permeabilising protein was suggested to involve steps additional to the N-terminal conformational change and oligomerisation in the mitochondrial membrane. These changes in BAX are not sufficient to commit to apoptosis and therefore do not represent commitment steps (Makin, Corfe et al. 2001). For BAK it was shown that N-terminal conformational change occurs before the execution phase (Griffiths, Dubrez et al. 1999).

In agreement with these studies I confirmed that BAK N-terminal conformational change does not represent the point of no return in BAK activation (Fig. 5.8) as truncating the N-terminal region did not result in “super-active” BAK.

It was proposed that BAK forms a symmetric BH3 groove homo-dimer building the subunit for the formation of high molecular weight complexes (Dewson, Kratina et al. 2008). Association of symmetric dimer into oligomers requires therefore another interface represented by helix α_6 (Dewson 2009). Therefore substitution of L78 with alanine should abolish BH3:groove dimer formation. Consequently, as the BH3:groove dimer represents the smallest subunit for oligomerisation no high molecular weight complexes can be formed. Therefore this mutant should not possess any proapoptotic function. Indeed I found that BAKL78A lost its killing activity. However it still formed dimers and high molecular weight

complexes at least as efficiently as wt BAK. Therefore BAK oligomerisation does not appear to be the final commitment step to apoptosis (Fig. 5.9).

Which step in BAK activation determines then the commitment of apoptosis?

CHAPTER 6:

**BIM_{EL} interacts with “active” BAK
after its displacement from BCL-X_L**

6.1 Introduction

According to the direct activation model activator BH3-only proteins (primarily BIM and tBID) are described to bind and directly activate BAK and BAX (Chipuk and Green 2008). Therefore in viable cells these activator proteins have to be held in check by anti-apoptotic proteins to maintain cell survival. Upon receiving an apoptotic stimulus they are displaced from their anti-apoptotic counterparts and become free to activate BAK and/or BAX. The precise nature of this interaction is not fully understood and most studies have focused on the association of activator BH3-only proteins with BAX rather than BAK.

It is proposed that direct association of BAX with activator BH3 proteins occurs in the cytoplasm driving its translocation and integration into the mitochondrial outer membrane. This association involves a site on the rear of BAX opposing its BH3 domain, where helix $\alpha 1$ and $\alpha 6$ form the interaction site for the BH3 domain of the activator proteins (Kim, Tu et al. 2009). After membrane insertion BAX homo-oligomerisation is induced by a second interaction with activator BH3-only proteins. However this association occurs through the classical BH3:groove interface (Kim, Tu et al. 2009). Another report suggests that activation of BAX by tBID first requires membrane insertion of tBID, which then recruits BAX inducing its membrane insertion and subsequent oligomerisation. This model also demonstrates the requirement of lipids in the outer mitochondrial membrane for this interaction to occur (Lovell, Billen et al. 2008).

BAK in contrast is already constitutively inserted in the mitochondrial membrane and therefore any potential interaction with activator BH3 proteins must occur at the membrane (Wei, Lindsten et al. 2000). So far interaction studies have concentrated mainly on tBID and BAK and any possible role of BIM has not been investigated (Wei, Lindsten et al. 2000; Ruffolo and Shore 2003).

Activator BH3-only proteins are proposed to be released when BAK and/or BAX oligomerises (Wei, Lindsten et al. 2000; Sundararajan and White 2001) resulting in a transient, “hit and run” interaction, which has so far proved difficult to detect.

Experiments in this chapter are aimed at investigating a potential role for activator BH3-only proteins, in particular BIM, in the stepwise activation of BAK. Using the BCL-X_L:BAK reconstitution system I found that primed BAK interacts with BIM_{EL} after its displacement from BCL-X_L after 30 min of ABT-737 exposure. Co-expression of BAK and BIM_{EL} at sub-lethal concentrations enhanced BAK pro-apoptotic function demonstrating that this

interaction represents an additional step in BAK activation. However BIM_{EL} did not induce the N-terminal conformational change nor oligomerisation of BAK as this interaction was observed to occur downstream of these events. The proportion of BIM_{EL} promoting the further activation of BAK does not seem to represent that sequestered by BCL-2 or BCL-X_L.

6.2 Results

6.2.1 BIM_{EL} resides in a complex with BAK

Activator BH3-only proteins are thought to directly activate BAK and the BH3-only proteins BIM and tBID are classified as direct activators. As ABT-737 activates the intrinsic mitochondrial pathway, an essential role for tBID in ABT-737 induced apoptosis can be excluded (Konopleva, Contractor et al. 2006) (Chapter 3). Although PUMA was recently shown to directly activate BAK, its direct activator role remains controversial (Kim, Tu et al. 2009). I therefore focused on a potential activator role of BIM_{EL} in the further activation of primed BAK.

Activator BH3-only proteins are proposed to induce BAK activation in a transient fashion making a direct interaction difficult to detect. Despite this I first addressed a possible physical interaction between BIM_{EL} and BAK following ABT-737 exposure using immunoprecipitation. BAK co-precipitated with BIM_{EL} in control as well as ABT-737 exposed Jurkat cells (Fig 6.1 A) and reciprocal immunoprecipitation using the BAK NT antibody produced identical results (Fig. 6.1 B). This suggested that BIM_{EL} is associated with BAK and this association is unaffected by ABT-737. Therefore BIM_{EL} appears to interact with BAK irrespective of the activation status of BAK.

Analysis of the supernatant of these immunoprecipitations showed that although the targeted protein was completely depleted from the supernatant an overall reduction in its co-precipitated binding partner was not detected (Fig. 6.1). This demonstrated that only a discrete proportion of cellular BIM_{EL} is constitutively associated with BAK.

Collectively these results demonstrate that a distinct proportion of BIM_{EL} interacts with BAK in control as well as ABT-737 exposed cells.

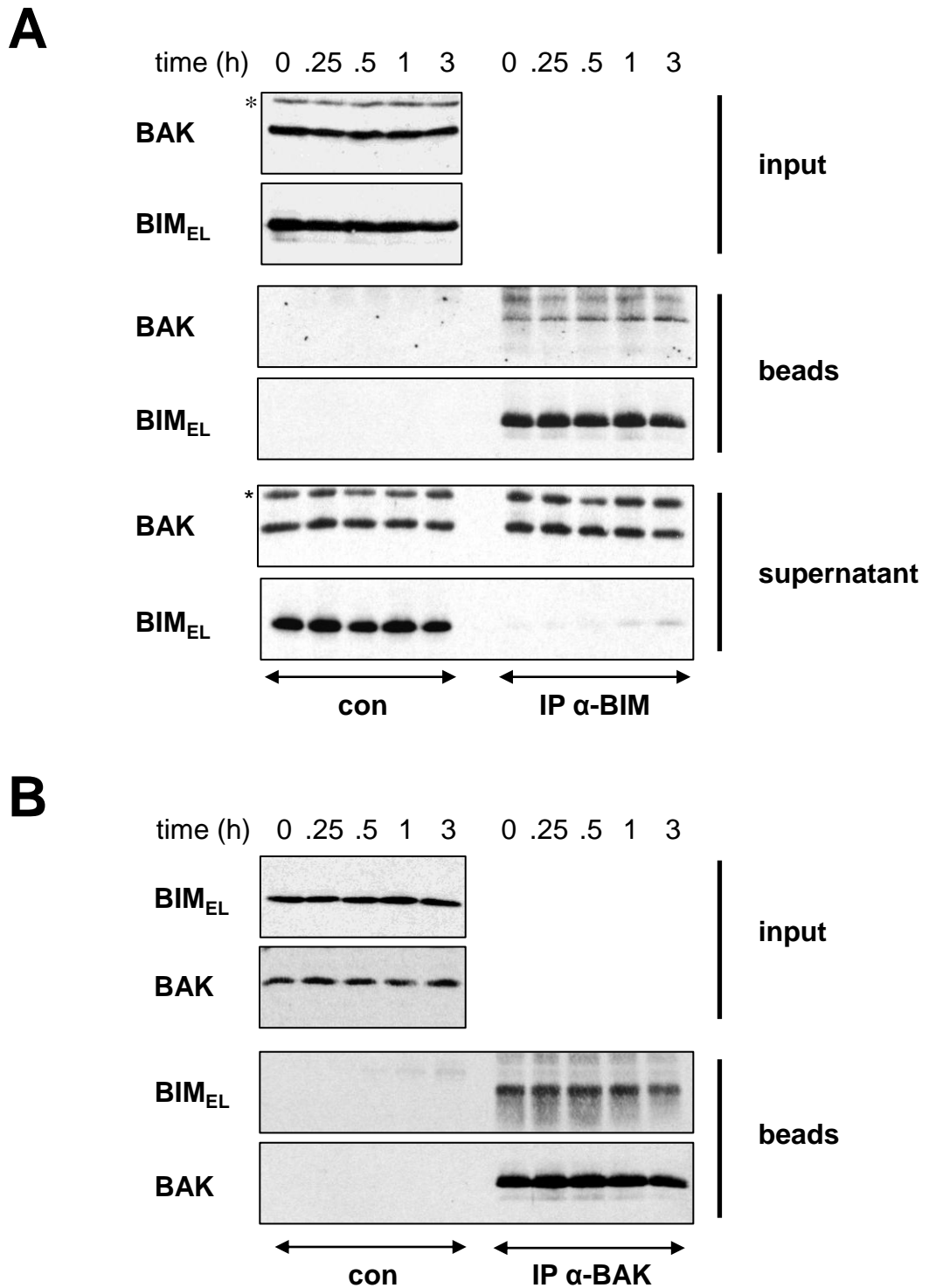


Figure 6.1 BIM_{EL} interacts with BAK

(A) Jurkat cells were exposed to 5 μ M ABT-737 for indicated times, lysed in 1 % CHAPS and subjected to immunoprecipitations using anti-BIM or (B) anti-BAK NT. Interaction with BAK and BIM_{EL} was analysed by Western blotting. Asterisk denotes unspecific band.

6.2.2 BIM_{EL} interacts with primed BAK after displacement from BCL-X_L

BIM_{EL} is proposed to activate BAK in a “hit and run” fashion resulting in a transient interaction (Wei, Lindsten et al. 2000). Therefore the pool of BAK constitutively associated with BIM_{EL} may also represent a different BAK pool to primed BAK involved in ABT-737 induced apoptosis.

I reasoned if BIM_{EL} interacts with primed BAK mediating its activation then an interaction between BIM_{EL} and primed BAK should occur after its displacement from BCL-X_L. To investigate if BIM_{EL} binds specifically to primed BAK after its displacement from BCL-X_L, I switched to the BCL-X_L:BAK reconstitution system (Fig. 4.3) and performed double immunoprecipitations. The first immunoprecipitation was directed against flag epitope to precipitate BCL-X_L. The supernatant of this immunoprecipitation was then subjected to immunoprecipitation using anti-strep in order to isolate primed BAK displaced from BCL-X_L (Fig. 6.2 A and Fig. 5.3).

In control cells all tetracycline induced BAK should be complexed with BCL-X_L (Fig 6.2 A a). Therefore after the first immunoprecipitation no BCL-X_L:BAK complex should reside in the supernatant. Consequently BAK cannot be immunoprecipitated from the supernatant of the anti-flag immunoprecipitation. In ABT-737 exposed cells however BAK is displaced from BCL-X_L (Fig. 6.2 A b). Assuming the displacement is complete the first immunoprecipitation should isolate BCL-X_L only. Consequently primed BAK should reside in the supernatant of this immunoprecipitation. The second anti-strep immunoprecipitation should therefore precipitate the BCL-X_L displaced primed BAK and any possible interacting proteins can then be analysed.

Analysis of the first immunoprecipitation from BCL-X_L:BAK reconstituted cells revealed that BCL-X_L was completely immunoprecipitated in control and ABT-737 exposed cells (Fig.6.2 C, middle panel) as no BCL-X_L was detectable in the second immunoprecipitation (Fig.6.2 C, right panel).

The first immunoprecipitation demonstrates that almost all induced BAK resides with BCL-X_L in a complex (Fig.6.2 C, middle panel) as very little BAK was immunoprecipitated in the second immunoprecipitation in control cells (Fig.6.2, right panel). ABT-737 displaced induced BAK from BCL-X_L in a time-dependent manner with complete dissociation occurring after 3 h (Fig.6.2 C, middle panel). Displacement of BAK from BCL-X_L by ABT-

737 was accompanied by the precipitation of BAK in the second immunoprecipitation (Fig.6.2 C, right panel).

BIM_{EL} co-precipitated with BCL-X_L in the first immunoprecipitation, whereby ABT-737 did not induce its displacement from BCL-X_L (Fig.6.2 C, middle panel). This result suggests that BIM_{EL} is a component of the reconstituted BCL-X_L:BAK. However the direct association with BAK within this complex is unlikely as BIM_{EL} remains associated with BCL-X_L whereas BAK is displaced following ABT-737 exposure. Analysis of the second immunoprecipitation revealed that BIM_{EL} co-precipitated with displaced primed BAK after exactly 30 min of ABT-737 exposure (Fig.6.3 C, right panel). This demonstrates that BIM_{EL} interacts with primed BAK after its displacement from BCL-X_L in a transient fashion.

Collectively these results demonstrate a transient interaction between BIM_{EL} and BAK. This interaction appears maximal after 30 min of ABT-737 exposure and occurs downstream of the displacement of primed BAK from BCL-X_L.

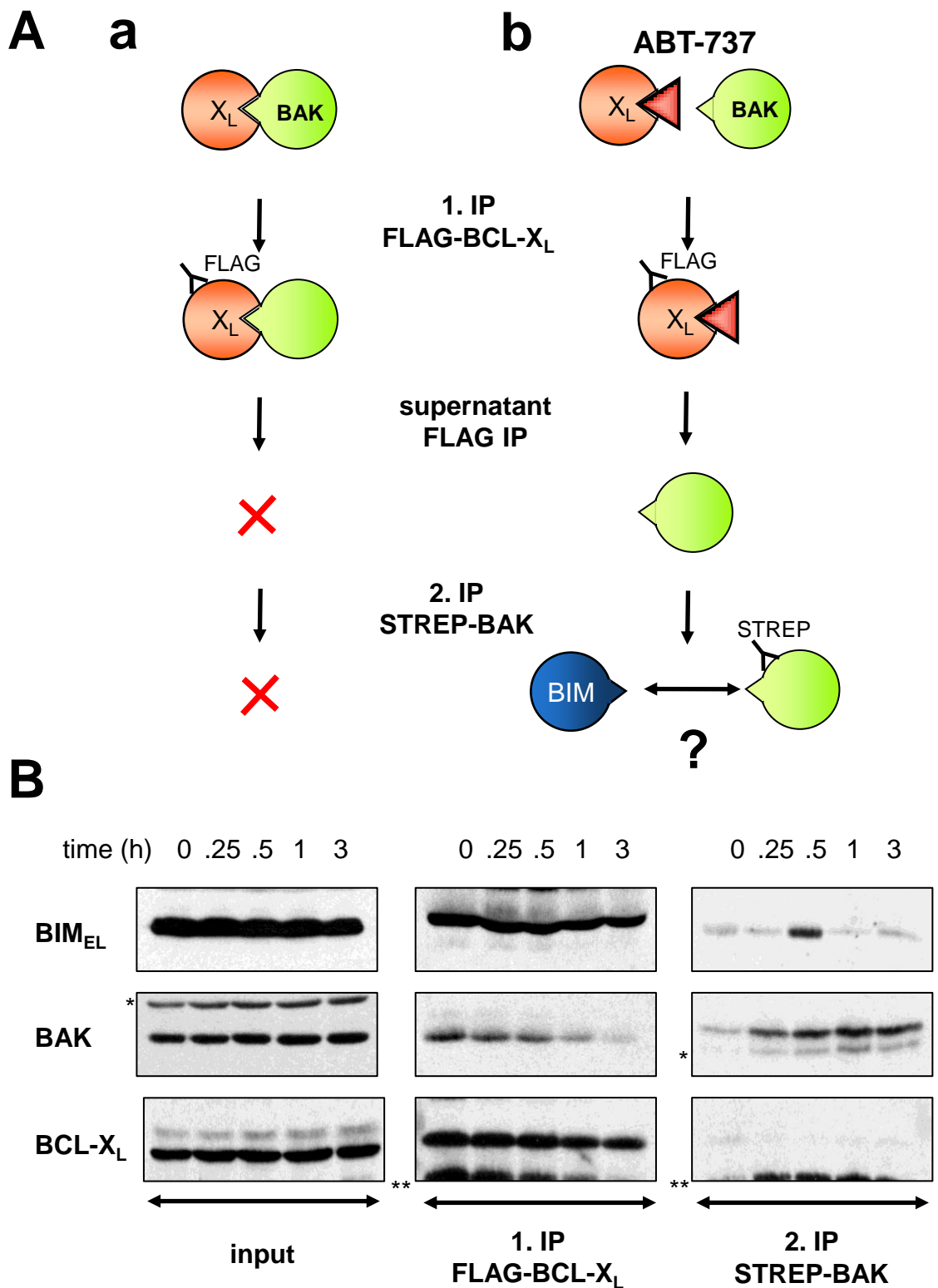


Figure 6.2 BIM_{EL} interacts with activated BAK

(A) Schematic representation of combined anti-flag / anti-strep immunoprecipitation. (B) HEK293T cells were reconstituted with BCL-XL:BAK complex and exposed to 5 μ M ABT-737 for indicated time, lysed in 1 % CHAPS and subjected to combined anti-flag / anti-strep immunoprecipitation. Interaction of BAK with BIM_{EL} was determined by Western blotting. *denotes unspecific band, ** denotes residual BAK signal.

6.2.3 BIM_{EL} enhances the pro-apoptotic function of BAK

If the direct interaction between BIM_{EL} and BAK detected after 30 min of ABT-737 exposure represents a further step in activation of primed BAK then co-transfecting BIM_{EL} and BAK should enhance BAK pro-apoptotic function resulting in increased cell death compared to BAK alone.

Transfection of either untagged BIM_{EL} or strep-tagged BAK alone induced cell death in a DNA concentration dependent manner in HEK293T cells (Fig. 6.3 A). At a DNA concentration of 200 ng no cell death was observed with BAK, similarly BIM_{EL} did not show killing activity until 400 ng. These sub-lethal concentrations of BAK and BIM_{EL} were therefore chosen for further experiments.

Co-expression of BAK with BIM_{EL} revealed that BIM_{EL} enhanced BAK pro-apoptotic function as determined by PS externalisation (Fig. 6.3 B) and reduced $\Delta\Psi_m$ (Fig. 6.3 C). This enhancing effect directly correlated with the concentration of BIM_{EL} and did not represent an addition of BIM_{EL} and BAK induced cell death as both proteins were expressed at sub-lethal levels. Furthermore BIM_{EL} has to enhance BAK killing function and not vice versa as BIM cannot kill in the absence of BAK (Willis, Fletcher et al. 2007).

To investigate whether this enhancing effect of BIM_{EL} was based on a direct interaction immunoprecipitations using anti-strep were performed. BIM_{EL} co-precipitated with strep-tagged BAK when co-expressed demonstrating the direct interaction between both proteins (Fig. 6.5 D).

Collectively these results demonstrate that BIM_{EL} appears to enhance BAK pro-apoptotic function. Therefore the direct interaction between BAK and BIM_{EL} represents a potential additional step in the activation of BAK.

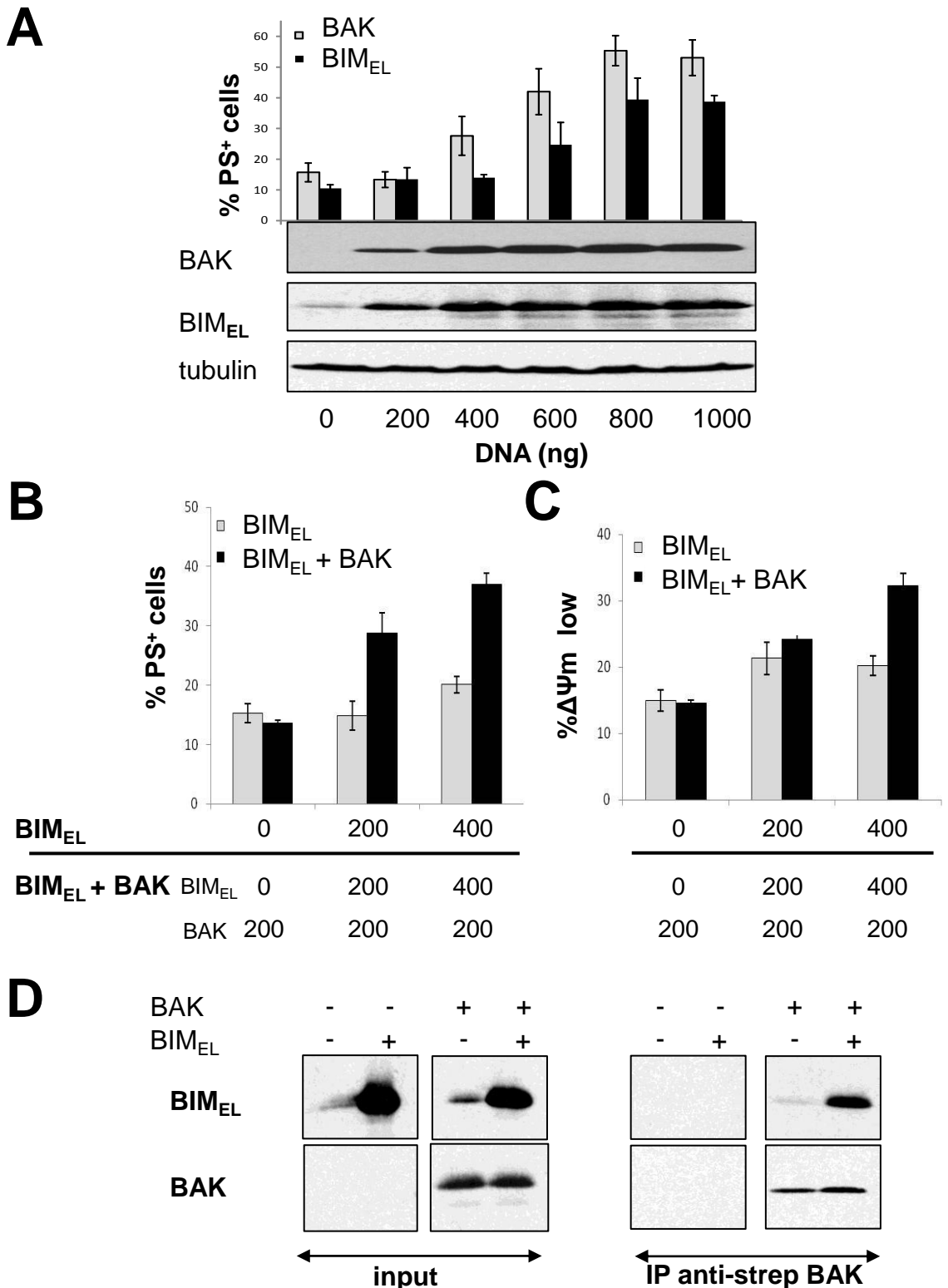


Figure 6.3 BIM_{EL} enhances the proapoptotic function of BAK

(A) HEK293T cells were transiently transfected with different DNA concentrations of strep-tagged BAK and untagged BIM_{EL}. Cell death was determined 16 h after transfection by PS externalisation. Data represent the mean S.E.M. of 5 experiments. (B) HEK293T cells were transiently co-transfected with 200 ng strep-tagged BAK and 200 or 400 ng BIM_{EL}. Cell death was determined after 16 h by PS externalisation or (C) reduced $\Delta\Psi_m$. (D) strep-tagged BAK and untagged BIM_{EL} were co-transfected HEK293T, lysed in 1 % CHAPS and subjected to immunoprecipitation using anti-strep. Interaction between BAK and BIM_{EL} was determined by Western blotting.

6.2.4 BIM_{EL} does not induce N-terminal conformational change or oligomerisation of BAK

Activators are proposed to induce the oligomerisation of BAK (Wei, Lindsten et al. 2000; Kim, Tu et al. 2009). To investigate if BIM_{EL} induces the N-terminal conformational change, which has to precede BAK oligomerisation (Fig.5.6) or oligomerisation per se after 30 min of ABT-737 exposure I analysed the conformational state of primed BAK in the BCL-X_L:BAK reconstitution system from control HEK293T cells.

To assess if induced BAK is N-terminal changed while bound to BCL-X_L I performed double immunoprecipitation from control BCL-X_L:BAK reconstituted HEK293T cells (Fig. 4.3 A). The AB-1 antibody was used for the first immunoprecipitation followed by a second immunoprecipitation using anti-BCL-X_L. Analysis of the first immunoprecipitation revealed that BCL-X_L co-precipitated with BAK suggesting that BAK is N-terminal conformationally changed while bound to BCL-X_L (Fig. 5. 3 A, middle panel). In the second immunoprecipitation BAK co-precipitated with BCL-X_L indicating that this primed BAK is N-terminal occluded. Therefore primed BAK when reconstituted in HEK293T cells is present as in MEF cells as a heterogenous population including N-terminal changed and N-terminal occluded BAK (Fig. 6.3 A and 5.3 B). However the majority of induced BAK is N-terminal conformationally changed while bound to BCL-X_L as the amount of BAK co-precipitated in the second immunoprecipitation is minor (Fig. 6.4 A).

To determine the oligomerisation state of induced BAK complexed with BCL-X_L, reconstituted cells were exposed to CuPhe and subjected to immunoprecipitation using anti-flag. A minor portion of induced BAK existed in the M_X conformation (Fig. 6.4 B) which correlated with the minor portion of N-terminal occluded primed BAK (Fig. 6.4 A). The majority of induced BAK was present as dimers and high molecular weight complexes while complexed with BCL-X_L (Fig 6.4 B). This demonstrates that primed BAK in the reconstituted BCL-X_L:BAK complex must be oligomerised.

Collectively these results demonstrate that induced BAK is N-terminal conformationally changed and oligomerised while complexed with BCL-X_L in the BCL-X_L:BAK reconstitution system in HEK293T cells. As both the N-terminal conformational change and oligomerisation have not been shown to be reversible for BAK ABT-737 must displace N-terminal conformationally changed/oligomerised BAK. Consequently BIM_{EL} cannot induce BAK

oligomerisation as the BIM_{EL} BAK interaction occurs downstream of the N-terminal conformational change and oligomerisation of BAK.

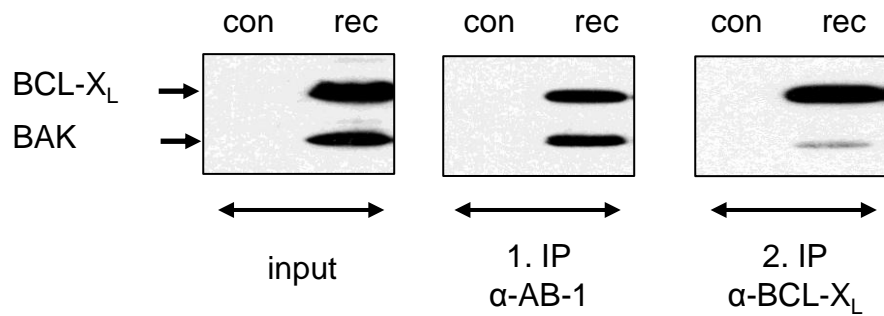
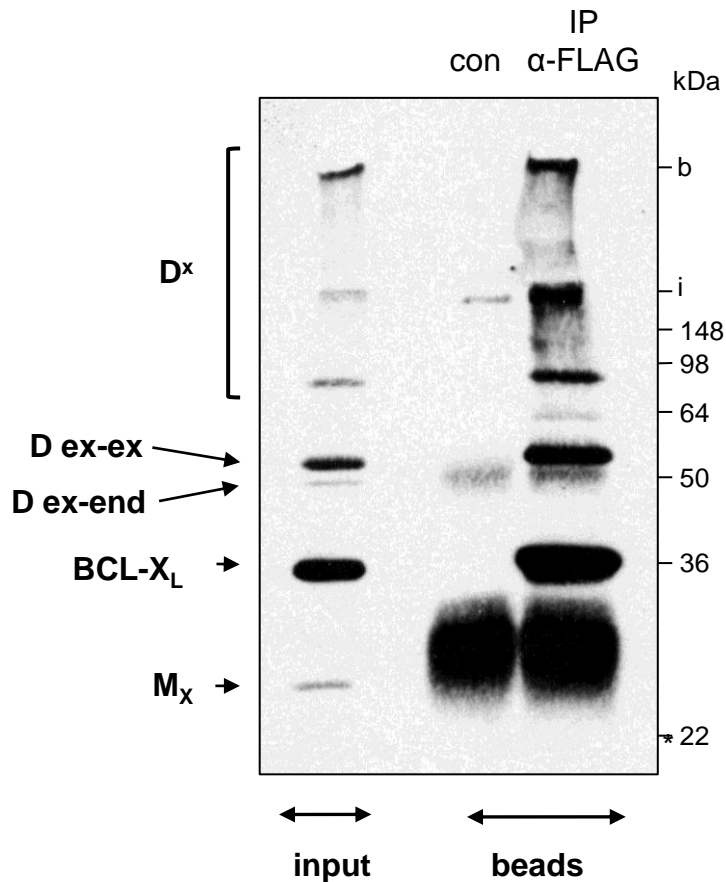
A**B**

Figure 6.4 BAK is N-terminal conformationally changed and oligomerised when reconstituted in HEK293T cells

(A) HEK293T cells reconstituted with BCL-X_L:BAK complex (rec). Cells were lysed in 1 % CHAPS and subjected to first immunoprecipitation using anti-AB-1. Supernatant of the AB-1 immunoprecipitation was subjected to a second immunoprecipitation against BCL-X_L. Immunoprecipitates were analysed by Western blotting using anti-strep. (B) BCL-X_L:BAK reconstituted HEK293T cells were fractionated into HM fraction and exposed to CuPhe. Disulphide linked HM fractions were lysed in 1 % CHAPS and subjected to immunoprecipitation using anti-FLAG antibody to precipitate flag-strep-double tagged BCL-X_L. Presence of dimers and high molecular weight complexes was analysed by Western blotting using anti-strep under denaturing conditions. Asterisk denotes Protein G band. ex: exogenous BAK, end: endogenous BAK

6.2.5 ABT-737 displaces BIM_{EL} from BCL-X_L but not BCL-2

According to the direct activation model activators are sequestered by anti-apoptotic BCL-2 proteins to prevent activation of BAK and therefore maintain cell survival. During apoptosis activators are displaced from their anti-apoptotic counterparts by sensitiser BH3-only proteins and are then free to activate BAK by direct interaction (Chipuk and Green 2008; Youle and Strasser 2008).

As ABT-737 neutralises BCL-2 and BCL-X_L I focused on these proteins as potential negative regulators of BIM_{EL}. To analyse if BIM_{EL} was sequestered by BCL-X_L and/or BCL-2 in Jurkat cells immunoprecipitations using anti-BCL-X_L (Fig. 6.5 A) or anti-BIM (Fig. 6.5 B) were performed. BIM_{EL} was found to be sequestered by both BCL-X_L and BCL-2 (Fig. 6.5). ABT-737 displaced BIM_{EL} from BCL-X_L and with complete dissociation detected after 3 h (Fig. 6.5 A) and reciprocal immunoprecipitation using anti-BIM confirmed these results (Fig. 6.5 B). Therefore displacement of BIM_{EL} from BCL-X_L followed slower kinetics than displacement of BAK where complete dissociation was detected after only 15 min of ABT-737 exposure (Fig. 5.3, 6.5 A). In contrast to BCL-X_L, displacement of BIM_{EL} from BCL-2 was not complete even after 3 h of ABT-737 exposure. This suggests that BIM_{EL} sequestered by BCL-2 was retained and is unlikely to be involved in the further activation of primed BAK.

To extend these results, BCL-2:BIM_{EL} as well as BCL-X_L:BIM_{EL} complexes were reconstituted analogous to the BCL-X_L:BAK reconstitution (Fig. 4.3). After induction of BIM_{EL}, cells were exposed for 3 h to two different ABT-737 concentrations and cell death assessed. Reconstitution of BCL-X_L:BIM_{EL} as well as BCL-2:BIM_{EL} complexes did not sensitise cells to ABT-737 unlike those reconstituted with a BCL-X_L:BAK complex (Fig. 6.6 A). Assuming that BIM_{EL} is sequestered by both antiapoptotic proteins this result could be explained either by an insufficient displacement of BIM_{EL} to activate endogenous BAK and/or no role for displaced BIM_{EL} in ABT-737 induced apoptosis.

To investigate if BIM_{EL} is displaced from antiapoptotic proteins in the reconstitution system BCL-2 and BCL-X_L were immunoprecipitated using anti-strep from control and ABT-737 exposed cells (Fig. 6.6 B). In control cells BIM_{EL} associated with both BCL-2 and BCL-X_L in agreement with the results obtained in Jurkat cells (Fig. 6.5). However BIM_{EL} was not displaced from BCL-2 in contrast to BCL-X_L which displayed a concentration dependent

displacement by ABT-737 was detectable. Complete dissociation of BIM_{EL} from BCL-X_L was not achieved in contrast to displacement of BAK from BCL-X_L (Fig. 5.3 C, Fig. 6.3 C).

Collectively these results demonstrated that BIM_{EL} cannot be as efficiently displaced from BCL-X_L by ABT-737 as BAK. No displacement was observed from BCL-2 suggesting that BIM_{EL} complexed with BCL-2 may have no role in ABT-737 induced apoptosis. Furthermore displacement of BIM_{EL} from BCL-X_L occurs downstream than the observed interaction between BIM_{EL} and primed BAK (Fig. 6.3 C). Therefore involvement of BCL-X_L complexed BIM_{EL} in ABT-737 induced cell death seems unlikely.

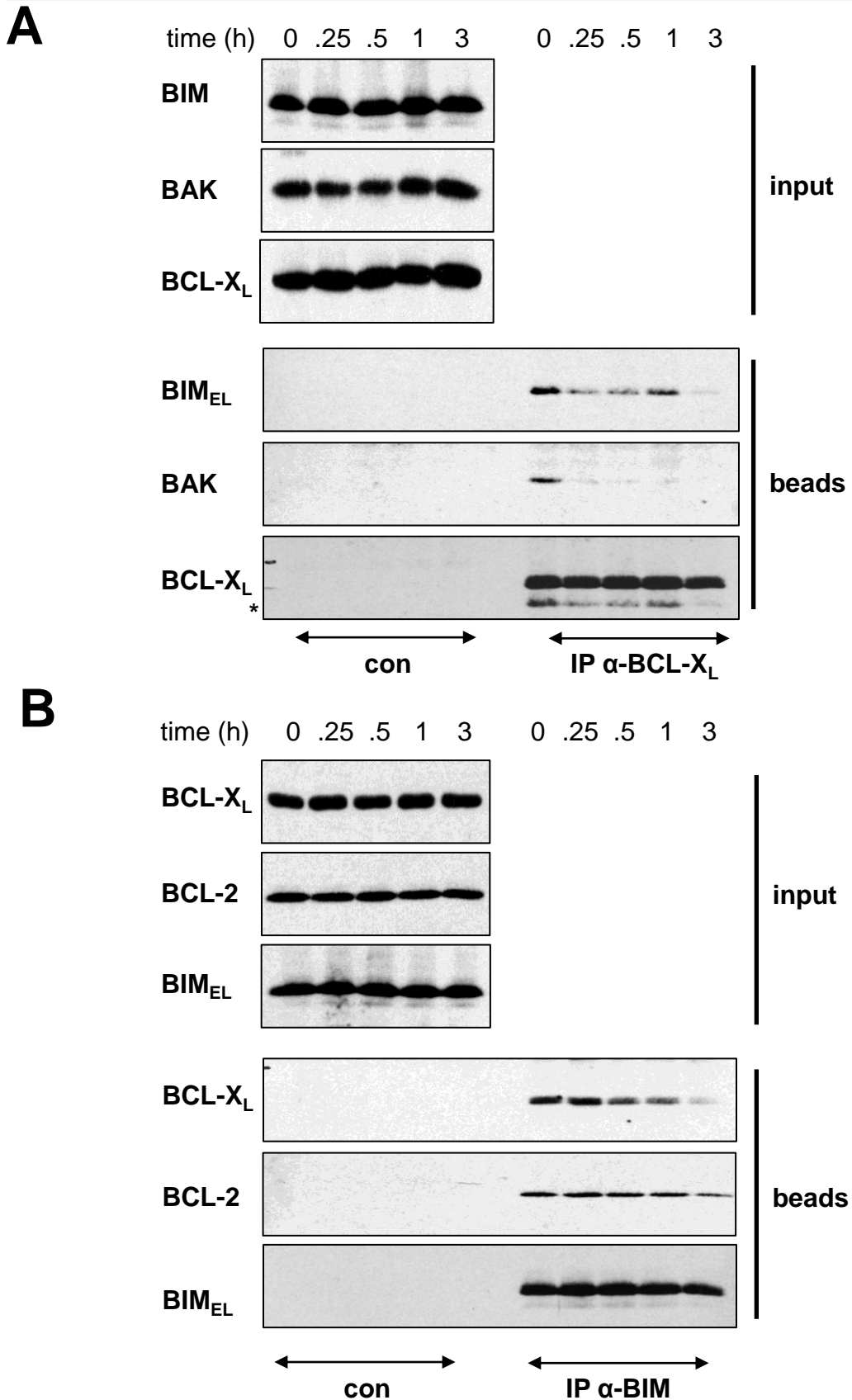


Figure 6.5 BIM_{EL} is displaced from BCL-XL by ABT-737

(A) Jurkat cells were exposed to ABT-737 for indicated times, lysed in 1% CHAPS and subjected to immunoprecipitations using BCL-XL antibody or (B) BIM antibody. Precipitates were analysed by Western blotting to analyse interaction partners.

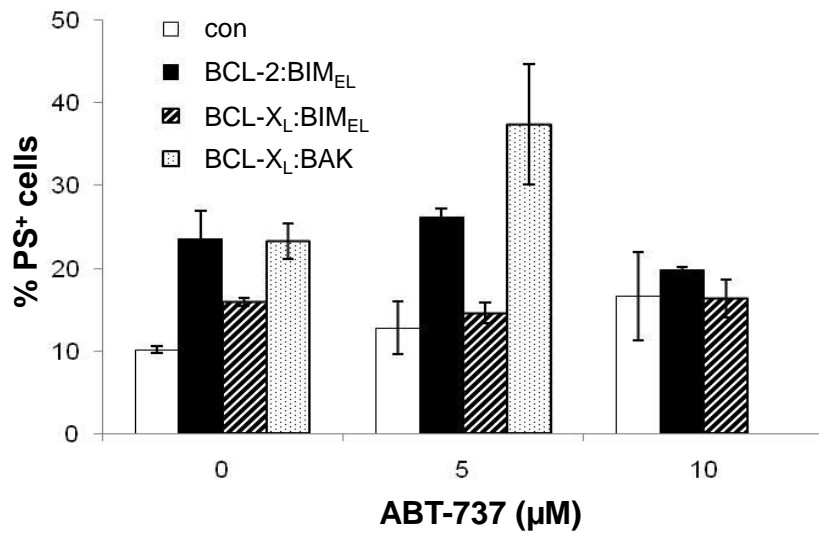
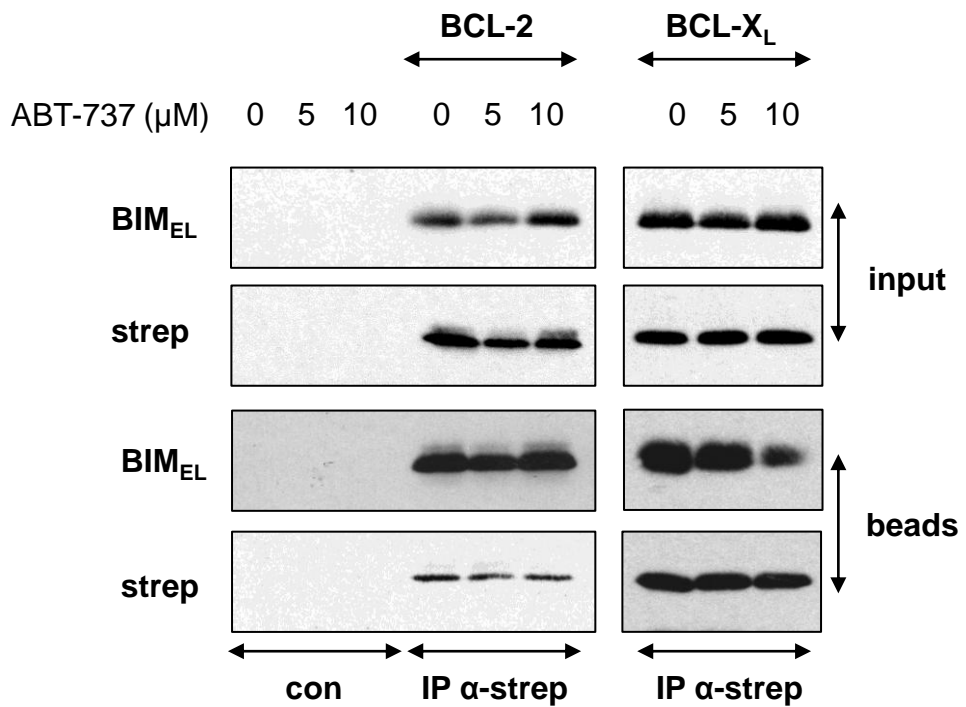
A**B**

Figure 6.6 BIM_{EL} is displaced from BCL-X_L by ABT-737

(A) HEK293T cells were reconstituted with BCL-2:BIM_{EL}, BCL-X_L:BIM_{EL} or BCL-X_L:BAK complexes and exposed to 5 or 10 µM ABT-737 for 3 h. BCL-2 was strep-tagged, BCL-X_L strep-flag double tagged and BIM_{EL} untagged. Cell death was analysed by PS externalisation. Data represent the mean S.E.M. of 4 experiments. (B) Reconstituted cells were lysed in 1% CHAPS and subjected to immunoprecipitation using anti-strep. Interaction with BIM_{EL} was analysed by Western blotting.

6.3 Discussion

BAK is described to be activated by direct interaction with t BID inducing its oligomerisation (Wei, Lindsten et al. 2000; Kim, Tu et al. 2009) however the underlying mechanism is not fully understood.

The BCL-X_L:BAK reconstitution system was therefore used to investigate a potential role of BIM_{EL} in the activation of primed BAK. After exactly 30 min of ABT-737 exposure BIM_{EL} interacts directly with primed BAK after its displacement from BCL-X_L. Furthermore co-expression experiments demonstrated that BIM_{EL} enhances BAK proapoptotic function. Therefore interaction of BIM_{EL} with BAK represents an additional step in the activation of BAK.

Interaction of BIM_{EL} and BAK occurred only at 30 min of ABT-737 exposure demonstrating the proposed transient “hit and run” nature of this interaction (Fig. 6.3 C). In this proposed model it was suggested that activator BH3-only proteins induce oligomerisation of BAK but are released when BAK oligomerises resulting in the transient nature of this interaction (Wei, Lindsten et al. 2000). In contrast I demonstrate that reconstituted primed BAK is already N-terminal conformationally changed and oligomerised while bound to BCL-X_L. As both of these activation steps are not reversible for BAK, BCL-X_L displaced primed BAK is after 30 min of ABT-737 exposure N-terminal conformationally changed and oligomerised. Consequently the interaction with BIM_{EL} occurs downstream of these activation steps and thus BIM_{EL} does not appear to induce either activation step (Fig. 6.4). Therefore the reason for a transient interaction is not given by the induction of BAK oligomerisation.

What effect does BIM then have on BAK? Based on the structural similarity of BAX to the membrane domain of diphtheria toxin and bacterial colicins it is proposed that efficient membrane permeabilisation requires the additional insertion of the pore domain (helix $\alpha 5$ and $\alpha 6$) of BAX (Muchmore, Sattler et al. 1996). This structural localisation is promoted by the interaction of BAX with tBID (Annis, Soucie et al. 2005). Based on the structural similarity between BAX and BAK insertion of helix $\alpha 5$ and $\alpha 6$ could also account for BAK mediated membrane permeabilisation. Thus interaction of BIM_{EL} with oligomerised BAK could potentially promote the insertion of the pore domain of oligomerised BAK.

To facilitate direct interaction activators must be either recruited to the mitochondria or displaced from anti-apoptotic proteins. BIM is localised at the mitochondria in hematopoietic

cells (Harada, Quearry et al. 2004; Konopleva, Contractor et al. 2006). Therefore BIM_{EL} needs to be kept in check by anti-apoptotic BCL-2 proteins to prevent activation of BAK to maintain cell survival. Indeed I found that BIM_{EL} is sequestered by BCL-X_L as well as BCL-2 in control Jurkat cells (Fig. 6.5) (Del Gaizo Moore, Brown et al. 2007).

Complete dissociation of displaced BIM_{EL} from BCL-X_L was detected after 3 h of ABT-737 exposure in Jurkat cells, whereas in the BCL-X_L:BIM_{EL} reconstitution system complete displacement by ABT-737 was not achieved. Thus displacement of BIM_{EL} follows delayed kinetics compared to the displacement of BAK from BCL-X_L (Fig 5.3 B, 6.5). Displacement of BIM_{EL} from BCL-2 was not detectable in both the endogenous situation or when BCL-2:BIM complex was reconstituted (Fig. 6.5 B, 6.6 B). In agreement with this an earlier study in primary CLL cells only detected displacement of BIM from BCL-2 by ABT-737 when immunoprecipitates were exposed to ABT-737 and no displacement in a cellular system was demonstrated (Del Gaizo Moore, Brown et al. 2007). Therefore the proportion of BIM_{EL} involved in the further activation of primed BAK is not represented by BCL-2complexed BIM_{EL}. It is also unlikely that BCL-X_L complexed BIM_{EL} is involved as displacement from BCL-X_L occurs downstream of the BIM_{EL}:BAK interaction (Fig. 6.3).

My observation on the role of BIM_{EL} in the activation of primed BAK does not reflect the classical one described in the direct activation model. I show that BIM_{EL} represents an additional activation step downstream of N-terminal conformational change and oligomerisation of BAK probably promoting insertion of helix $\alpha 5$ and $\alpha 6$ in the mitochondrial membrane.

CHAPTER 7:
Discussion

The point of no return during apoptosis is perturbation of the mitochondrial membrane which leads to the release of cytochrome *c* from the intermitochondrial membrane space. BAK represents a crucial mediator of MOMP but the underlying structural changes as well as the involvement of other members of the BCL-2 protein family leading to the conversion of inactive BAK to a membrane permeabilising pore remain unclear.

In this thesis I have demonstrated that BAK undergoes several conformational changes in order to adapt an active conformation. These changes include exposure of its BH3 domain, followed by an N-terminal conformational change leading to its oligomerisation and finally the insertion of the pore domain mediated by direct interaction with BIM_{EL} (Fig. 7.1). Thus the activation of BAK comprises a multiple step mechanism providing several points of regulation controlling the execution of apoptosis.

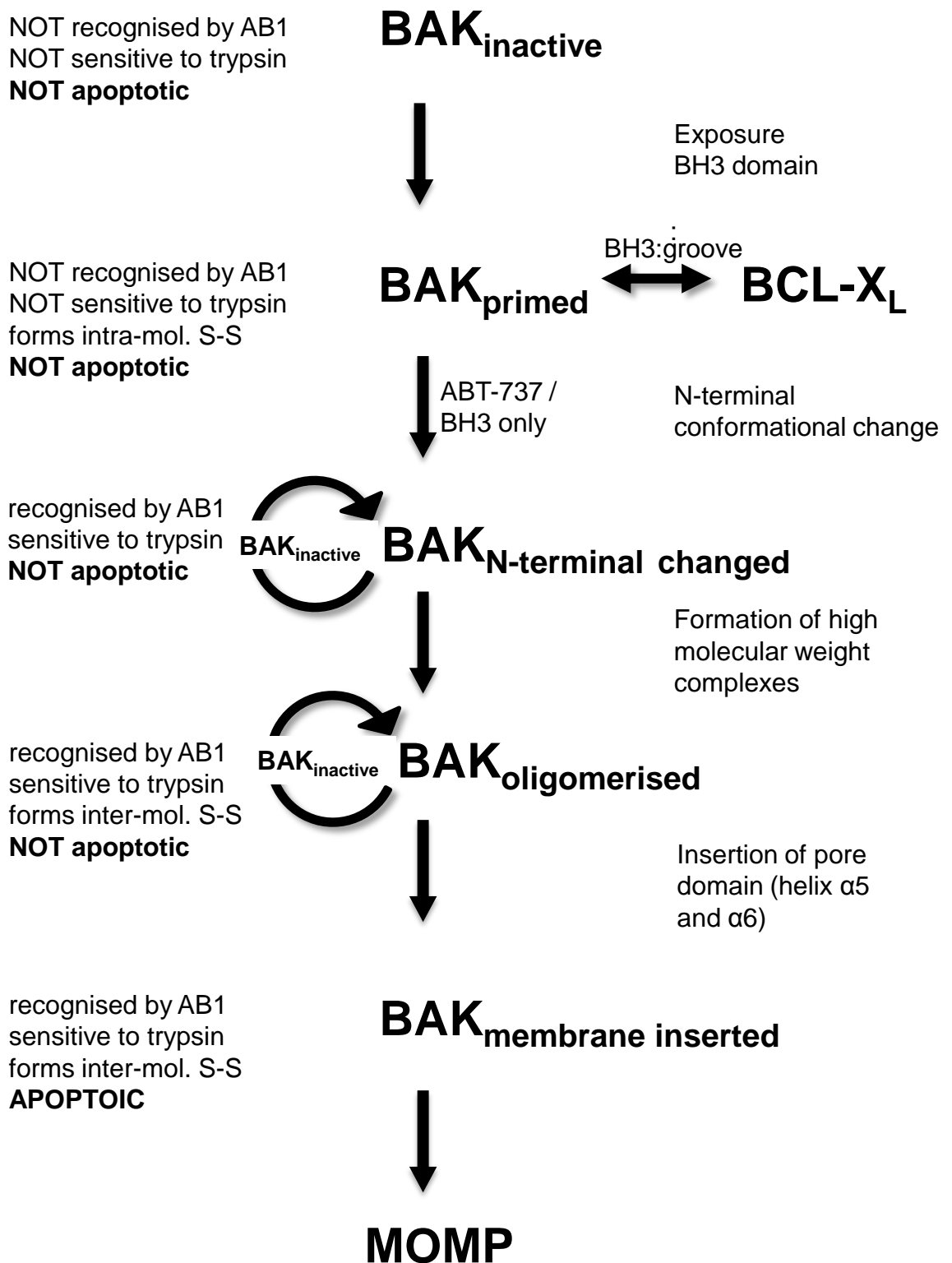


Figure 7.1 BAK activation- a multiple step mechanism

Inactive BAK exposes its BH3 domain resulting in primed BAK which is sequestered by BCL-X_L to prevent further activation. After displacement of primed BAK from BCL-X_L by ABT-737 or BH3-only proteins it undergoes an N-terminal conformational change followed by its oligomerisation. To achieve full proapoptotic function membrane insertion of the pore domain is necessary which is mediated by direct interaction with BIM_{EL}. This results in the permeabilisation of the outer mitochondrial membrane and subsequent cytochrome c release.

7.1 Exposure of the BH3 domain

One of the first steps in BAK activation must involve the exposure of its BH3 domain. In line with earlier observations (Willis, Chen et al. 2005) I demonstrate that in control Jurkat cells BAK is sequestered by BCL-X_L (Fig. 4.1 A). This interaction occurs through the classical BH3:groove interface (Sattler, Liang et al. 1997) as ABT-737 can displace BAK from BCL-X_L by competing for the hydrophobic groove of BCL-X_L (Fig. 4.1 A and 4.4). Furthermore mutation of the BAK BH3 domain abolished interaction with BCL-X_L providing further evidence for association through a BH3:groove interface (Fig. 4.7 C).

The BH3:groove interface is mainly stabilized by hydrophobic interactions where L78 was described to represent the most critical residue in complex stabilization (Sattler, Liang et al. 1997). I found that substitution of L78 with alanine did not alter binding to BCL-X_L and compensation by other hydrophobic residues within the BAK BH3 domain is likely (Fig. 4.7). A BAKD83A mutant abolished binding to BCL-X_L reflecting the importance of electrostatic interactions in BH3:groove complex stabilization (Fig. 4.7).

The crystal structure of inactive BAK reveals that the critical residues in the BAK BH3 domain face the protein core and therefore are not available to insert into the hydrophobic groove of BCL-X_L (Moldoveanu, Liu et al. 2006). Consequently BAK has to undergo a structural rearrangement prior to binding to BCL-X_L. This conformational change includes rotation of BH3 domain containing-helix $\alpha 3$ in order to expose critical residues to the protein surface. Rotation of helix $\alpha 3$ coincidentally opens the hydrophobic binding groove of BAK by relocating R88 and Y89 two residues that sterically hinder the groove (Moldoveanu, Liu et al. 2006). Therefore BAK sequestered by BCL-X_L is characterized by an exposed BH3 domain and open hydrophobic binding groove a conformation referred to as “primed”.

The proportion of primed BAK sequestered by BCL-X_L does not represent total cellular BAK as primed BAK eluted on sucrose density gradients in fractions corresponding to around 150 kDa (although total cellular BAK was present in every fraction) (Fig. 4.2). Additionally immunoprecipitations showed that although BCL-X_L was completely depleted only a distinct proportion of BAK seems to be complexed with BAK and vice versa (Fig. 4.1). This suggests that BAK must also be complexed with other proteins in control cells (e.g. VDAC2) potentially providing alternative BAK regulation mechanisms (Cheng, Sheiko et al. 2003).

The presence of primed BAK in the Jurkat cells could reflect the fact that these cells are tumor cells. Therefore the continuous conversion from inactive to primed BAK occurs but cells escape apoptosis by overexpressing BCL-X_L which blocks further activation of primed BAK. This impaired apoptosis leads then to tumour development.

To specifically focus on the further activation of primed BAK during apoptosis, I have chosen the BH3 mimetic ABT-737. Out of six tested putative BH3 mimetics only ABT-737 acted as an authentic BCL-2 inhibitor by specifically inducing the intrinsic apoptotic pathway in a BAK and/or BAX and caspase-9-dependent manner (Fig. 3.1 and 3.2). Furthermore I demonstrate that ABT-737 induces the classical apoptotic hallmarks like reduction in $\Delta\Psi_m$, cytochrome *c* release, caspase activation and PS externalisation in Jurkat cells (Fig. 3.3, 3.4 and 3.5). ABT-737 mimics the binding profile of the BH3-only protein BAD and therefore neutralises the anti-apoptotic BCL-2 proteins BCL-X_L, BCL-2 and BCL-w. Therefore exposure to ABT-737 should result in the displacement of primed BAK from BCL-X_L. Indeed I found that primed BAK is displaced from BCL-X_L by ABT-737 as demonstrated in an endogenous situation in Jurkat cells (Fig. 4.1). Furthermore reconstituting BCL-X_L:BAK complexes in resistant cells resulted in sensitisation to ABT-737 demonstrating that this discrete proportion of BAK is primarily involved in ABT-737 induced apoptosis (Fig. 4.3). Therefore ABT-737 was used as a tool to further investigate the activation steps of primed BAK after its displacement from BCL-X_L.

7.2 N-terminal conformational change and oligomerisation of primed BAK

BAK is described to be activated during apoptosis and this is characterised both by an N-terminal conformational change and also its oligomerisation into higher molecular weight complexes. At what stage in BAK activation do these conformational changes occur? Is primed BAK is N-terminal conformationally changed and/or oligomerised while complexed to BCL-X_L or do these conformational changes occur after displacement from BCL-X_L? The relevance of these conformational changes for the formation of a membrane permeabilising BAK pore is also unclear.

I demonstrate that BAK undergoes an N-terminal conformational change, as determined by exposure of the AB1 epitope as well as increased trypsin sensitivity following 15 min of ABT-737 exposure (Griffiths, Dubrez et al. 1999; Wei, Lindsten et al. 2000) (Fig. 5.1). This

N-terminal conformational change represents a reorganisation of the N-terminal region rather than a simple exposure of helix α_1 , and involves the initial repositioning of the overlying helix α_2 followed by rotation of helix α_1 (Fig. 5.2).

Using double immunoprecipitation, I demonstrate that this N-terminal conformational change occurs after the displacement of primed BAK from BCL-X_L in the endogenous situation in the Jurkat cells (Fig. 5.3). Consequently primed BAK complexed with BCL-X_L is not N-terminally conformationally changed and the N-terminal conformational change must occur after displacement of BAK from BCL-X_L (Fig. 5.3). Thus the N-terminal conformational change occurs separate/independent and downstream to the exposure of the BH3 domain likely facilitated by the long loop between helix α_1 and α_3 (Moldoveanu, Liu et al. 2006). However in the reconstitution system a portion of BAK sequestered by BCL-X_L is N-terminally conformationally changed (Fig. 5.3). This probably reflects the fact that due to overexpression of BAK it auto-activates itself and undergoes the subsequent conformational changes. Thus BCL-X_L sequesters BAK in different conformational states resulting in the heterogeneous population of N-terminal conformationally changed and N-terminal occluded BAK.

Next to the N-terminal conformational change the formation of dimers and high molecular weight complexes is a characteristic of BAK activation. Exposure to the redox catalyst CuPhe retains BAK in a closed M_X conformation in control cells indicating that the N-terminal C14 is constrained near C166 which is located in helix α_6 . After 15 min of ABT-737 exposure, the M_X conformation is reduced and this is accompanied by the detection of dimers and high molecular weight complexes (Fig. 5.5). Considering that primed BAK is completely displaced from BCL-X_L at this time point (Fig. 5.3 and 6.7), this demonstrates that together with the N-terminal conformational change the formation of dimers and high molecular weight complexes must also occur after displacement of primed BAK from BCL-X_L.

Both BAK activation steps occur after 15 min of ABT-737 exposure. This time dependency could imply that both steps occur coincidentally. However analysis of their relationship revealed that the N-terminal change has to precede oligomerisation, as no high molecular weight species were detectable when BAK was restrained in the M_X conformation prior to activation (Fig. 5.6). This is in agreement with earlier findings that helix α_6 , which is exposed due to the N-terminal conformational change, represents an oligomerisation interface (Dewson, Kratina et al. 2009). Furthermore these results also demonstrate that the initial

proportion of N-terminal conformationally changed BAK detected at 15 min following ABT-737 reflects that which is oligomerised at this time point, as oligomerisation cannot occur without the N-terminal conformational change (Fig. 5.6).

N-terminal conformationally changed as well as oligomerised BAK which was detectable as soon as 15 min following ABT-737 exposure seems to nucleate N-terminal occluded, monomeric BAK in the Jurkat cells. Following 15 min of ABT-737 exposure, primed BAK was completely displaced from BCL-X_L (Fig. 5.3 and 6.7). Therefore the increase in N-terminal conformationally changed as well as oligomerised BAK between 15 min and 3 h of ABT-737 exposure is the result of a feed forward loop (Fig. 5.1, 5.3 and 5.5), where the initial N-terminal changed/ oligomerised BAK induces a conformational change/oligomerisation in inactive BAK. However the N-terminal conformational change and oligomerisation of BAK are not sufficient to transform BAK into a membrane permeabilising pore (Fig. 5.8 and 5.9). A BAK L78A mutant lost proapoptotic activity yet still formed dimers and high molecular weight complexes (Fig. 5.9). Therefore neither the N-terminal conformational change nor oligomerisation represent the points of no return in BAK activation.

The L78A BAK mutant would also be useful as a tool to investigate the composition of the pore by which cytochrome *c* is released. Neither the structure nor the composition of this pore is known as its transient nature makes it difficult to analyse. The L78A mutant apparently oligomerises into the same high molecular weight species like wt BAK (Fig. 5.9), suggesting that oligomerisation is not impaired with this mutant. Thus the static formation of L78A BAK oligomers could provide further insights into the composition and structure of the pore responsible for cytochrome *c* release.

7.3 Interaction with BIM_{EL}

Activator BH3-only proteins are described to activate BAK by direct interaction (Chipuk and Green 2008). I found that BIM_{EL} interacts with BAK in control as well as ABT-737 exposed cells (Fig. 6.1). To analyse if BIM_{EL} specifically interacts with the proportion of primed BAK after its displacement from BCL-X_L I performed double immunoprecipitations on BCL-X_L:BAK reconstituted cells. Following ABT-737 exposure BAK is displaced from BCL-X_L in a time dependent manner and specifically at 30 min BIM_{EL} was found to interact with the displaced BAK reflecting the transient nature of this interaction (Fig. 6.2).

Is the interaction with BIM_{EL} then promoting BAK proapoptotic function? Co-transfection of BIM_{EL} with sub-lethal concentrations of BAK revealed that BIM_{EL} can enhance BAK proapoptotic function (Fig. 6.3). This demonstrates that association of BAK with BIM_{EL} may represent an additional step in BAK activation and may be required to achieve the proapoptotic function of BAK.

BIM is described to induce the oligomerisation of BAK (Wei, Lindsten et al. 2000). In the BCL-X_L:BAK reconstitution I demonstrate that system BAK is N-terminal conformationally changed as well as oligomerised while still complexed with BCL-X_L (Fig. 6.3). Consequently after its displacement from BCL-X_L, BAK still exists in an N-terminal conformational changed/oligomerised conformation as these steps are not reversible. Therefore BIM_{EL} must interact with N-terminal changed oligomerised BAK placing this interaction downstream of both the N-terminal conformational change and oligomerisation. Thus in this system, BIM_{EL} does not induce oligomerisation of BAK. What step is BIM_{EL} then involved in?

Active BAK assembles into a pore in the outer mitochondrial membrane big enough to release cytochrome c. In order to penetrate the mitochondrial outer membrane BAX was described to insert after its transmembrane domain (helix $\alpha 9$) also the pore domain (helix $\alpha 5$ and $\alpha 6$) (Annis, Soucie et al. 2005). This embedding of the pore domain was demonstrated to be driven by BIM. Considering the structural similarities between BAK and BAX, additional insertion of the pore domain is also a reasonable hypothesis for BAK. In this scenario, BIM_{EL} would induce the insertion of the pore domain of oligomerised BAK (helix $\alpha 5$ and $\alpha 6$). This step occurs downstream of displacement of primed BAK from BCL-X_L, the N-terminal conformational change as well as oligomerisation and therefore may represent the point of no return in BAK activation.

ABT-737 displaces primed BAK from BCL-X_L which could then spontaneously undergo N-terminal change and oligomerisation. However I demonstrate that oligomerised BAK is not sufficient to permeabilise the mitochondria but instead requires interaction with BIM_{EL} to fully achieve its proapoptotic function. This reinforces the idea that ABT-737 acts as a derepressor BH3-only protein as the pool of BIM_{EL} involved in the further activation of BAK does not represent the one displaced from BCL-X_L by ABT-737 (Fig. 6.6 and 6.7).

These findings suggest that ABT-737 can only release apoptosis by displacing BAK from BCL-X_L and not directly induce apoptosis.

The activation of BAK thus represents a multiple step mechanism, where each step provides a potential target for therapeutic intervention in diseases of premature cell death or unchecked cellular survival. Therefore the identification and characterisation of each steps required for the transition from inactive BAK to a membrane permeabilising pore is crucial.

I demonstrate that the activation of BAK comprises a multiple step mechanism. One of the first steps is its exposure of the BH3 domain, which facilitates binding to the hydrophobic groove of BCL-X_L. After displacement of BAK from BCL-X_L during apoptosis BAK undergoes an N-terminal conformational change and subsequent oligomerisation. However oligomerisation is not the critical event to trigger the permeabilisation of the outer mitochondrial membrane. I demonstrate that BIM_{EL} transiently interacts with BAK, whereby this interaction occurs downstream of the N-terminal conformational change and probably promotes further membrane insertion (helix $\alpha 5$ and $\alpha 6$).

7.4 Direct or indirect activation

The results presented show aspects of both models and would combine the indirect with the direct model. BAK exists in a preactivated state, which is characterised by an exposed BH3 domain. Cell survival is maintained by the sequestration of primed BAK by BCL-X_L and apoptosis is induced when primed BAK is displaced from BCL-X_L. These findings correlate with the indirect activation model.

In agreement with the direct activation model I demonstrate that BIM interacts with BAK. It was postulated that direct activators induce the oligomerisation of BAK drawn from experiments involving incubation of heavy membrane fractions with tBID followed by analysis of BAK oligomerisation (Wei, Lindsten et al. 2000). Problematic with this conclusion is that direct activators fulfill a dual role- they also can act as sensitizer BH3-only proteins by displacing BAK from antiapoptotic proteins and both roles cannot be separated by experiments like this. By using ABT-737 to release BAK from BCL-X_L I showed that BIM interacts with BAK after its oligomerisation which positions the interaction of BIM with BAK further downstream as postulated in the direct activation model. Therefore BIM promotes probably the insertion of the BAK pore domain rather than its oligomerisation providing the critical commitment step to apoptosis.

Another feature of the direct model is that BIM is sequestered by antiapoptotic proteins and is displaced during apoptosis to activate BAK. However, my results suggest that although BIM is sequestered by antiapoptotic proteins its displacement is delayed compared to the displacement of BAK from BCL-X_L. This would suggest that the portion of BIM which is sequestered by antiapoptotic proteins is not the one involved in the direct activation BAK.

Consequently my results suggest that the underlying mechanism of BAK activation does not strictly follow either model but rather suggest a combination of aspects of both models.

CHAPTER 8:
References

- Adams, J. M. and S. Cory (2007). "The Bcl-2 apoptotic switch in cancer development and therapy." *Oncogene* **26**(9): 1324-37.
- Annis, M. G., E. L. Soucie, et al. (2005). "Bax forms multispinning monomers that oligomerize to permeabilize membranes during apoptosis." *EMBO J* **24**(12): 2096-103.
- Antonsson, B., S. Montessuit, et al. (2001). "Bax is present as a high molecular weight oligomer/complex in the mitochondrial membrane of apoptotic cells." *J Biol Chem* **276**(15): 11615-23.
- Balakrishnan, K., W. G. Wierda, et al. (2008). "Gossypol, a BH3 mimetic, induces apoptosis in chronic lymphocytic leukemia cells." *Blood* **112**(5): 1971-80.
- Bradford, M. (1976). "A rapid and sensitive for the quantitation of microgram quantities of protein utilizing the principle of protein-dye binding." *Anal. Biochem.* **72**: 248-254.
- Cain, K., D. G. Brown, et al. (1999). "Caspase Activation Involves the Formation of the Aposome, a Large (~700 kDa) Caspase-activating Complex." *J. Biol. Chem.* **274**(32): 22686-22692.
- Cartron, P. F., T. Gallenne, et al. (2004). "The first alpha helix of Bax plays a necessary role in its ligand-induced activation by the BH3-only proteins Bid and PUMA." *Mol Cell* **16**(5): 807-18.
- Certo, M., V. Del Gaizo Moore, et al. (2006). "Mitochondria primed by death signals determine cellular addiction to antiapoptotic BCL-2 family members." *Cancer Cell* **9**(5): 351-65.
- Chen, L., S. N. Willis, et al. (2005). "Differential targeting of prosurvival Bcl-2 proteins by their BH3-only ligands allows complementary apoptotic function." *Mol Cell* **17**(3): 393-403.
- Cheng, E. H., T. V. Sheiko, et al. (2003). "VDAC2 inhibits BAK activation and mitochondrial apoptosis." *Science* **301**(5632): 513-7.
- Chipuk, J. E. and D. R. Green (2008). "How do BCL-2 proteins induce mitochondrial outer membrane permeabilization?" *Trends Cell Biol* **18**(4): 157-64.
- Chipuk, J. E., T. Moldoveanu, et al. "The BCL-2 family reunion." *Mol Cell* **37**(3): 299-310.
- Cohen, G. M. (1997). "Caspases: the executioners of apoptosis." *Biochem J* **326** (Pt 1): 1-16.
- Conradt, B. and H. R. Horvitz (1998). "The C. elegans protein EGL-1 is required for programmed cell death and interacts with the Bcl-2-like protein CED-9." *Cell* **93**(4): 519-29.
- Danial, N. N. and S. J. Korsmeyer (2004). "Cell death: critical control points." *Cell* **116**(2): 205-19.
- Del Gaizo Moore, V., J. R. Brown, et al. (2007). "Chronic lymphocytic leukemia requires BCL2 to sequester prodeath BIM, explaining sensitivity to BCL2 antagonist ABT-737." *J Clin Invest* **117**(1): 112-21.
- Dewson, G., T. Kratina, et al. (2009). "Bak activation for apoptosis involves oligomerization of dimers via their alpha6 helices." *Mol Cell* **36**(4): 696-703.
- Dewson, G., T. Kratina, et al. (2008). "To trigger apoptosis, Bak exposes its BH3 domain and homodimerizes via BH3:groove interactions." *Mol Cell* **30**(3): 369-80.
- Ellis, R. E. and H. R. Horvitz (1991). "Two C. elegans genes control the programmed deaths of specific cells in the pharynx." *Development* **112**(2): 591-603.
- Falke, J. J., A. F. Dernburg, et al. (1988). "Structure of a bacterial sensory receptor. A site-directed sulfhydryl study." *J Biol Chem* **263**(29): 14850-8.
- Fesik, S. W. (2005). "Promoting apoptosis as a strategy for cancer drug discovery." *Nat Rev Cancer* **5**(11): 876-85.
- Frank, S., B. Gaume, et al. (2001). "The role of dynamin-related protein 1, a mediator of mitochondrial fission, in apoptosis." *Dev Cell* **1**(4): 515-25.

- Gavathiotis, E., M. Suzuki, et al. (2008). "BAX activation is initiated at a novel interaction site." *Nature* **455**(7216): 1076-81.
- Green, D. R. and G. I. Evan (2002). "A matter of life and death." *Cancer Cell* **1**: 19-30.
- Green, D. R. and G. I. Evan (2002). "A matter of life and death." *Cancer Cell* **1**(1): 19-30.
- Green, D. R. and G. Kroemer (2004). "The pathophysiology of mitochondrial cell death." *Science* **305**(5684): 626-9.
- Griffiths, G. J., B. M. Corfe, et al. (2001). "Cellular damage signals promote sequential changes at the N-terminus and BH-1 domain of the pro-apoptotic protein Bak." *Oncogene* **20**(52): 7668-76.
- Griffiths, G. J., L. Dubrez, et al. (1999). "Cell damage-induced conformational changes of the pro-apoptotic protein Bak in vivo precede the onset of apoptosis." *J Cell Biol* **144**(5): 903-14.
- Hanahan, D. and R. A. Weinberg (2000). "The hallmarks of cancer." *Cell* **100**(1): 57-70.
- Harada, H., B. Quearry, et al. (2004). "Survival factor-induced extracellular signal-regulated kinase phosphorylates BIM, inhibiting its association with BAX and proapoptotic activity." *Proc Natl Acad Sci U S A* **101**(43): 15313-7.
- Hengartner, M. O., R. E. Ellis, et al. (1992). "Caenorhabditis elegans gene ced-9 protects cells from programmed cell death." *Nature* **356**(6369): 494-9.
- Hengartner, M. O. and H. R. Horvitz (1994). "C. elegans cell survival gene ced-9 encodes a functional homolog of the mammalian proto-oncogene bcl-2." *Cell* **76**(4): 665-76.
- Horvitz, H. R. (1999). "Genetic control of programmed cell death in the nematode Caenorhabditis elegans." *Cancer Res* **59**(7 Suppl): 1701s-1706s.
- Hsu, Y. T. and R. J. Youle (1997). "Nonionic detergents induce dimerization among members of the Bcl-2 family." *J Biol Chem* **272**(21): 13829-34.
- Karbowski, M., Y. J. Lee, et al. (2002). "Spatial and temporal association of Bax with mitochondrial fission sites, Drp1, and Mfn2 during apoptosis." *J Cell Biol* **159**(6): 931-8.
- Kaufmann, S. H., S. Desnoyers, et al. (1993). "Specific proteolytic cleavage of poly(ADP-ribose) polymerase: an early marker of chemotherapy-induced apoptosis." *Cancer Res* **53**(17): 3976-85.
- Kerr, J. F., A. H. Wyllie, et al. (1972). "Apoptosis: a basic biological phenomenon with wide-ranging implications in tissue kinetics." *Br J Cancer* **26**(4): 239-57.
- Kim, H., H. C. Tu, et al. (2009). "Stepwise activation of BAX and BAK by tBID, BIM, and PUMA initiates mitochondrial apoptosis." *Mol Cell* **36**(3): 487-99.
- Kitada, S., M. Leone, et al. (2003). "Discovery, characterization, and structure-activity relationships studies of proapoptotic polyphenols targeting B-cell lymphocyte/leukemia-2 proteins." *J Med Chem* **46**(20): 4259-64.
- Ko, C. H., S. C. Shen, et al. (2007). "Gossypol reduction of tumor growth through ROS-dependent mitochondria pathway in human colorectal carcinoma cells." *Int J Cancer* **121**(8): 1670-9.
- Konopleva, M., R. Contractor, et al. (2006). "Mechanisms of apoptosis sensitivity and resistance to the BH3 mimetic ABT-737 in acute myeloid leukemia." *Cancer Cell* **10**(5): 375-88.
- Kuwana, T., L. Bouchier-Hayes, et al. (2005). "BH3 domains of BH3-only proteins differentially regulate Bax-mediated mitochondrial membrane permeabilization both directly and indirectly." *Mol Cell* **17**(4): 525-35.
- Kuwana, T., M. R. Mackey, et al. (2002). "Bid, Bax, and lipids cooperate to form supramolecular openings in the outer mitochondrial membrane." *Cell* **111**(3): 331-42.
- Lazebnik, Y. A., S. H. Kaufmann, et al. (1994). "Cleavage of poly(ADP-ribose) polymerase by a proteinase with properties like ICE." *Nature* **371**(6495): 346-7.

- Leber, B., J. Lin, et al. (2007). "Embedded together: the life and death consequences of interaction of the Bcl-2 family with membranes." *Apoptosis* **12**(5): 897-911.
- Letai, A., M. C. Bassik, et al. (2002). "Distinct BH3 domains either sensitize or activate mitochondrial apoptosis, serving as prototype cancer therapeutics." *Cancer Cell* **2**(3): 183-92.
- Ley, R., K. E. Ewings, et al. (2005). "Regulatory phosphorylation of Bim: sorting out the ERK from the JNK." *Cell Death Differ* **12**(8): 1008-14.
- Lockshin, R. A. and C. M. Williams (1965). "Programmed Cell Death--I. Cytology of Degeneration in the Intersegmental Muscles of the Pernyi Silkworm." *J Insect Physiol* **11**: 123-33.
- Lovell, J. F., L. P. Billen, et al. (2008). "Membrane binding by tBid initiates an ordered series of events culminating in membrane permeabilization by Bax." *Cell* **135**(6): 1074-84.
- Makin, G. W., B. M. Corfe, et al. (2001). "Damage-induced Bax N-terminal change, translocation to mitochondria and formation of Bax dimers/complexes occur regardless of cell fate." *EMBO J* **20**(22): 6306-15.
- Martin, S. J., C. P. Reutelingsperger, et al. (1995). "Early redistribution of plasma membrane phosphatidylserine is a general feature of apoptosis regardless of the initiating stimulus: inhibition by overexpression of Bcl-2 and Abl." *J Exp Med* **182**(5): 1545-56.
- Martinou, J. C. and D. R. Green (2001). "Breaking the mitochondrial barrier." *Nat Rev Mol Cell Biol* **2**(1): 63-7.
- Meier, P., A. Finch, et al. (2000). "Apoptosis in development." *Nature* **407**: 796-801.
- Miyashita, T. and J. C. Reed (1993). "Bcl-2 oncoprotein blocks chemotherapy-induced apoptosis in a human leukemia cell line." *Blood* **81**(1): 151-7.
- Moldoveanu, T., Q. Liu, et al. (2006). "The X-ray structure of a BAK homodimer reveals an inhibitory zinc binding site." *Mol Cell* **24**(5): 677-88.
- Muchmore, S. W., M. Sattler, et al. (1996). "X-ray and NMR structure of human Bcl-xL, an inhibitor of programmed cell death." *Nature* **381**(6580): 335-41.
- Nguyen, M., R. C. Marcellus, et al. (2007). "Small molecule obatoclax (GX15-070) antagonizes MCL-1 and overcomes MCL-1-mediated resistance to apoptosis." *Proc Natl Acad Sci U S A* **104**(49): 19512-7.
- Oltersdorf, T., S. W. Elmore, et al. (2005). "An inhibitor of Bcl-2 family proteins induces regression of solid tumours." *Nature* **435**(7042): 677-681.
- Oltersdorf, T., S. W. Elmore, et al. (2005). "An inhibitor of Bcl-2 family proteins induces regression of solid tumours." *Nature* **435**(7042): 677-81.
- Oltvai, Z. N., C. L. Millman, et al. (1993). "Bcl-2 heterodimerizes in vivo with a conserved homolog, Bax, that accelerates programmed cell death." *Cell* **74**(4): 609-19.
- Pagliari, L. J., T. Kuwana, et al. (2005). "The multidomain proapoptotic molecules Bax and Bak are directly activated by heat." *Proc Natl Acad Sci U S A* **102**(50): 17975-80.
- Puthalakath, H., A. Villunger, et al. (2001). "Bim: a proapoptotic BH3-only protein regulated by interaction with the myosin V actin motor complex, activated by anoikis." *Science* **293**(5536): 1829-32.
- Roy, S. S., A. M. Ehrlich, et al. (2009). "VDAC2 is required for truncated BID-induced mitochondrial apoptosis by recruiting BAK to the mitochondria." *EMBO Rep* **10**(12): 1341-7.
- Ruffolo, S. C. and G. C. Shore (2003). "BCL-2 selectively interacts with the BID-induced open conformer of BAK, inhibiting BAK auto-oligomerization." *J Biol Chem* **278**(27): 25039-45.
- Sattler, M., H. Liang, et al. (1997). "Structure of Bcl-xL-Bak peptide complex: recognition between regulators of apoptosis." *Science* **275**(5302): 983-6.

- Sentman, C. L., J. R. Shutter, et al. (1991). "bcl-2 inhibits multiple forms of apoptosis but not negative selection in thymocytes." *Cell* **67**(5): 879-88.
- Shawgo, M. E., S. N. Shelton, et al. (2008). "Caspase-mediated Bak activation and cytochrome c release during intrinsic apoptotic cell death in Jurkat cells." *J Biol Chem* **283**(51): 35532-8.
- Sun, X. M., S. B. Bratton, et al. (2002). "Bcl-2 and Bcl-xL inhibit CD95-mediated apoptosis by preventing mitochondrial release of Smac/DIABLO and subsequent inactivation of X-linked inhibitor-of-apoptosis protein." *J Biol Chem* **277**(13): 11345-51.
- Sundararajan, R. and E. White (2001). "E1B 19K blocks Bax oligomerization and tumor necrosis factor alpha-mediated apoptosis." *J Virol* **75**(16): 7506-16.
- Suzuki, M., R. J. Youle, et al. (2000). "Structure of Bax: coregulation of dimer formation and intracellular localization." *Cell* **103**(4): 645-54.
- Takahashi, A., E. S. Alnemri, et al. (1996). "Cleavage of lamin A by Mch2 alpha but not CPP32: multiple interleukin 1 beta-converting enzyme-related proteases with distinct substrate recognition properties are active in apoptosis." *Proc. Natl. Acad. Sci. U. S. A.* **93**: 8395-8400.
- Terradillos, O., S. Montessuit, et al. (2002). "Direct addition of BimL to mitochondria does not lead to cytochrome c release." *FEBS Lett* **522**(1-3): 29-34.
- Towbin, H., T. Staehelin, et al. (1992). "Electrophoretic transfer of proteins from polyacrylamide gels to nitrocellulose sheets: procedure and some applications. 1979." *Biotechnology* **24**: 145-9.
- Tsujimoto, Y., J. Yunis, et al. (1984). "Molecular cloning of the chromosomal breakpoint of B-cell lymphomas and leukemias with the t(11;14) chromosome translocation." *Science* **224**(4656): 1403-6.
- Uren, R. T., G. Dewson, et al. (2007). "Mitochondrial permeabilization relies on BH3 ligands engaging multiple prosurvival Bcl-2 relatives, not Bak." *J Cell Biol* **177**(2): 277-87.
- van Delft, M. F., A. H. Wei, et al. (2006). "The BH3 mimetic ABT-737 targets selective Bcl-2 proteins and efficiently induces apoptosis via Bak/Bax if Mcl-1 is neutralized." *Cancer Cell* **10**(5): 389-99.
- Vaux, D. L., S. Cory, et al. (1988). "Bcl-2 gene promotes haemopoietic cell survival and cooperates with c-myc to immortalize pre-B cells." *Nature* **335**(6189): 440-2.
- Vogler, M., D. Dinsdale, et al. (2009). "Bcl-2 inhibitors: small molecules with a big impact on cancer therapy." *Cell Death Differ* **16**(3): 360-7.
- Vogler, M., K. Weber, et al. (2009). "Different forms of cell death induced by putative BCL2 inhibitors." *Cell Death Differ* **16**(7): 1030-9.
- Walensky, L. D., A. L. Kung, et al. (2004). "Activation of apoptosis in vivo by a hydrocarbon-stapled BH3 helix." *Science* **305**(5689): 1466-70.
- Wei, M. C., T. Lindsten, et al. (2000). "tBID, a membrane-targeted death ligand, oligomerizes BAK to release cytochrome c." *Genes Dev* **14**(16): 2060-71.
- Wei, M. C., W. X. Zhong, et al. (2001). "Proapoptotic BAX and BAK: a requisite gateway to mitochondrial dysfunction and death." *Science* **292**: 727-730.
- Wei, M. C., W. X. Zong, et al. (2001). "Proapoptotic BAX and BAK: a requisite gateway to mitochondrial dysfunction and death." *Science* **292**(5517): 727-30.
- Willis, S. N., L. Chen, et al. (2005). "Proapoptotic Bak is sequestered by Mcl-1 and Bcl-xL, but not Bcl-2, until displaced by BH3-only proteins." *Genes Dev* **19**(11): 1294-305.
- Willis, S. N., J. I. Fletcher, et al. (2007). "Apoptosis initiated when BH3 ligands engage multiple Bcl-2 homologs, not Bax or Bak." *Science* **315**(5813): 856-9.
- Wolf, B. B. and D. R. Green (1999). "Suicidal tendencies: apoptotic cell death by caspase family proteinases." *J. Biol. Chem.* **274**(29): 20049-20052.

- Yethon, J. A., R. F. Epand, et al. (2003). "Interaction with a membrane surface triggers a reversible conformational change in Bax normally associated with induction of apoptosis." J Biol Chem **278**(49): 48935-41.
- Youle, R. J. and A. Strasser (2008). "The BCL-2 protein family: opposing activities that mediate cell death." Nat Rev Mol Cell Biol **9**(1): 47-59.
- Zha, H. and J. C. Reed (1997). "Heterodimerization-independent functions of cell death regulatory proteins Bax and Bcl-2 in yeast and mammalian cells." J Biol Chem **272**(50): 31482-8.
- Zhai, D., C. Jin, et al. (2006). "Comparison of chemical inhibitors of antiapoptotic Bcl-2-family proteins." Cell Death Differ **13**(8): 1419-21.
- Zhang, M., H. Liu, et al. (2007). "Gossypol induces apoptosis in human PC-3 prostate cancer cells by modulating caspase-dependent and caspase-independent cell death pathways." Life Sci **80**(8): 767-74.
- Zhong, W. X., T. Lindsten, et al. (2001). "BH3-only proteins that bind pro-survival Bcl-2 family members fail to induce apoptosis in the absence of Bax and Bak." Gnes and Dev. **15**: 1481-1486.
- Zou, H., Y. Li, et al. (1999). "An APAF-1.cytochrome c multimeric complex is a functional apoptosome that activates procaspase-9." J. Biol. Chem. **274**(17): 11549-11556.

CHAPTER 9:
Appendix

PRIMERS**BAK truncations:**

Strep BAK M1-23

5' cgggatccaccatggctagctggagccacccgcagttcgaaaaagccgaggagcaggtagcccagg 3'

Strep BAK M1-42

5' cgggatccaccatggctagctggagccacccgcagttcgaaaaagcccatcagcaggaacaggaggc 3'

Strep BAK M1-S69

5' cgggatccaccatggctagctggagccacccgcagttcgaaaaagccaccatggggcaggtgggac 3'

Strep BAK N83-212

5' cgggatccaccatggctagctggagccacccgcagttcgaaaaaggcgccaaccgacgtatgactcag 3'

BAK Mutants - Quikchange Primers

Y38R

Forward: 5'-gaggaggtttccgcagccgcgtttttaccgcatca-3'

Reverse: 5'-tgatggcggtaaaaaacgcggctcggaaaaacctcctc-3'

F35A

Forward: 5'-ccaggacacagaggaggttgcggcagctacg-3'

Reverse: 5'-cgtagctcgggcaacctcctctgtgtcctgg-3'

T31R

Forward: 5'-agcaggtagcccaggacagagagggtt-3'

Reverse: 5'-aacctcctctctgtcctgggctacctgct-3'

M60A

Forward: 5'-cctgccgaccagaggcggtcaccttacctct-3'

Reverse: 5'-agagtaaggtgaccgctctgggtcggcagg-3'

L63R

Forward: 5'-cccagagatggtcacccgacctctgcaacctagc-3'

Reverse: 5'-gctaggttgagagggtcgggtgacctctctggg-3'